A Combinatorial Engineering Approach to Increase the Productivity of CHO Cells, and Proteomic Analysis of Cell Culture Supernatant

Von der Fakultät Energie-, Verfahrens- und Biotechnik der Universität Stuttgart

zur Erlangung der Würde eines Doktors der Naturwissenschaften (Dr. rer. nat.)

genehmigte Abhandlung

vorgelegt von

Eric Becker

aus Ottweiler

Hauptberichter: Prof. Dr. K. Pfizenmaier

Mitberichter: Prof. Dr. R. Kontermann

Tag der mündlichen Prüfung:

10.Dez.2008

Institut für Zellbiologie und Immunologie

2008

Unser Kopf ist rund,
damit das Denken die Richtung ändern kann

Francis Picabia (1879–1953)

1 INDEX

2 LIST OF ABBREVIATIONS

°C	Degrees Celsius
2-AB	2-Aminobenzamide
2D-DIGE	Differential twodimensional gel electrophoresis
2D-GE	Two-dimensional gel electrophoresis
amp	Ampicillin
BI	Boehringer Ingelheim
CCF	Cell culture fluid
cDNA	complementary DNA
CEDEX	Cell density examination system
CERT	Ceramide transfer protein
CFA	Colony formation assay
CHO	Chinese hamster ovary
CMV	Cytomegalovirus
cT	Cycle threshold
Da or D	Dalton
d	Day(s)
DEPC	Diethylpyrocarbonate
DNA	Deoxyribonucleic acid
DO	Dissolved oxygen
ECL	Enhanced chemiluminescence
EDTA	Ethylenediamine tetraacetate
EGTA	Ethyleneglycol tetraacetic acid
ELISA	Enzyme-Linked ImmunoSorbent Assay
ER	Endoplasmic reticulum
ERSE	ER stress response element
FACS	Fluorescent activated cell sorting
FC	Flow cytometry
FCS	Fetal Calf Serum
FITC	Fluorescein isothiocyanate
FRET	Fluorescence resonance energy transfer
GFP	Green fluorescent protein
h	Hour(s)
HPLC	High-pressure liquid chromatography
HRP	Horseradish peroxidase
HSA	Human serum albumin
HTRF	Homogeneous time-resolved fluorescence assay
IEF	Isoelectric focusing
IgG	Immunoglobulin G
IRE1	Inositol requiring enzyme 1

IRES	Internal ribosomal entry site
IVC	Integral of viable cells
L	Liter(s)
M	Molar
m	Meter(s)
mAb	Monoclonal antibody
MCS	Multiple cloning site
min	Minute(s)
mRNA	messenger RNA
Mw	Molecular weight
neo	Neomycin
NIR	Near infrared
PBS	Phosphate-buffered saline
PCR	Polymerase chain reaction
PES	Polyethersulfone
pI	isoelectric point
Prefix m	milli = 10^{-3}
Prefix µ	mu = 10^{-6}
Prefix n	nano = 10^{-9}
Prefix p	piko = 10^{-12}
puro	Puromycin
PVDF	Polyvinylidene fluoride
Qp	Specific productivity
qPCR	Quantitative real time PCR
RNA	Ribonucleic acid
rpm	Rotations per minute
RT-PCR	Real-time PCR
SDS-PAGE	Sodium dodecylsulfate polyacrylamide gel electrophoresis
STIP1	Stress-induced phosphoprotein 1
TCA	Trichloroacetic acid
UPR	Unfolded protein response
V	Volt(s)
WCB	Working cell bank
XBP-1(s)	Unspliced form of X-box-binding protein 2
XBP-1(u)	Spliced form of X-box-binding protein 1
XIAP	X-linked inhibitor of apoptosis

3 ZUSAMMENFASSUNG

Die Verbesserung von Produktionsprozessen zur biotechnologischen Herstellung therapeutischer Proteine ist und bleibt eine ständige Herausforderung. Durch den Einsatz von optimierten Expressionsvektoren und die gezielte genetische Veränderung von Zellen auf den Ebenen der Transkription und Translation konnten deutliche Prozessverbesserungen erzielt werden. Dennoch waren zu Beginn des Projektes aus der Literatur keine eindeutigen Ergebnisse bekannt die belegen, dass der gezielte genetische Eingriff in die Post-translationale und Transportmaschinerie der Zelle zu einer weiteren Steigerung der Ausbeute führen kann.

In der vorliegenden Arbeit konnte gezeigt werden, dass die Überexpression des humanen Transkriptionsfaktors X-box-binding protein 1 (XBP-1) in Ovarienzellen des Chinesischen Hamsters (CHO) zu einer Erweiterung des endoplasmatischen Retikulums führte. Ausserdem konnte die spezifische Produktivität von in Suspension wachsenden monoklonalen Antikörper (mAb) produzierenden CHO-Zellen durch heterologe Expression der gesplicten Form des Transkriptionsfaktors X-box-binding protein 1 (XBP-1(s)) um 60% verbessert werden. Dies führte auch in einem Fed-batch Produktionsprozess zu deutlich gesteigerten Antikörperausbeuten. Eine Analyse der Produktqualität zeigte keinerlei Veränderungen in Bezug auf das Glykosilierungsmuster und die physikochemischen Eigenschaften des produzierten monoklonalen Antikörpers. Damit konnte gezeigt werden, dass eine gezielte genetische Veränderung von Produktionszellen durch Engineering des Endoplasmatischen Retikulums zu verbesserten Prozessausbeuten führen kann. Während dieser Evaluierung wurden jedoch auch negative Einflüsse der XBP-1 Überexpression beobachtet: Es konnten nur wenige monoklonale Zellen isoliert werden, die eine hohe Expression des heterologen Transkriptionsfaktors zeigten. Gleichzeitig wurde eine gewisse Dosisabhängigkeit beobachtet, bei der Zellen mit höherem intrazellulären Gehalt von XBP-1(s) auch den höchsten Effekt auf

die spezifische Produktivität aufwiesen. Des Weiteren konnte gezeigt werden, dass die Expression des heterologen Proteins über die Zeit instabil war und dadurch auch die spezifische Produktivität mit zunehmendem Zellalter abnahm. Diese Beobachtungen wurden anhand eines Koloniebildungstests überprüft. Deutlich geringere Koloniezahlen nach XBP-1 Überexpression bestätigten einen vermuteten Überlebensnachteil der Zellen durch die gezielte genetische Veränderung. Darüber hinaus konnte in einem weiteren Versuchsansatz gezeigt werden, dass die Überexpression von XBP-1 in CHO Zellen zu erhöhter Apoptose führt. In Anlehnung an die beobachtete Dosisabhängigkeit und um eine höchstmögliche Steigerung der Produktivität zu erreichen, sollte im Weiteren versucht werden, den Anteil der Zellen zu erhöhen, die eine gesteigerte Expressionsrate des heterologen Transkritptionsfaktors aufwiesen. Dazu wurde versucht, durch die gemeinsame Expression des anti-apoptotisch wirkenden Proteins x-linked inhibitor of apoptosis (XIAP) zusammen mit XBP-1 dessen bereits gezeigte, negative Einflüsse zu kompensieren. Einen ersten Hinweis auf einen möglichen Erfolg dieses Ansatzes wurde erreicht, indem in Koloniebildungstests eine Koexpression beider Proteine zu höheren Koloniezahlen führte und damit der negative Einfluss der XBP-1(s) Expression ausgeglichen werden konnte. Des Weiteren wurde ausgehend von einem antikörperproduziereden Produktionsklon gezeigt, das auf Ebene von polyklonalen Zelllinien die kombinierte Expression beider Proteine zu einem verbesserten Prozess mit gesteigerter Ausbeute führt. Um die Anwendbarkeit dieses kombinatorischen, gentechnischen Optimierungsansatzes für die kommerzielle Zelllinienentwicklung zu zeigen, wurden monoklonale Zellen generiert und untersucht. In dieser Arbeit konnten allerdings keine Klone gefunden werden, die den produktivitätssteigernden Effekt zeigten. Eine mögliche Ursache könnte in dem sehr stringenten Klonierungsansatz mittels Einzelzellablage in serum-freien Medium liegen.

Die Daten zeigen, dass es prinzipiell möglich ist, Prozesse durch die kombinierte Expression von anti-apoptotischen und sekretionssteigernden Proteinen zu verbessern. Gleichzeitig wird

jedoch deutlich, dass die Übertragung solcher Ansätze von Modellsystemen zu einer kommerziellen Anwendung schwierig sein kann.

Ein weiterer, wichtiger Baustein für einen stabilen Produktionsprozess für Biopharmazeutika ist eine ausgereifte Prozesskontrolle. Ein zusätzliches Ziel dieser Arbeit war es, eine Methode zu etablieren, mit deren Hilfe Proteine im Zellkulturüberstand identifiziert werden können, die als Marker für bestimmte Prozessphasen dienen können. Hierzu sollte das Proteom im Zellkulturüberstand von Prozessen mit Hilfe der differenziellen zweidimensionalen Gelelektrophorese (2D-DIGE) untersucht werden. Um den Einfluß des Protein-Produktes von Produktionszellen auf die Proteintrennung der Methode zu eliminieren, wurde zuerst eine Modellzelle generiert. Diese zeigte die gleichen Wachstumseigenschaften wie Produktionszellen, ohne dabei ein Therapeutikum zu produzieren. Im Folgenden wurden verschiedene Wege getestet, um die Proteinkonzentration im Zellkulturüberstand zu erhöhen und schließlich wurde eine Ultrafiltrationsmethode ausgewählt. Für einen ersten Test des gesamten Analyseverfahrens wurden anschliessend Überstände von verschiedenen Prozesstagen eines Batch-Prozesses mit Hilfe der 2D-DIGE Methode analysiert. Mittels Massenspektroskopie konnten dabei Proteine identifiziert werden, die zu den verschiedenen Messzeitpunkten in unterschiedlichen Konzentrationen vorlagen, was die Voraussetzung für mögliche Prozessmarker darstellt. Anhand eines Proteins wurde das Ergebnis dieser Analyse mittels eines immunologischen Nachweises verifiziert und bestätigt. Damit konnte gezeigt werden, dass die in dieser Arbeit etablierte Methode für die Suche nach Markerproteinen im Überstand von biotechnologischen Prozessen geeignet ist. Sie kann somit als Grundlage für die weitere Charakterisierung des Proteoms im Überstand von Zellkulturprozessen herangezogen werden. Anhand möglicher identifizierter Markerproteine können so neue Verfahren zur Prozesskontrolle entwickelt werden, welche die Grundlage für weiter verbesserte Produktionsprozesse bilden.

4 SUMMARY

The optimization of production processes for therapeutic antibodies is a continuing challenge in pharmaceutical biotechnology. It has been demonstrated that vector design and host cell engineering can improve transcriptional and translational efficiency, resulting in the generation of high producer cell lines. However, the introduction of transgenes into production cell lines that regulate protein transport or affect post-translational modifications have been reported in the literature to lead to inconsistent results regarding the improvement of industrial processes.

The present study shows that heterologous expression of the spliced form of transcription factor X-box-binding protein 1 (XBP-1(s)) leads to an increase in ER content in adherently growing Chinese hamster ovary (CHO) cells. Furthermore, specific therapeutic antibody productivity was elevated by 60% in CHO cells grown in inoculum suspension cultures. This dose-dependent effect translated into significantly increased overall antibody titers in a fed-batch format where cells were grown in chemically defined serum-free media. Protein-A purified antibody products from mock cells and XBP-1 transfected cells were found to be of comparable quality with regard to glycosylation pattern and physicochemical characteristics. The data demonstrated the potential of XBP-1 engineering to improve mammalian cell culture production processes to yield high amounts of a therapeutic protein product of desired quality. However, only low numbers of cells expressing the transgene at high levels were found during the generation of stable cell lines. Additionally, XBP-1(s) expression in monoclonal cell lines was found to decrease over a prolonged period of seed-stock cultivation. These observations were verified by colony formation assays (CFA) where XBP-1(s) expression led to significantly lower colony counts. In an additional experimental setting it was demonstrated that XBP-1(s) expression enhanced apoptosis in CHO cells. Altogether, the data demonstrated a survival disadvantage upon XBP-1(s) overexpression in engineered CHO

cells, hampering a possible commercial cell line development program based on XBP-1 engineered cells. Consequently, to elevate the frequency of high XBP-1(s)-expressing cells to thereby maximize the XBP-1(s) dose dependent effect on productivity, a combinatorial approach was investigated. To overcome the XBP-1(s) mediated apoptosis, co-expression of the anti-apoptotic protein x-linked inhibitor of apoptosis (XIAP) and XBP-1(s), combining secretion engineering and anti-apoptosis engineering, was evaluated. The proof-of-concept was demonstrated by colony formation assays (CFA), where concomitant XIAP and XBP-1(s) expression was able to restore colony counts. Moreover, when an mAb-producing CHO cell line was engineered, the bicistronic overexpression of both transgenes showed highest specific productivities and final titers in fed-batch cultures of polyclonal cell lines when compared with control cells. To test the applicability of this approach in a setting relevant for commercial use, the polyclonal cell lines were cloned by a serum-free single cell cloning step and subsequently tested for their productivity. In this study, however, no clones with elevated specific productivity could be found. This unexpected result may be explained by the stringent cloning procedure.

The data demonstrated a path toward optimized mammalian production processes. However, despite the proof-of-concept for the two transgenes approach on a pool level it proved challenging to transfer this idea from a model system to the final stages of industrial cell line development.

An additional building block for reproducible high-yielding production processes is sophisticated process monitoring. To be able to identify marker proteins which as a result of their concentration can indicate, for example, transitions between process phases during a production run, an analytical method was developed to investigate changes in the proteome of cell culture supernatant samples. In this approach, the proteome of the supernatant was analyzed by differential two-dimensional gel electrophoresis (2D-DIGE). In order to

eliminate interfering effects of the protein product of producer cell lines on the separation method, a mock cell line was generated. This mock cell line was selected to closely simulate production processes with comparable cellular growth characteristics but without product formation. For the concentration of supernatant samples precipitation and ultrafiltration were compared and the filtration method was finally selected. A first analysis of supernatant samples derived from three different process times of a batch culture demonstrated the applicability of the method to separate and finally identify proteins with different abundance in process supernatant samples - a prerequisite for possible process marker proteins. Furthermore, the results of this first study were verified by Western blot analysis for one protein.

The established method based on separation of the proteins from the supernatant by 2D-DIGE and subsequent identification by peptide mass fingerprinting using mass spectrometry can now be used as a starting point for further characterization studies. The identification of such process marker proteins is the first step toward next-generation bioprocess monitoring and control and provides an opportunity for further improved high-yielding production processes.

.

5 INTRODUCTION

5.1 Production of biopharmaceuticals

The market for biopharmaceuticals for use in human therapy continued to grow over more than the last two decades to more than 165 biopharmaceuticals approved worldwide in 2006 (Walsh, 2006). In 2008, 132 pharmaceuticals based on 96 active ingredients were approved in Germany (VFA, 2008). One of the main classes of therapeutic proteins was monoclonal antibodies (mAb), which represent 20% of the approved recombinant therapeutics in Germany. At present, 502 new biopharmaceuticals are being evaluated in clinical studies and sales of US$140 billion are estimated for 2014 (22% of the total pharma market) (Decision Resources/Pharmaview, 2008). This class of human therapeutics can be produced in a variety of hosts: (i) bacterial cells, (ii) fungi , (iii) insect cells, (iv) plants and plant cells, (v) transgenic animals and (vi) mammalian cells including human-derived cell lines (Schirrmann et al., 2008). Currently, the majority of biopharmaceuticals (~70%) is produced from mammalian cells because of their ability to correctly process and modify human proteins (Wurm, 2004). Successful processing and high-yield production of biopharmaceuticals are essential characteristics of any suitable recombinant mammalian producer cell line. Commonly used cell lines for the production of therapeutics include: mouse myeloma (NS0, SP2/0), human embryonic kidney (HEK-293), baby hamster kidney (BHK) and more recently the human retina-derived (PerC6) cell lines (Kuystermans et al., 2007; Chu and Robinson, 2001). Nevertheless, currently the most common industrial mammalian host cell system for the production of biopharmaceuticals is immortalized Chinese hamster ovary (CHO) cells, which are used to produce 27 approved therapeutic products (Jayapal et al., 2007).

Since many biopharmaceuticals have to be applied at high and often repeated doses to be effective (this is especially true of monoclonal antibodies) large amounts of products are

required to supply the market, and as a consequence there is an urgent need to lower costs by by increasing process yields.

5.2 Cell engineering strategies for improved production processes

Initial genetic engineering strategies to improve mammalian production cell lines focused on generating cells with the ability to grow in suspension and serum-free media. Stable expression of transferrin and insulin-like growth factor 1 (IGF-1) in CHO-K1 cells resulted in a cell line that can proliferate under protein-free conditions (Pak et al., 1996).

As apoptosis has been shown to be the predominant cause of cell death in mammalian cell culture production processes (al-Rubeai and Singh, 1998), the effect of expression of anti-apoptotic genes in mammalian host cells on culture viability was thoroughly investigated. Most anti-apoptosis engineering strategies focus on the overexpression of anti-apoptotic genes of the Bcl-2 family (e.g., Bcl-2 or BclxL (Kaufmann and Fussenegger, 2003)) or caspase inhibitors such as x-linked inhibitor of apoptosis (XIAP) (Sauerwald et al., 2002).

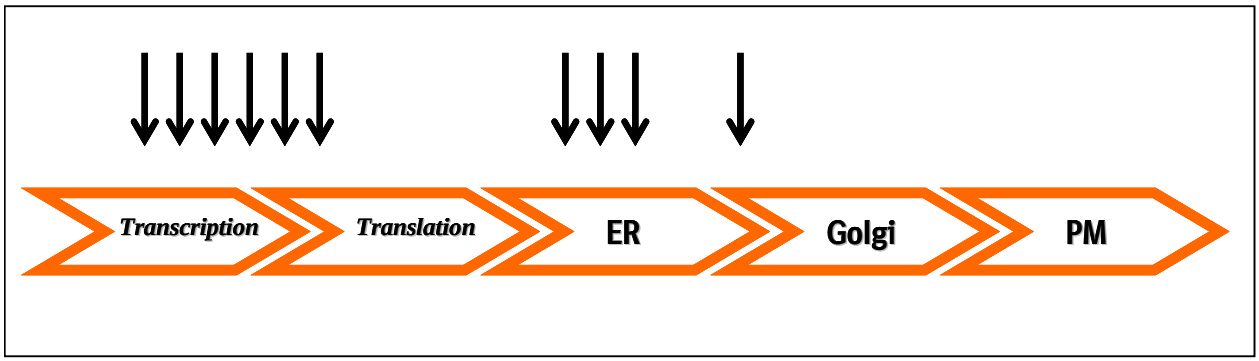

Figure 1: Symbolic path of a secreted protein and points of action for engineering approaches

What is shown here is the intracellular path of a secreted therapeutic protein. Arrows mark the area or location for engineering approaches described in the literature.

By increasing the cellular resistance to apoptotic stimuli during fermentation, such as nutrient depletion and waste byproduct accumulation, production processes with apoptosis engineered cell lines showed prolonged culture viability and in some cases an increase in product yield (Chiang and Sisk, 2005).

However, the most obvious parameter for optimizing production processes for biopharmaceuticals is the specific productivity of the individual cell in the bioreactor. Here, the main focus for improving the expression system was based on the modification of the early events in protein synthesis (Figure 1), namely, enhancing the copy number by amplification, the mRNA level by the use of strong promotors and mRNA stability by optimized polyA signals (for review see (Kuystermans et al., 2007)).

Other approaches for improving specific cell line productivity included the use of regulatory DNA elements encoded by the product expressing vectors aiming to target or create transcriptional hot spots. Regulatory elements such as S/MARs (Scaffold/matrix-associated regions) which affect chromatin structure and UCOEs (Ubiquitous chromatin opening elements) derived from housekeeping genes were both shown to positively affect specific productivities of recombinant proteins produced from CHO cell lines (Benton et al., 2002; Kim et al., 2004). Further improvements of the expression system include the modification of selection markers (Sautter and Enenkel, 2005) and the screening of optimal signal peptides (Knappskog et al., 2007). Recently, due to an increased understanding of the mechanistic action of microRNAs (miRNA) they have been suggested as a possible next-generation tool for cellular engineering of production cell lines (Muller et al., 2008).

Since biopharmaceutical protein products are secreted from the cells during the production process, the secretory transport machinery of the production cell line is another interesting target for novel host cell engineering strategies. In general, the yield of any biopharmaceutical

production process depends to a great extend on the amount of protein product that the producing cells secrete over time when grown under process conditions. Many complex intracellular processes are necessary to synthesize, process and secrete a protein from a eukaryotic cell. All these steps such as transcription, RNA transport, translation, post-translational modification and protein transport are tightly regulated in the wild-type host cell line and will have an impact on the specific productivity of any producer cell line derived from this host.

Many engineering approaches have employed the growing understanding of the molecular networks that drive processes such as transcription and translation to increase the yield of these steps in protein production. However, as in any multi-step process, widening a bottleneck during early steps of the process chain possibly creates bottlenecks further downstream, especially post translation. Up to a certain threshold, the specific productivity of a production cell has been reported to correlate linearly with the level of product gene transcription (Barnes et al., 2007; Jiang et al., 2006; Schlatter et al., 2005). Further enhancement of product expression at the mRNA level, however, may lead to an overload of the protein synthesis, folding or transport machinery, resulting in intracellular accumulation of the protein product, as also suggested by the authors of a recent review (Mohan et al., 2008). Indeed, this can frequently be observed in current manufacturing processes, for example by flow cytometric analysis (Fieder and Kaufmann, unpublished data).

Protein secretion is a complex multistep mechanism: proteins destined to be transported to the extracellular space or the plasma membrane are first co-translationally imported into the endoplasmic reticulum (ER). From there, they are packed into lipid vesicles and transported to the Golgi apparatus and finally from the trans-Golgi network (TGN) to the plasma membrane, where they are released into the culture medium (Seth et al., 2006). Although the key features of this multistep process are well known, there is still no detailed mechanistic

and molecular understanding of the regulatory network governing protein transport to the plasma membrane. Accordingly, the task of defining specific engineering approaches to target and successfully by-pass a potential bottleneck in the secretory pathway is hampered by the at present incomplete knowledge of the underlying molecular mechanisms.

The first studies on engineering the intracellular transport of secreted therapeutic proteins centered around the overexpression of molecular chaperones hosted within the endoplasmic reticulum (ER), such as binding protein BiP/GRP78 and protein disulfide isomerase (PDI). Chaperones are cellular proteins which assist the folding and assembly of newly synthesized proteins. In contrast to what would have been expected, BiP overexpression in mammalian cells has been shown to reduce rather than increase the secretion of proteins (Dorner and Kaufman, 1994). Likewise, PDI overexpression in CHO cells reduced the expression of a TNFR:FC fusion protein (Davis et al., 2000). However, in another case the specific production rate of an antibody was increased by 40% (Borth et al., 2005). A possible explanation for these apparently contradictory findings is that the increase of the cell's protein folding capacity may create a transport bottleneck further downstream. This is supported by a report describing ER to cis-Golgi transport problems for IFN-gamma production in a CHO cell line (Hooker et al., 1999).

So far, the engineering approach acting furthest downstream focused on the use of ceramide transport protein (CERT, also known as Goodpasture antigen-binding protein) overexpression. CERT is a cytosolic protein essential for the non-vesicular delivery of ceramide from its production site at the ER to Golgi membranes, where conversion to sphingomyelin (SM) takes place (Hanada et al., 2003). The overexpression of CERT has been shown to enhance the specific productivity of the non-glycosylated single-chain protein human serum albumin (HSA) under seed-stock culture and fed-batch production conditions. Also, the overexpression of CERT was shown to be effective in elevating specific

productivity of monoclonal antibodies by around 30% for medium (10-30 pg/(c*d)) and high-producing cell lines (>30 pg/(c*d)) (Florin et al.submitted).

Instead of overexpressing a gene with a distinct function such as chaperone activity or lipid transport, the overexpression of more globally acting genes such as transcription factors may lead to more consistent results in cell line engineering.

5.3 Physiological roles of XBP-1

XBP-1 is a transcription factor activated by splicing. During activation, XBP-1 mRNA is spliced by the endoribonuclease activity of the ER-membrane associated kinase inositol-requiring enzyme 1α (IRE1α). IRE1 removes a 26 nucleotide intron from the XBP-1 mRNA, resulting in the synthesis of a potent transcription factor (Calfon et al., 2002; Lee et al., 2002; Yoshida et al., 2001) regulating genes involved in maintaining ER homeostasis and expansion (Lee et al., 2003a; Yoshida et al., 2003). The resulting spliced form of the protein (XBP-1(s)) translocates to the nucleus and activates the transcription of its downstream targets by binding and activating the so-called ER stress responsive elements (ERSE). The ERSE element is located within the promotors of a wide spectrum of secretory pathway genes, resulting in (i) a physical expansion of the ER, (ii) increased mitochondrial mass and function, (iii) larger cell size and (iv) enhanced total protein synthesis (Shaffer et al., 2004).

With these functions, XBP-1 is one of the master-regulators in differentiation of plasma cells, a specialized cell type optimized for high-level production and secretion of antibodies (Iwakoshi et al., 2003). Furthermore, XBP-1 not only regulates plasma cell differentiation, a terminal differentiation program with a cellular lifespan of days to a few weeks (Manz and Radbruch, 2002), but also plays an important role in the unfolded protein response (UPR) of mammalian cells (Brewer and Hendershot, 2005). The UPR represents a complex signal transduction network activated by the accumulation of misfolded proteins in the endoplasmic

reticulum. The UPR coordinates adaptive responses to this stress situation, including induction of ER resident molecular chaperone and protein foldase expression to increase the protein folding capacity of the ER, induction of phospholipid synthesis, attenuation of general translation, and upregulation of ER-associated degradation to decrease the unfolded protein load of the ER. Upon severe or prolonged ER stress, the UPR ultimately induces apoptotic cell death (Groenendyk and Michalak, 2005; Kim et al., 2006).

Due to its roles in expanding the secretory capacity of cells, XBP-1 appears to be an interesting target gene for improving the specific productivity of mammalian producer cell lines. The aim of the present work was to evaluate and characterize this novel engineering approach under industrially relevant settings. These include the use of suspension cells growing in chemically defined media as well as the characterization of the long-term stability of transgene expression.

5.4 Proteomic changes in the process culture fluid

In addition to the optimal producer cell line, process monitoring and control during cell culture are other key factors in the manufacture of biopharmaceuticals. After the selection of the stable, high-producing cell clone, the cell culture parameters need to be optimized to establish a robust high-yield process based on this cell line. Nearly all bioreactors used for commercial production are equipped with monitoring and control systems for temperature, pH and dissolved oxygen (DO). New probes and techniques are being constantly developed to measure various culture parameters such as cell number, cell viability and nutrient concentrations (Jain and Kumar, 2008). However, the information encoded in the proteomic changes of the supernatant of production processes has so far not been analyzed and employed for use in process monitoring and control. During a production process, the cell - as factory for the pharmaceutical product - actively secretes proteins in addition to the therapeutic. The content of this protein mixture and the kinetics of its composition during cell culture are driven by complex regulation networks inside the cell and depend on the culture conditions. Therefore, developing a methodology to monitor and analyze the cell culture fluid proteome should provide access to a completely new class of monitoring data and process control concepts. A typically fed-batch production process is divided into different phases: (i) the exponential growth phase, where cell mass accumulates due to cell division; (ii) the stationary phase, where cell doubling ceases and no further biomass is produced; (iii) the decline or death phase, when cell viability drops and the number of viable cells per culture volume decreases. Knowing exactly the onset of these process phases provides an opportunity for process optimization, e.g. the transfer times during scale-up of seed-train cultures (Sitton and Srienc, 2008). Also, identifying marker proteins that indicate a phase transition would open up the possibility of monitoring these proteins for, e.g. batch-to-batch comparison, proving comparability to the authorities. Furthermore, based on the profiles of such marker

proteins, feeding strategies or times could be adopted during process development with the aim of prolonging the growth phase and increasing peak cell density and consequently the process yield through higher overall integrated viable cell number. By contrast, recent approaches focus on the analysis of the intracellular proteome. Also, changes in the proteome of cells grown under different process conditions have been analyzed (reviewed in (O'Callaghan and James, 2008)). Since such an analysis of the cellular proteome is labor- and time-intensive, its use for process monitoring and control is limited. Instead, a strategic approach might be for marker proteins in the cell culture fluid identified by a proteomic survey to be quickly and easily monitored by, e.g. antibody microarrays, realizing an at-line rather than an off-line control element. The use of such protein chips would dramatically cut the time from sampling to the result compared with conventional proteome techniques, thus providing direct process control.

The best established technique for the investigation of the total protein composition of a sample is two-dimensional gel electrophoresis (2D-GE). Proteins are first separated in one dimension according to their charge (pI) by isoelectric focusing (IEF) and subsequently by their molecular weight using sodium dodecylsulfate polyacrylamide gel electrophoresis (SDS-PAGE) in the second dimension. Prerequisites for the separation and comparison of complex protein mixtures by 2D-GE are high resolution and reproducibility. Separated protein samples can then be identified using peptide mass fingerprinting by different mass spectrometry techniques (Lahm and Langen, 2000). Comparison of different samples and gels is greatly enhanced by a modification of the original 2D-GE protocol. Using fluorescent dyes tagging multiple samples differently allows a direct comparison of two samples run on one gel (Unlu et al., 1997). This technique is called difference or differential gel electrophoresis (DIGE). Serveral gels are compared by using a third sample per gel representing a mixture of all samples tagged uniquely by a third dye.

Since the first step of this novel approach is the global description of the cell culture fluid proteome during a production run, a method for the proteomic analysis of supernatant samples had to be developed. Therefore, the cell culture fluid containing low concentrations of proteins needed to be concentrated and separated by 2D-DIGE methods. Subsequently, proteins with different abundance in the various process phases had to be identified by mass spectrometry. The aim of this work was to develop such a method and test it for its applicability to process samples generated during production processes using suspension cells grown in chemically defined media.

6 RESULTS

6.1 An XBP-1-dependent bottleneck in the production of IgG subtype antibodies in chemically defined serum-free Chinese hamster ovary (CHO) fed-batch processes

This study, using CHO cells grown in suspension in chemically defined serum-free media assesses the possibility of improving fed-batch processes by stable expression of the active spliced form of human XBP-1. The transcription factor was identified as an engineering candidate due to its physiological functions. Its utility for improving biopharmaceutical production processes was tested in a setting closely reflecting industrial needs, namely the use in CHO cells grown in suspension in chemically defined serum-free media.

6.1.1 Functional expression of human XBP-1(s) in CHO-K1 cells

One of the morphological changes occurring during the differentiation of a B-cell to an antibody-secreting plasma cell is a massive enlargement of the ER. The activated spliced variant of the X-box-binding protein (XBP-1(s)) has been shown to be one of the keyregulators of this process (Reimold et al., 2001). To test whether human XBP-1(s) has similar functions in CHO cells as described during B-cell differentiation, the functional expression of XBP-1(s) transgene upon transient expression in CHO-K1 cells was initially assessed by analyzing the cellular ER content with the fluorescent dye ER-Tracker^{TM}. For this purpose, cells were trypsinated 48h after transfection with mock plasmids or pBIP-XBP-1 expressing XBP-1(s). Detached cells were stained with ER-Tracker^{TM} and the signal intensity was quantified by flow cytometry.

A slight increase in fluorescence intensity in cells treated only with transfection reagents (without DNA) as well as in cells transfected with mock plasmid containing a puromycin resistance cassette (Mock) was observed when compared with untransfected control cells (Figure 2).

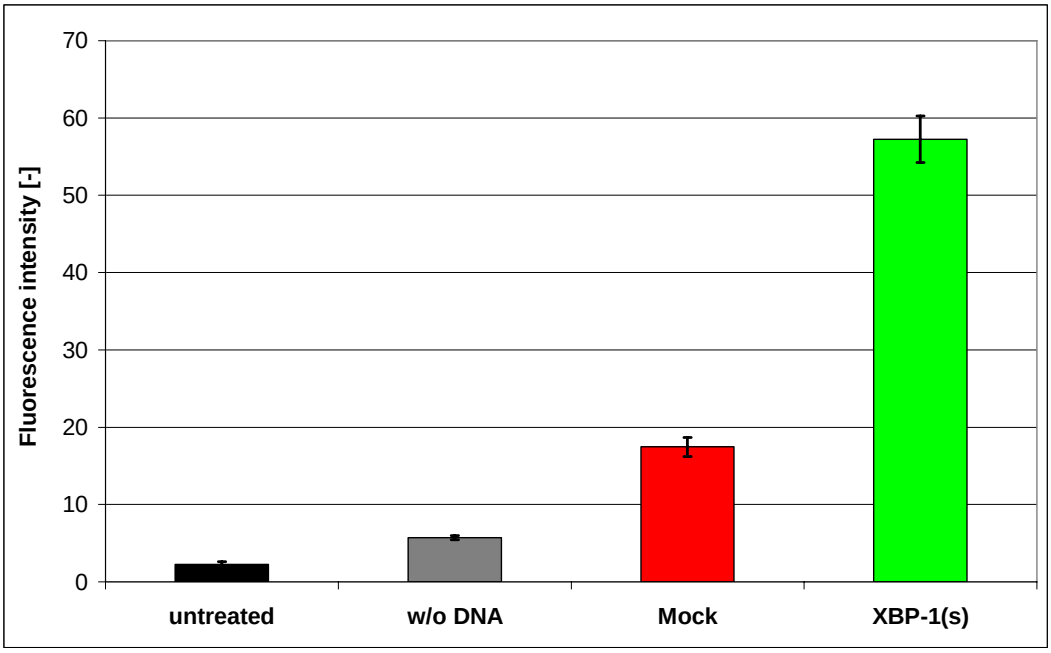

Figure 2: **Transient heterologous expression of human XBP-1(s) leads to an increase in ER content in CHO-K1 cells.**
Fluorescence intensity of ER-Tracker™ signal blotted for untreated, without DNA transfected, mock transfected and XBP-1(s) transfected cells.

Compared with the mock control, the fluorescence signal detected in XBP-1(s) transfected cells was elevated three-fold, indicating that heterologous introduction of human XBP-1(s) leads to a significant increase in ER content in CHO-K1 cells. These phenotypic changes confirmed the functional expression of human XBP-1(s) in hamster cells and suggested accompanying alterations in the protein folding and transport machinery similar to the changes observed during B-cell differentiation.

6.1.2 Generation of IgG producing CHO-DG44 cell lines stably expressing human XBP-1(s)

To analyze the potential benefit of XBP-1(s) overexpression in industrially relevant monoclonal antibody-producing cells, a CHO-DG44 cell line expressing a therapeutic IgG molecule (referred to herein as “parental”) was used. This cell line was selected because of its well characterized, proven stability in production. Furthermore, the cell line showed a “medium” specific productivity of 15 pg/(cell*d), providing the opportunity to detect positive as well as negative impacts of transgene expression, and is thus a suitable model cell line for studying the effects from transgene expression.

This CHO IgG cell line was transfected with a plasmid encoding XBP-1(s) under the control of a CMV promoter/enhancer combination or, as mock control, with the vector backbone alone. Stable cell pools containing the mock or the XBP-1(s) plasmid were generated by selection using puromycin and were subcloned by limited dilution. Clonally growing colonies were further propagated to give rise to cell lines. XBP-1(s) transgene expression was analyzed by Western blot using lysates from transient mock and XBP-1(s) transfections in CHO-K1 cells as negative and positive control, respectively. Nuclear extracts from 14 XBP-1 transfected monoclonal cell lines were analyzed but only four were found to be XBP-1(s) positive. Of these, the two monoclonal cell lines XBP1_E23 and XBP1_E27 showed the lowest and highest XBP-1(s) expression, respectively, (Figure 3) and were therefore selected for further analysis. As a stringent control of the significance of any effect of XBP-1(s) on productivity, five mock clones were also screened and the monoclonal cell line with the highest specific productivity was selected as reference for all further experiments (Mock_E5). All cell lines were cultivated according to a 2d-2d-3d rhythm that is typically used in industrial inoculum schemes for large-scale manufacturing. Cell culture supernatants were collected during cell passaging and analyzed for antibody concentration by IgG-ELISA over 5

to 11 passages. Viable cell counts for each passage were then used to calculate the average specific productivities of the cell lines.

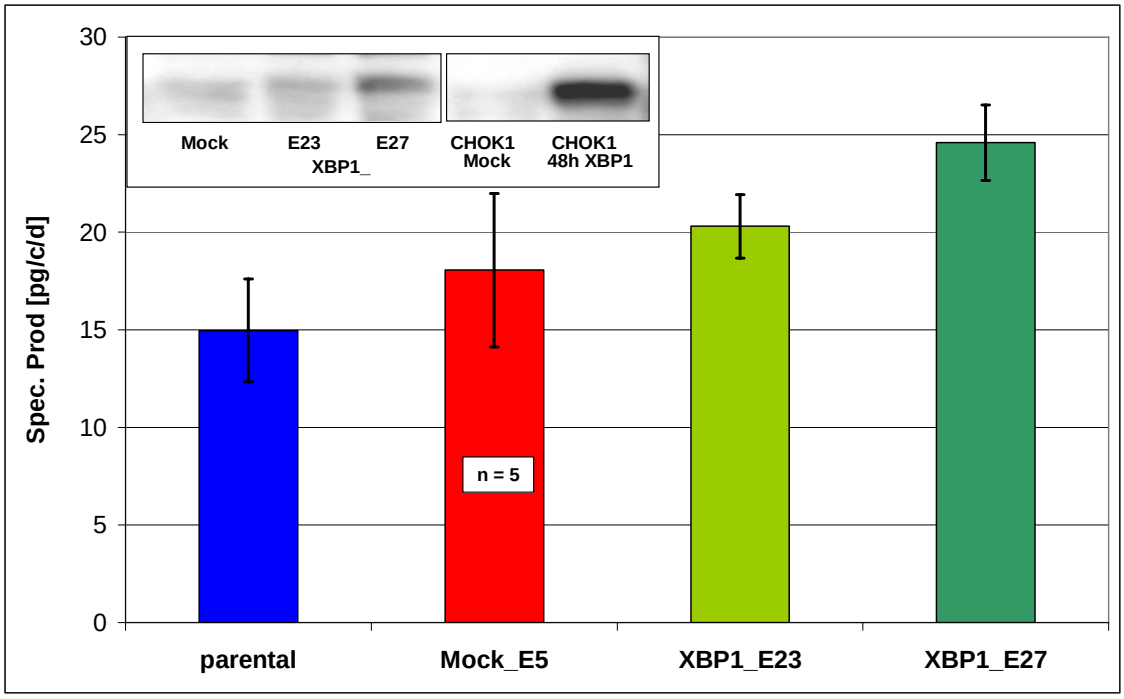

Figure 3: **Stable transfection of CHO-DG 44 IgG production cell lines with human XBP 1 enhances their specific IgG productivity in inoculum suspension cultures.**

The specific productivities of antibody-producing CHO-DG44 cells (parental), one mock clone (E5) and two monoclonal XBP-1(s)-expressing cell lines E_23 and E_27. The values are represented as mean values and error bars represent the standard deviations of the serial passages of n=11 or n=5 passages.

Insert: Western blot of nuclear extracts from the same clones to confirm XBP-1 expression. Lysates from transiently transfected cells served as negative (Mock) and positive control (48h XBP1).

As shown in Figure 3, the mock clone selected showed a 20% increase in specific productivity compared with the parental cell line when cultured in serial stock cultures. By comparison, the specific productivity of the cells expressing XBP-1(s) was enhanced by up to 60% when compared with the parental cell line. Notably, this effect was more pronounced in clone XBP-1_E27, which exhibited a higher XBP-1 expression, whereas it was less

significant in clone E23, which showed only a weak XBP-1 signal in the Western blot. This indicates a positive correlation between transgene expression and specific productivity.

6.1.3 Fed-batch production of an IgG subtype antibody from XBP-1(s) expressing CHO cells grown in chemically defined serum-free media

To test whether the increased specific productivity obtained during serial cultivation also translated into higher antibody yield in a production process, the monoclonal cell lines described (parental, mock_E5, XBP1_E23 and XBP1_E27) were analyzed in a scale-down screening fed-batch process format. The shake flask screening model has been shown to be predictive for the performance of cell lines in controlled bioreactors (Liu and Hong, 2001). Shake flasks were inoculated with 0.25 $x10^6$ cells/mL and cultivated for 10 days. Feed solution was added daily at a fixed volume proportion. The pH was measured daily and adjusted to pH 7.0 by adding carbonate buffer to closely simulate controlled bioreactor conditions.

As seen in Figure 4 A, parental and mock cell lines showed an almost identical growth profile. Peak cell densities reached were approximately $13x10^6$ viable cells/mL for both cell lines. The XBP-1(s)-expressing cell lines showed a slightly different growth profile with maximum viable cell densities of about $11x10^6$ viable cells/mL. Overall, the introduction of XBP-1(s) into an IgG-producing CHO cell line led to a comparable growth profile when compared with parental and mock transfected cell lines but notably to a 15% lower peak cell density in the fed-batch format described.

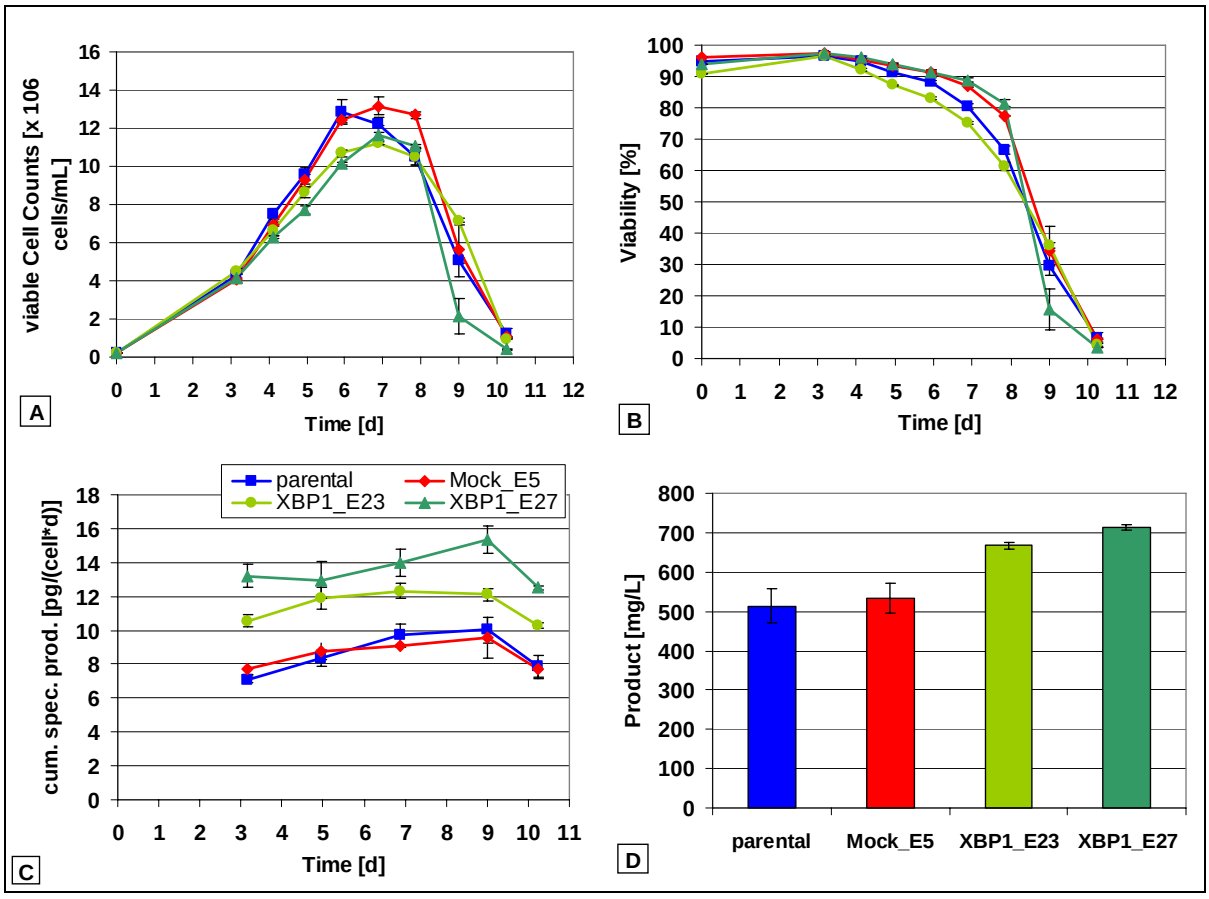

Figure 4: Heterologous expression of h-XBP-1 in CHO cells can lead to higher antibody (IgG) yield in chemically defined serum-free fed-batch processes.

A fed-batch was performed in shake flasks (n=3). Viable cell count (A) and viability (B) were assessed by the CEDEX system. On the harvest day, the product concentration was determined by ELISA (D). The specific productivity (C) was calculated as product concentration divided by IVC (integral of viable cells). Error bars represent the standard deviation.

A comparison of viability profiles revealed similar patterns for the four cell lines compared, with highest differences on d8 showing 60% and 80% for XBP1_E23 and XBP1_E27, respectively. Notably, clone XBP1_E27 exhibited the highest drop in viability between d8 and d9 of culture, declining from 80% to 15%. When the specific productivities (Qp) during fed-batch cultivation were compared, there was no significant difference between the parental and mock cell lines with an average Qp of 9 pg/(cell*d) (Figure 4 C). By contrast, both XBP-1(s)-expressing cell lines showed significantly increased specific productivities with

clone XBP1_E27 (55% increased) again being superior to XBP1_E23 (33% increased). When final IgG yield was compared (Figure 4 D), the elevated specific productivities transmitted into higher final harvest concentrations for the cells engineered with XBP-1(s). Parental and mock cell lines reached a final yield of 520 mg/L on average compared with a 29% increase for clone XBP1_E23 and 38% more product by XBP1_E27. The overall increase in final product did not match the level of increase observed in specific productivity. This fact was a consequence of lower peak cell densities. The difference in Qp between serial stock cultivation (Figure 3) and fed-batch performance (Figure 4 C) was frequently observed during the development of production cell lines and is accompanied by an increase in growth rate in the production medium.

In conclusion, the productivity as well as the final yield of XBP-1(s) engineered cell lines outperformed the parental and mock transfected control cell lines. In percent, the increase in final titer was lower than the enhancement in specific productivity due to lower cell growth in the fed-batch process.

6.1.4 Purification and physicochemical analysis of an IgG antibody secreted from XBP-1(s) expressing CHO cells grown in a chemically defined serum-free fed-batch format

Next, the possible impact of an engineered post-translational cellular machinery on the quality of a secreted therapeutic protein product was assessed. To this end, the initial capture step that is generally used at the beginning of most commercial antibody purification processes was run. Cell culture fluid was separated from the cells by centrifugation and the product was purified by affinity chromatography using protein A. The samples were then subjected to SDS-PAGE and IEF analysis.

Figure 5 depicts the purified IgG molecules secreted from the different CHO production cell lines separated according to either molecule size (SDS-PAGE) or charge (IEF). As expected for an IgG product, a main band of about 150 kD was seen in all samples on a non-reducing SDS-PAGE.

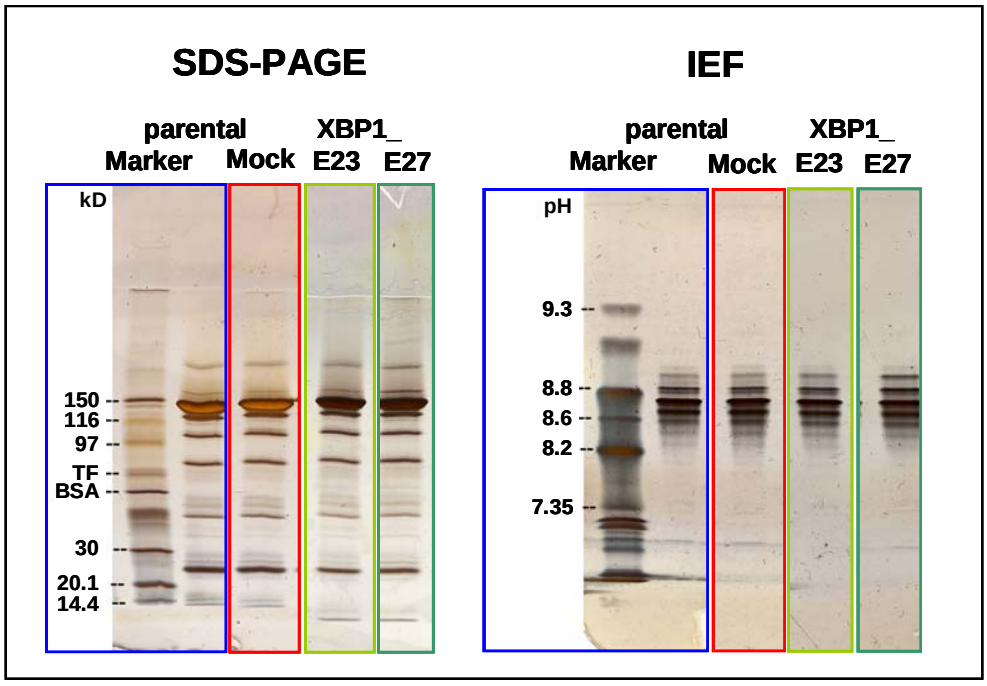

Figure 5: Physico-chemical properties of IgG molecules purified from the supernatants of XBP-1 CHO cultures analyzed by SDS-PAGE and IEF

After ProtA purification the secreted mAb product was separated by size on a 4-15% SDS-PAGE gel and for charge on a Phast Dry IEF gel. Protein was visualized by silver staining. For simplification only one of n=3 samples is shown.

The IgG product secreted from parental, mock and XBP-1(s) engineered cells was comparable with regard to the protein band intensities as well as the band pattern (Figure 5). On IEF gels, the band pattern centered around a pI of 8.7. A very similar pattern was seen for a standard sample consisting of purified commercial bulk product of the same therapeutic antibody. Furthermore, the product was analyzed for aggregate formation using size exclusion

chromatography and showed a monomer content of more than 99% in all samples (data not shown).

In summary, protein-A purified IgG material produced from the different cell lines was comparable and within the range of typical batch-to-batch variations with regard to size, charge distribution and aggregate formation as shown by the methodologies described.

6.1.5 Carbohydrate mapping of IgG molecules purified from the supernatants of XBP-1(s) CHO fed-batch cultures

As XBP-1(s) engineering of CHO cells leads to an enlargement of the endoplasmic reticulum and the function of this organelle is crucial for the correct N-glycosylation of secreted proteins, an important question was whether this engineering step influenced the carbohydrate structures of the antibody produced in XBP-1(s) expressing cell lines. Glycan distribution was analyzed by a quality control laboratory.

Protein-A purified IgG products secreted by the different cell lines in the fed-batch cultures described were analyzed by carbohydrate mapping. Affinity purified product samples were digested by PNGase-F to separate the carbohydrate structures from the protein backbone.

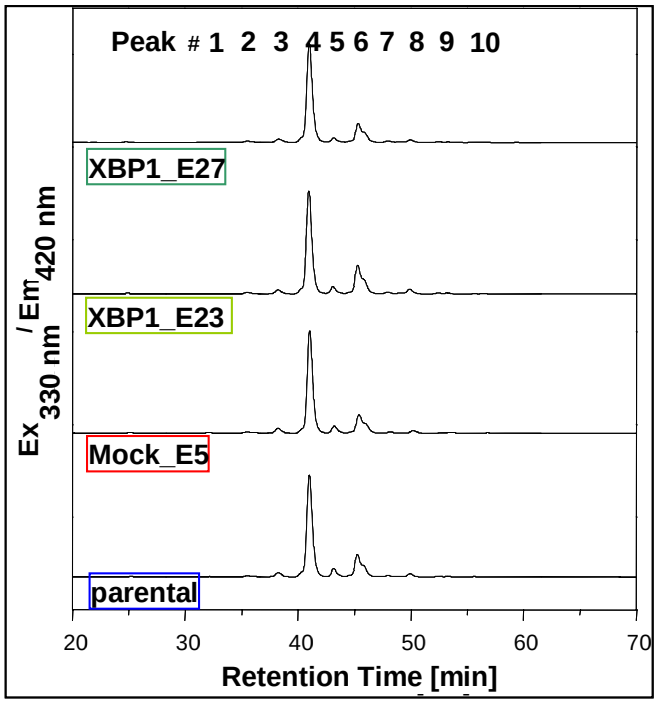

Figure 6: Carbohydrate mapping of IgG molecules purified from the supernatants of XBP-1(s) CHO cultures

HPLC retention profiles of PNGase-F digested IgG produced in XBP-1(s) expressing cell lines E23, E27, mock clone E5 and the parental cell line.

After HPLC separation of the glycan structures, the profiles were compared and the peak areas were quantitatively analyzed.

As shown in Figure 6, the glycan-specific peak profile of the respective samples was highly similar between the materials produced by the different cell lines. No absent or additional peaks were detected and the peak area distribution was comparable.

Table 1: Quantification of relative peak area

The peak area was calculated in percent of total area using the HPLC-analysis software. The mean peak area and the standard error are given for n=3 samples.

Peak No.:	**1**	**2**	**3**	**4**	**5**	**6**	**7**	**8**	**9**	**10**
parental	**0.2** ± 0.02	**0.9** ± 0.01	**3.3** ± 0.39	**65.5** ± 0.26	**5.3** ± 0.06	**20.1** ± 0.4	**1.3** ± 0.32	**2.3** ± 0.23	**0.8** ± 0.1	**0.4** ± 0.01
Mock	**0.3** ± 0.01	**0.7** ± 0.07	**3.6** ± 0.07	**67.3** ± 0.30	**4.9** ± 0.17	**18.6** ± 0.26	**1.4** ± 0.08	**1.9** ± 0.06	**0.9** ± 0.04	**0.3** ± 0.01
XBP1_E23	**0.0** ± 0.00	**0.7** ± 0.08	**2.4** ± 0.06	**62.0** ± 0.08	**4.4** ± 0.05	**24.5** ± 0.12	**1.0** ± 0.03	**3.4** ± 0.05	**1.1** ± 0.01	**0.5** ± 0.03
XBP1_E27	**0.0** ± 0.00	**0.7** ± 0.15	**2.6** ± 0.13	**70.2** ± 0.14	**3.2** ± 0.11	**19.1** ± 0.11	**1.1** ± 0.12	**2.1** ± 0.13	**0.8** ± 0.02	**0.3** ± 0.01

Furthermore, peak quantification indicated that the microheterogeneity caused by IgG glycosylation variants was within normal batch-to-batch variation across all materials analyzed (Table 1).

It can therefore be concluded that ER engineering by introduction of heterologous XBP-1(s) did not alter the physicochemical properties of a secreted therapeutic IgG product produced from CHO cells in serum-free chemically defined fed-batch cultures.

6.2 Impact of overexpression of XBP-1(s) in CHO cells

The stability of transgene expression as well as a stable antibody productivity is important for the regulatory approval of any production cell line and was assessed in long-term seed-stock culture to further characterize the engineered cell lines.

6.2.1 Genotypic and phenotypic stability of XBP-1(s) expression in CHO cells

To investigate the stability of heterologous XBP-1(s) expression in the stable CHO cell lines XBP1_E23 and XBP1_E27 for both cell lines, a cell bank was generated in passage 8 after the first cell expansion from 96-well plates. The cells were kept in a long-term seed-stock culture. At the outset, in passage 10 and after additional 25 passages the abundance of XBP-1(s) mRNA was quantitatively analyzed by real-time PCR. To normalize for possible RNA concentration differences in the samples, the beta tubulin mRNA levels were used as normalization parameter.

The qPCR in Figure 7 confirmed the Western blot result of Figure 3 with a higher XBP-1 mRNA level in clone XBP1_E27 compared with clone XBP1_E23. For both clonal cell lines, mRNA level was higher in early passages than in the passage examined later. For clone XBP1_E27 the absolute drop in XBP-1 mRNA level was highest within the data set. In passage 35 the mRNA level of clone XBP1_E27 was equal to the mRNA level of clone XBP1_E23 in early passage. Overall, comparing the percental decrease, XBP-1 mRNA level dropped for both clones over 25 passages to about 35% of their respective starting value.

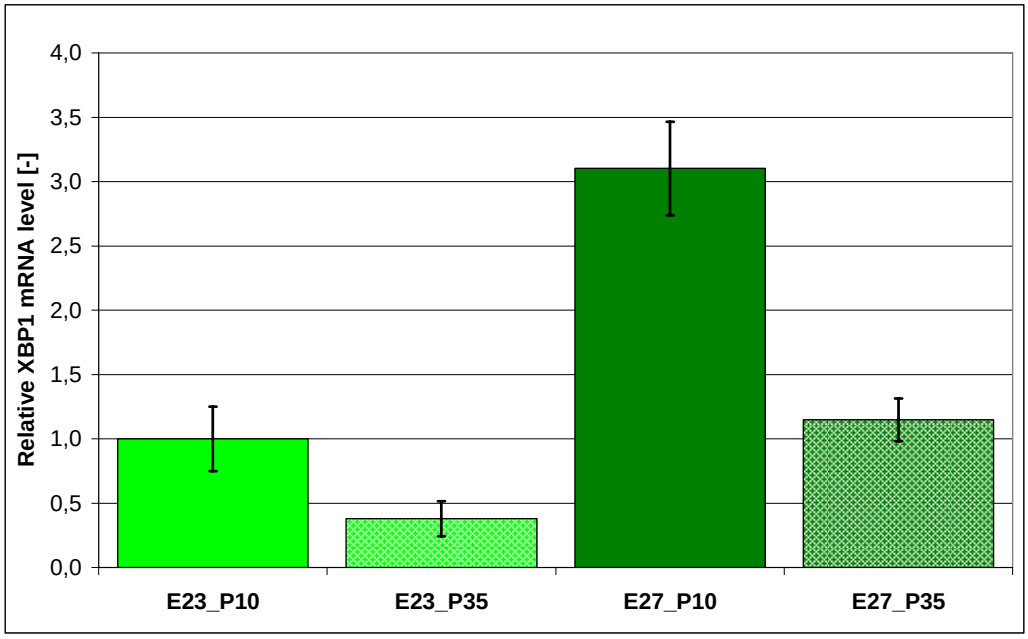

Figure 7: Quantitative analysis showed a decrease of XBP-1(s) mRNA during long-term cultivation.

The two stable XBP-1(s) expressing cell lines E23 and E27 were cultivated for 35 passages and XBP-1 mRNA levels were measured in an early (P10, solid bars) and in a later passage (P35, structured bars). The expression level was normalized to the beta tubulin level of the same sample and subsequently to the level of E23 in early passage 10. Error bars represent the standard deviation of triplicate PCR samples from one mRNA preparation.

To test the impact of this loss in heterologous mRNA expression, a fed-batch process was run with cells of different ages. The specific antibody production rate (Qp) was determined at four timepoints during the 10-day process when product titer was measured by ELISA (Figure 8). To calculate Qp, the product concentration was divided by the integral of viable cells. Again, the mean specific productivity calculated for the fed-batch run decreased with culture age. For clone XBP1_E23 Qp decreased from about 17 pg/(cell*d) to about 14 pg/(cell*d) without statistical significance. By contrast, for clone XBP1_E27 the loss in specific productivity is higher and statistically significant. Specific productivity was also determined in serial stock cultivation. However, over 25 passages no significant drop in specific productivity was observed (data not shown).

In summary, both monoclonal cell lines that were engineered by heterologous XBP-1(s) expression to secrete more antibody product showed a phenotype that was not stable over prolonged periods of time in continuous seed-stock culture. These data indicate a potential hurdle for using XBP-1 engineered host cells for manufacturing.

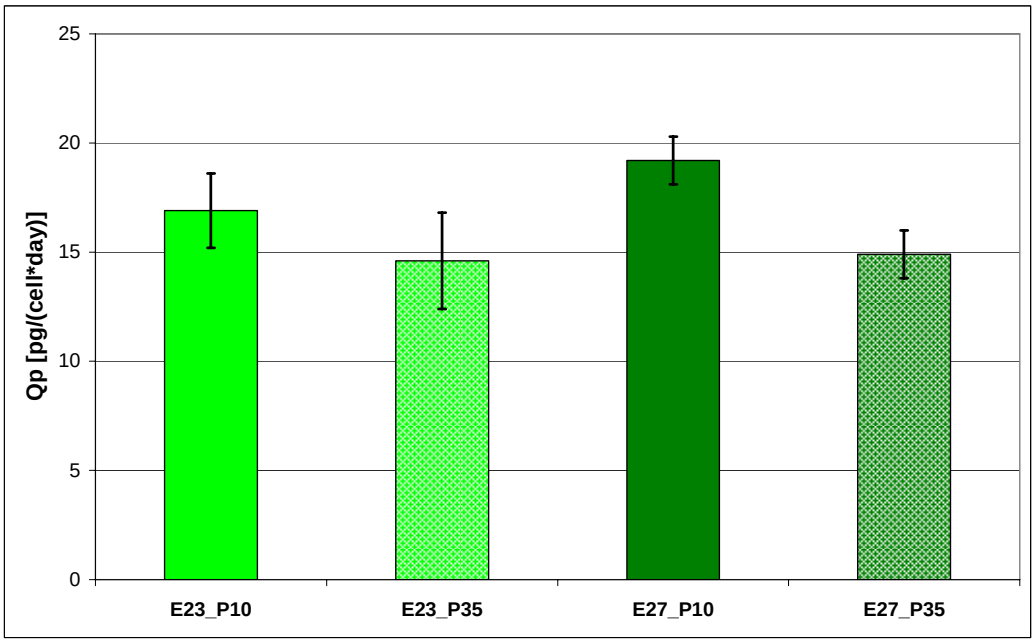

Figure 8: The specific antibody production per cell decreased with culture age for clone XBP1_E27.

Clonal cell lines E23 and E27 were cultivated in a fed-batch process format for 10 days and the specific antibody production rate was calculated for four timepoints during the process when titer was determined by ELISA. The mean specific productivity of the four measurements represented, as well as the standard deviation.

6.2.2 Colony formation assay in CHO-K1 cell line expressing XBP-1(s)

Instability of transgene expression can be a result of different cellular mechanisms such as DNA methylation or overgrowing of cells with low transgene expression. To understand the underlying mechanism of the instability observed it was investigated whether XBP-1(s) expression exerts a negative impact on growth or survival of CHO cells.

To assess a possible negative impact of human XBP-1(s) expression, a colony formation assay was run using the adherently growing CHO-K1 cell line as a model system. In this assay the overall survival of cells is affected by transfection, stable integration of the plasmid DNA, cell death due to transgene expression, alteration of attachment characteristics of the cell, resistance to selective pressure and proliferation capability. The colony formation assay integrates all effects by quantifying the number of colonies finally formed by surviving cells. The adherent cell system was chosen for its highly reproducible transfection rate of 70% (compared with 20% for suspension CHO-DG44 cells) by lipid mediated DNA transfer. Transfection efficiency was determined by transfection of plasmids encoding a fluorescent protein.

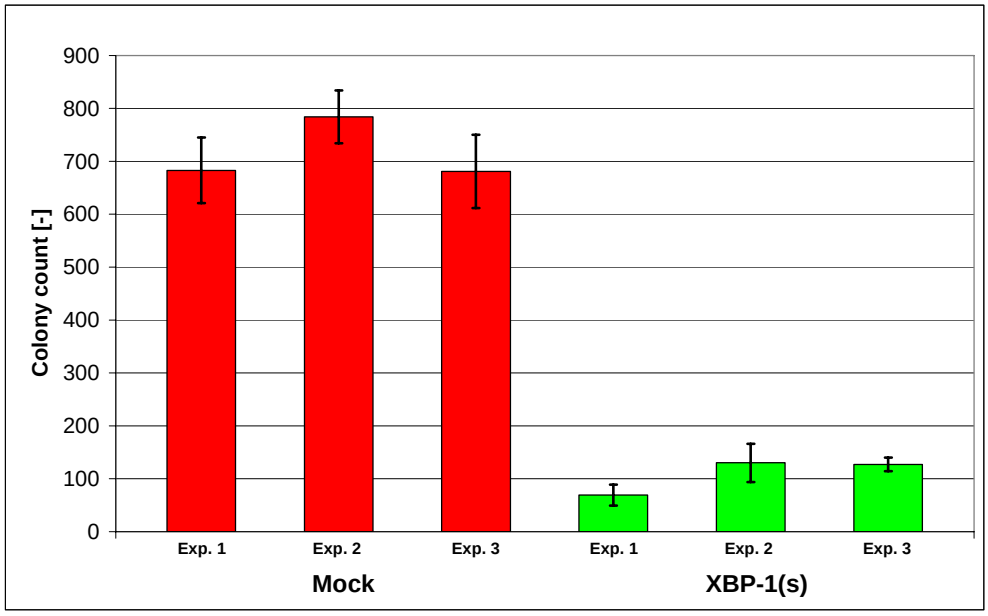

Figure 9: The expression of XBP-1(s) results in a survival disadvantage in CHO-K1 cells.

The data represent the mean colony count per plate for three independent experiments. Error bars represent the standard deviation of triplicate samples.

CHO-K1 cells were transfected either with a mock control plasmid or the same amount XBP-1(s) plasmid. After 24 h the cells of one well of a 6-well plate were trypsinized and completely seeded in a Petridish to allow them to adhere and obtain a low cell density so that growing cells could form single colonies. Another 24 h later, the selection antibiotic puromycin was added to a concentration of 15 mg/L. The cells were cultivated under selective conditions where only cells with stable integrated plasmid DNA could grow to form colonies.

After 14 days in culture, cells were fixed and stained with Giemsa stain and colonies were counted for each experiment. Adherent, living cells were stained purple and colonies became visible to the naked eye when more than 6 to 8 cells were close to each other. The purple colonies were then counted.

For cells transfected with the human active spliced form of XBP-1, the mean colony count was 7 times lower compared with mock transfection (Figure 9). For the mock transfection, an average of 700 colonies/dish were counted compared with an average of 100 colonies/dish in XBP-1(s) transfected cells.

The data indicated that the survival of cells, as summarized in the CFA, was negatively impacted by the expression of XBP-1(s). This result implies that expression of heterologous XBP-1(s) in CHO cells negatively affected the first steps in cell line development possibly complicating the generation of a new host cell line based on this approach. This finding was in agreement with the observation made in chapter 6.1.2, where a low frequency of clones with high XBP-1(s) expression was noted. On the other hand, high expression of XBP-1(s) correlated with its beneficial effect on specific productivity, indicating a possible hurdle for the use of XBP-1(s) in cell line engineering.

6.2.3 Physiological roles of XBP-1(s) in mammalian cells

As described in the introduction, in the native cellular environment XBP-1 can have two main functions. As transcription factor it plays a major role in the cellular stress response to misfolded proteins, the so called unfolded protein response (UPR). The second physiological role of XBP-1 is during the late phases of the terminal differentiation program of B-cells to antibody secreting plasma cells. Both signalling cascades have features in common: an unresolved, persisting UPR leads to cell cycle arrest and finally apoptosis (Groenendyk and Michalak, 2005; Kim et al., 2006) and the maturation of a plasma cell is a terminal cell differentiation program leading to proliferation blockade with a life span of days to a few weeks (Manz and Radbruch, 2002).

6.2.4 Apoptosis induction in transiently transfected CHO-K1 cells expressing XBP-1(s)

The observation of reduced colony counts in CFA together with the observed difficulties in obtaining high XBP-1(s) expressing clones posed to the question whether there is a common mechanism explaining both phenomena. Induction of apoptosis upon high-level expression of this active transcription factor would explain less surviving cells in CFA and low abundance of clones expressing high levels of the transgene.

To analyze apoptosis induction associated with heterologous XBP-1(s) expression, CHO-K1 cells were transfected either with XBP-1(s) or mock plasmid and analyzed by Annexin V assay 48 h later. Transient transfection is the first step in any cell line generation. Furthermore, transgene levels are highest during this period, thus providing the opportunity to detect a possible apoptosis induction solely by the presence of high XBP-1(s) levels when compared with mock transfected cells. The results of three independent experiments are summarized in Figure 10. The apoptosis rate of mock transfected cells was set to 100% and

compared with apoptosis rates in XBP-1(s) transfected cells. On average, 25% more cells were Annexin V positive when transfected with XBP-1(s) compared with mock transfected cells.

These data indicate that heterologous XBP-1(s) expression could lead to apoptosis in CHO cells, complicating the use of XBP-1 as suitable transgene for a general improvement in biopharmaceutical processes.

6.3 Evaluation of a combinatorial engineering approach to overcome a survival disadvantage of XBP-1(s) expressing cells

To overcome the previously shown negative influence of XBP-1(s) on the survival of transgenic CHO cells, the strategy of a combinatorial approach was investigated. Due to its shown effect to induce apoptosis (Figure 10), the combination of the secretion-enhancing XBP-1(s) together with an anti-apoptotic protein was investigated. Although the apoptotic program is highly complex and the cellular events involve the activation of many signalling cascades, two main pathways predominate: the intrinsic mitochondrial-mediated pathway and the extrinsic cell surface-mediated death receptor pathway (Arden and Betenbaugh, 2004). In both pathways the death signal is transmitted by a set of cysteine proteases called caspases and this cascade is tightly regulated by the presence of anti-apoptotic proteins (Kaufmann and Fussenegger, 2004). As the exact mechanism of XBP-1(s) apoptosis induction is unknown, a suitable candidate for the combinatorial expression together with XBP-1(s) should inhibit apoptosis on several levels. Therefore, one promising engineering candidate was the caspase inhibitor X-linked inhibitor of apoptosis (XIAP) which inhibits caspases 3, 7 and 9 (Deveraux et al., 1998; Deveraux et al., 1997). Caspases 3 and 7 are executioner caspases, whereas caspase 9 is an initiator caspase. Furthermore, overexpression of XIAP in CHO and HEK293 cells has been shown to inhibit apoptosis after exposure to toxins such as etoposide or

cisplatin (Sauerwald et al., 2002). To test the effect of XIAP expression on the XBP-1(s) phenotypes described, both genes were coexpressed in CHO cells to monitor apoptosis and survival in transient transfections and colony formation assays.

6.3.1 Apoptosis analysis after transient expression of XBP-1(s) in CHO-K1 cells

To prove that a combination of XIAP and XBP-1(s) leads to less cell death, CHO-K1 cells were transfected with both expression plasmids and the percentage of early and late apoptotic cells was determined 48 h after transfection by Annexin V and PI counter staining. Only counterstaining enabled a distinction to be made between viable, early apoptotic, late apoptotic and necrotic cells, as in late apoptotic cells Annexin V binds to the phosphatidylserine residues on the inner plasma membrane. These data were compared with single plasmid experiments when either XIAP or XBP-1(s) or a mock plasmid were introduced into the same cells. For each transfection the same amount of total DNA was used by adding mock plasmid to the transfections where only one protein was to be tested. The experiment was repeated twice. In one of the three independent experiments, cells were washed 24 h after transfection and serum deprived by addition of serum-free growth media to test whether an apoptosis stimulus would influence the result. The data of the three experiments were summarized and the apoptosis rate of the mock control was set to 100%. The experimental transfections were plotted relative to the control in Figure 10.

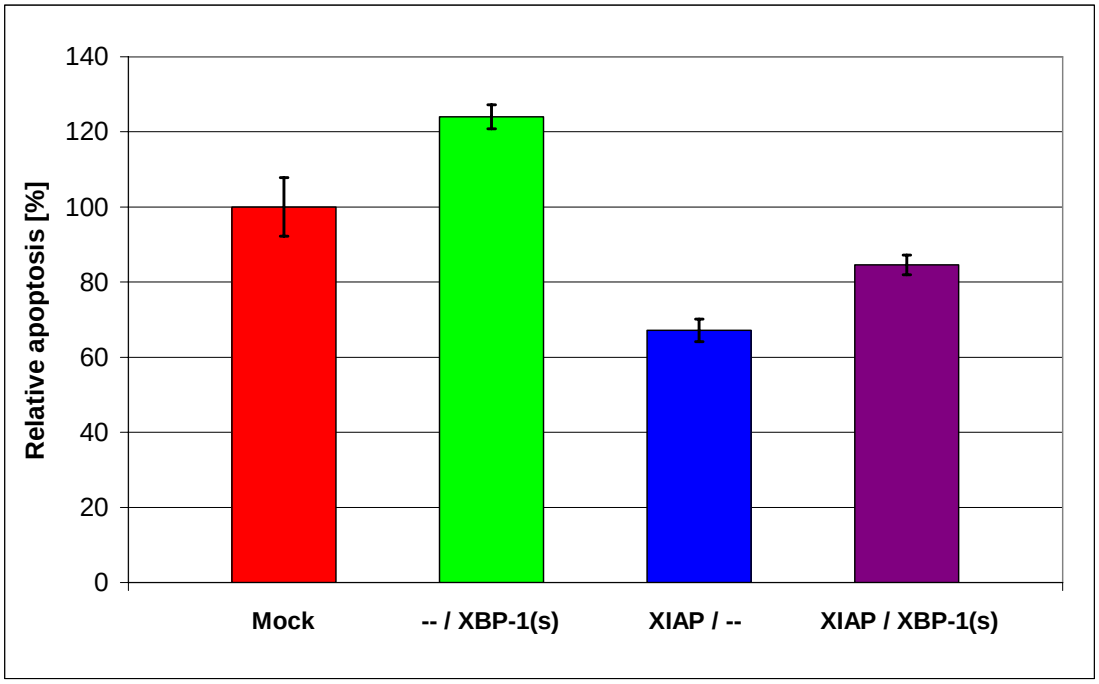

Figure 10: The combination of XBP-1(s) together with XIAP results in a lower apoptosis rate compared with mock and XBP-1(s) transfected cells after transient heterologous expression in CHO-K1 cells.

CHO-K1 cells were transfected either with the empty plasmid (mock), XBP-1(s), XIAP or both plasmids together. The data show the relative apoptosis rate (early plus late apoptosis) compared with mock 48 h after transfection as determined by annexin-V/PI staining. The data and error bars represent the mean of three independent experiments run in triplicate samples.

As seen in the previous set of experiments, transfecting XBP-1(s) into CHO-K1 cells led to 25% more apoptotic cells compared with the control, while transfecting XIAP resulted in a significantly smaller fraction of apoptotic cells (35% compared with the control and 50% compared with XBP-1(s) expressing cells). Interestingly, combining XIAP and XBP-1(s) showed 15% less apoptotic cells when compared with the control as well as 40% reduced apoptosis when compared with XBP-1(s). The data indicate the capability of XIAP to reduce apoptosis induction of human XBP-1(s) expression in CHO cells.

6.3.2 Colony formation assay in CHO-K1 cell line expressing XIAP and XBP-1(s)

As a next step, the combination of XIAP together with XBP-1(s) was tested in the colony formation assay to show if the lower apoptosis rate resulted in the formation of more colonies. As the output of a CFA is the sum of several effects from transient transgene expression to stable integration and cell growth characteristics, the results provide a deeper insight into the applicability of the approach with regard to the benefit of XIAP co-expression for cell line generation. To be able to select for both transgenes simultaneously and to avoid effects due to different death kinetics of different selection markers, bicistronic expression constructs using an internal ribosomal entry site (IRES) from ECMV virus were designed. The translation of both proteins of interest originates from the same mRNA template. All expression constructs were designed according to a common construction principle where the anti-apoptotic protein is expressed in the first cistron and the secretion-enhancing protein in the second. The expression of the transgenes was under the control of the CMV promoter/enhancer combination.

The colony formation assay was performed as described in chapter 6.2.2: however, to improve the resolution of individual colonies on the plate by lowering the total colony count, only $1x10^5$ cells of total cell count were used (instead of the total cells of one 6-well). The colony count was averaged and normalized to the mock control (Figure 11). Expression of XBP-1(s) consistently led to twice lower colony counts. The expression of XIAP led to higher colony numbers but exhibited a higher variation between two experiments. More consistently, higher colony numbers were found when both proteins were expressed indicating that XIAP could compensate the negative effect of XBP-1(s) on cell survival.

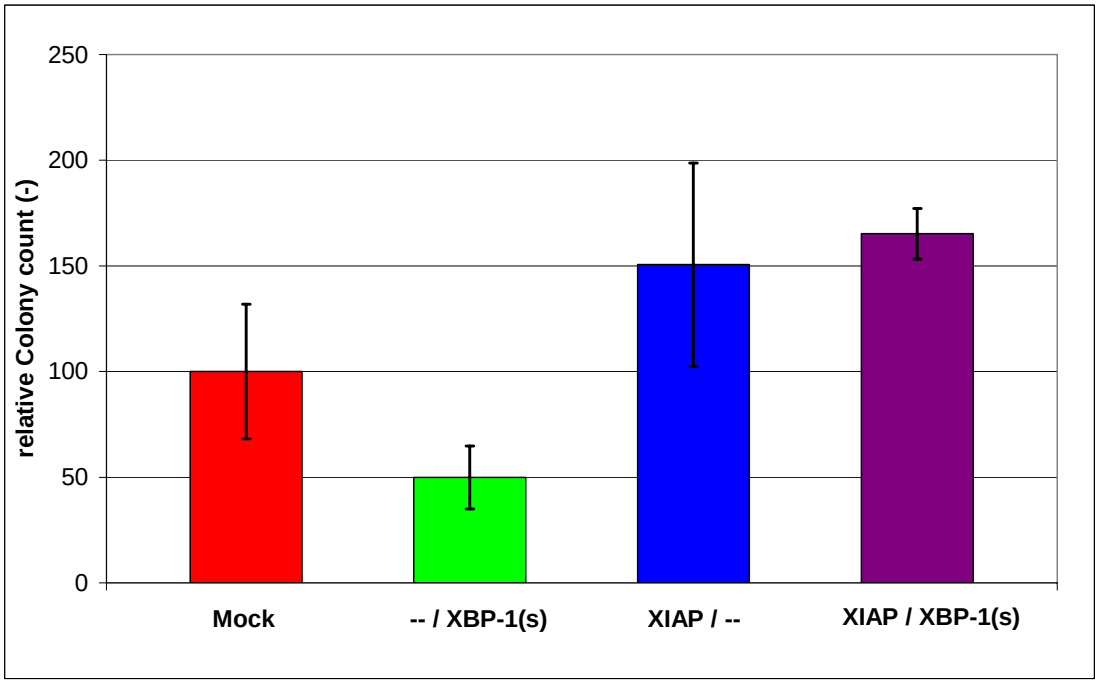

Figure 11: The combination of XBP1-(s) with XIAP leads to higher survival rates in CFA in CHO-K1 cells when compared with mock and XBP-1(s) transfected cells.

The data represent the mean colony count of two independent experiments with triplicate samples normalized to the mock control. The error bars represent the deviation of measurements.

These results are in agreement with the data obtained in the apoptosis assay and confirmed that XIAP could counteract negative effects of XBP-1(s) expression in CHO cells and even conferred a survival advantage when both proteins were expressed simultaneously. As the colony formation assay in CHO-K1 cells summarized transfection, attachment, plasmid integration, cell death and proliferation, the data open up the perspective of improved bioprocesses. All mentioned aspects of this assay except for attachment are important for the generation of an improved, engineered cell line.

6.3.3 XIAP and XBP-1(s) expression analysis in polyclonal IgG-producing cell lines

The next important question was to test this new two transgene approach under production-relevant conditions. As shown earlier in chapter 6.1.2, high XBP-1(s) levels are desirable for enhancing specific productivity. However, enhanced apoptosis levels as found in transient expression experiments impair the generation of cell lines expressing high XBP-1(s) levels. As the co-expression of XBP-1(s) together with XIAP led to a reduction in apoptotic cells and the formation of more colonies in the CFA, this approach was to be tested in antibody-producing suspension cells. To test if XIAP co-expression can lead to higher XBP-1(s) levels in antibody-producing cell lines, thus enhancing productivity beyond the single engineering approach, the same parental cell line expressing a human IgG antibody as used in the previous studies was transfected with the constructed bicistronic plasmids.

For each expression construct, three transfections were performed and cells selected for growth in 10 mg/L puromycin containing media. After two weeks, stably growing cell pools were expanded and cultivated in seed-stock cultures to determine the specific antibody productivity and their transgene expression by real-time PCR.

The XIAP mRNA expression was analyzed by qPCR and normalized to beta tubulin mRNA levels (Figure 12). Different expression levels were found for cell pools transfected ranging from 1- to 6-fold over beta tubulin levels. The XIAP expression level and range of variation was the same when cells expressing solely XIAP and cells expressing both engineering proteins were compared.

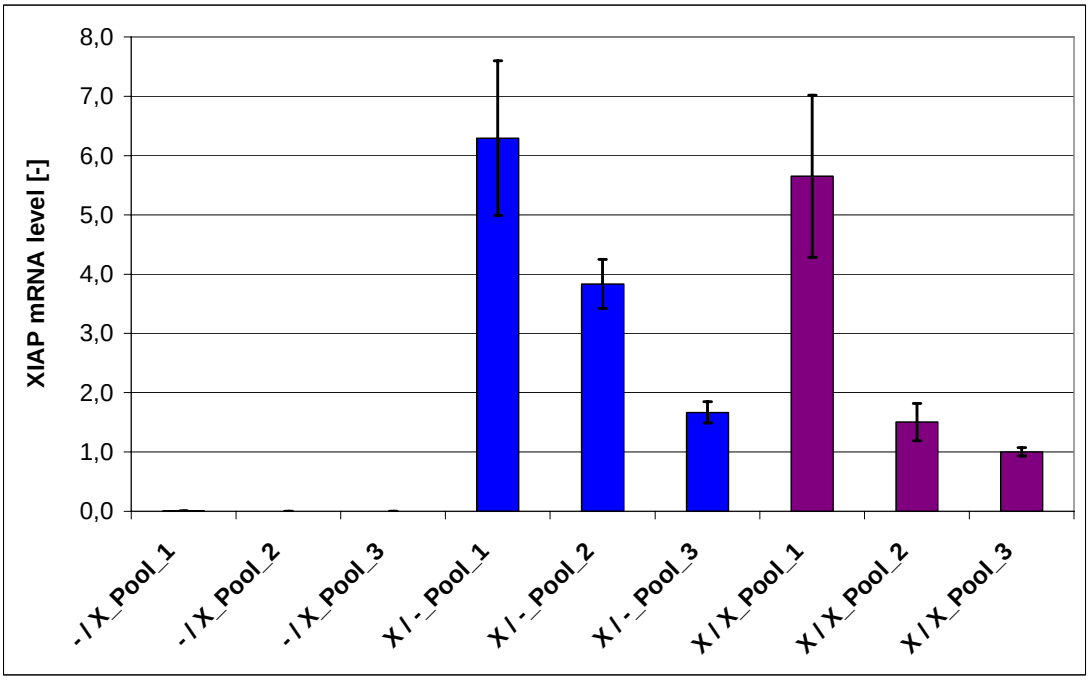

Figure 12: XIAP mRNA expression level in stable cell pools is comparable.

The XIAP mRNA abundance was measured by qPCR. Beta tubulin mRNA level was used for normalization. Solely XBP-1(s) expressing pools served as negative control. The analysis was run in triplicate samples from one mRNA preparation and error bars represent the standard deviation.

The mRNA expression analysis of XBP-1(s) by qPCR also showed variations in specific transcript level among the transgenic cell pools (Figure 13). For the bicistronic expression of both transgenes a similar profile was found for XIAP and for XBP-1(s), confirming the expression linked by an IRES element. Highest XBP-1(s) mRNA abundance was found in pool no. 1 expressing both trangenes with about a 4-fold increase over beta tubulin. The highest solely XBP-1(s) expressing pool showed a 2.5-fold increase over tubulin. However, the enhanced XBP-1(s) level in double engineered pools was not consistent, as the two remaining pools examined showed expression levels in the order of the solely XBP-1(s)-expressing pools. In the limited data set, the highest XBP-1(s)-expressing pool was indeed found in the two transgene expressing cells supporting the working hypothesis that XIAP co-expression allowed cells to survive high levels of XBP-1(s).

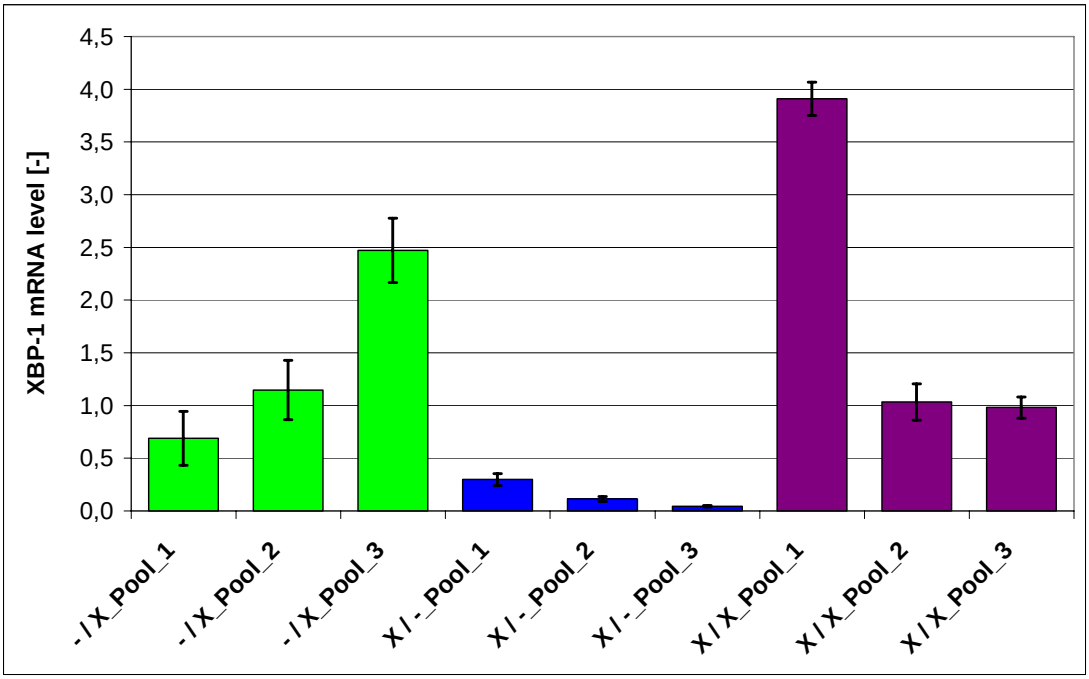

Figure 13: The XBP-1 mRNA expression level in stable pools was not increased by the co-expression of XIAP in general.

The XBP-1 mRNA abundance was measured by qPCR. Beta tubulin mRNA level was used for normalization. Solely XIAP-expressing pools served as negative control. The analysis was run in triplicate samples from one mRNA preparation, and error bars represent standard deviation.

6.3.4 Analysis of IgG productivity in seed-stock cultures of polyclonal cell lines expressing XIAP and XBP-1(s)

To determine whether the specific antibody production rate of the generated CHO cells was altered, cell pools were cultivated in seed-stock cultures. Cells were passaged at 2-2-3 day intervals and supernatant samples were analyzed for product concentration on three consecutive passages: the mean specific productivity was calculated (Figure 14). For mock transfected, XBP-1(s) and solely XIAP-expressing cell pools the specific productivity varied around 15 pg/(cell*d), the same productivity found for the parental cell line (compare Figure 3). Mock pool no. 3 and the solely XIAP-expressing pool no. 1 exhibited a reduced

productivity of 7 pg/(cell*d) and 9 pg/(cell*d), respectively. For two of the three cell pools expressing both transgenes, pool no. 1 and pool no. 2, the specific productivity was increased to 22 pg/(cell*d) and 18 pg/(cell*d), respectively. The third pool showed an insignificantly increased productivity of 17 pg/(cell*d). For polyclonal populations no increase in specific productivity was found for XBP-1(s)-expressing cells, whereas double engineered pools showed higher secretion rates.

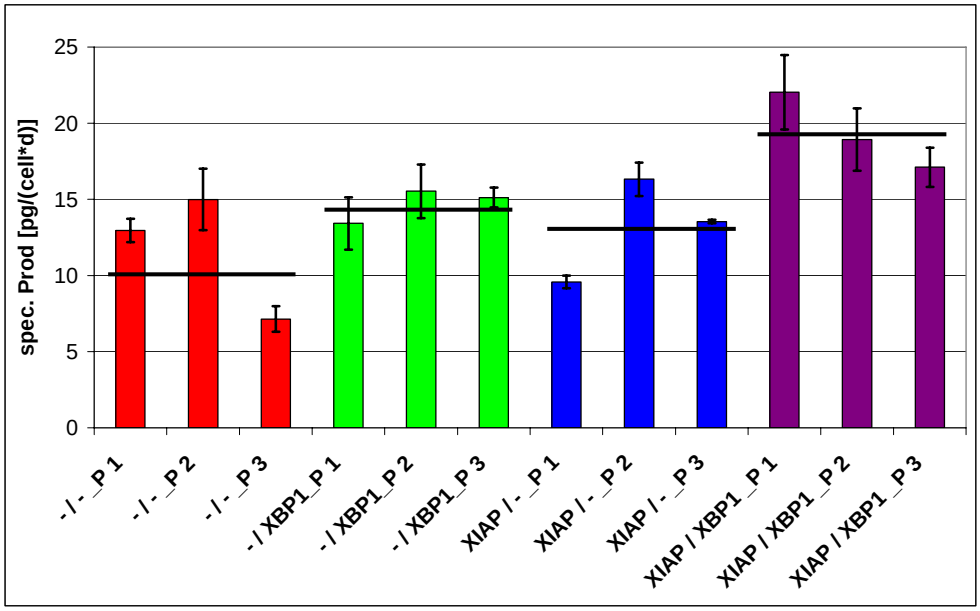

Figure 14: The specific antibody productivity of stable cell pools is enhanced in seed-stock cultures for two of three pools expressing both transgenes.

The cell culture supernatant was analyzed for antibody concentration over three passages in serial seed-stock culture. The error bars represent the standard deviation of the triplicate measurement. Horizontal bars represent the mean Qp of the three pools.

For solely XBP-1(s)-expressing cell pools no correlation was found between the specific antibody productivity and the transgene expression level as determined by qPCR. Also, no correlation between transgene expression and specific productivity was observed for the solely XIAP-expressing pools. By contrast, for the pools transfected with the plasmid

encoding both proteins, the specific productivity in seed-stock cultures correlated with XBP-1(s) mRNA abundance. Pool no. 1 with highest transgene expression showed the highest specific productivity. For pool no. 3 the contrary observation was made.

Even though XBP-1(s) expression was confirmed on the mRNA level for single and double engineering, only cell pools expressing both transgenes exhibited an enhanced Qp as determined in seed-stock cultures. In cell pools, the measured productivity is a mean value, resulting from different cellular production rates. As the productivity of monoclonal cell lines is expected to be higher than in parental pools, these results indicate the potential to select highest producing clones from double engineered cell pools, thus supporting the hypothesis that the combinatorial approach is beneficial. Nevertheless, the final conclusion can only be drawn on the clone level as all cells finally selected for production have to be of monoclonal origin.

6.3.5 Fed-batch production of an IgG antibody from cell pools expressing XIAP and XBP-1(s)

In a next step, the performance of the cell pools was tested in a fed-batch process as described in chapter 6.1.3. The growth profile showed a peak cell density of about 9×10^6cells/mL (Figure 15 A). The three mock pools showed the most divergent growth profiles, with an average peak cell density of 6×10^6cells/mL varying between 4×10^6cells/mL to 8×10^6cells/mL. Repetition of the experiment revealed the same growth characteristics (data not shown) proving that the observed growth profiles were significant. The viability chart in Figure 15 B shows a comparable profile. Surprisingly, no XIAP dependent viability extension for pools stably expressing the anti-apoptotic protein were observed. When the harvest titers where compared by ELISA, the mean of the three cell pools expressing both transgenes

yielded 600 mg/L on average (Figure 15 C). All pools expressing either XIAP or XBP-1(s) varied around a final titer of around 400 mg/L. The same ranking as for final titer was observed when the specific antibody productivity was compared.

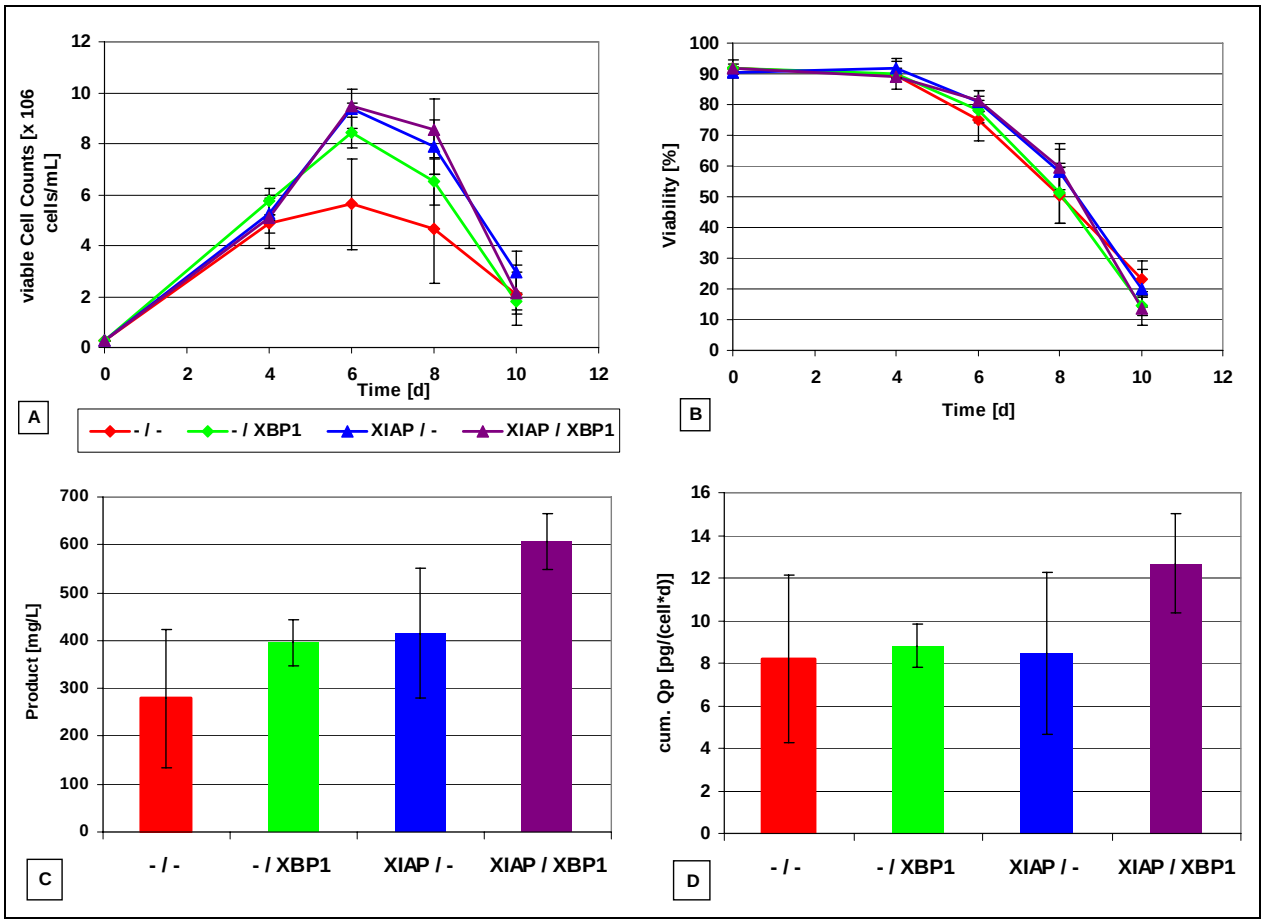

Figure 15: Bicistronic expression of h-XBP-1(s) in combination with h-XIAP in CHO cells led to higher antibody (IgG) yield in a chemically defined serum-free fed-batch process on the pool level.

A fed-batch experiment was performed in shake flasks (n=2). Viable cell count (A) and viability (B) were assessed by the CEDEX system. The product concentration was determined by ELISA (C) and shown for the harvest d10. The specific productivity (D) was calculated as product concentration divided by IVC (integral of viable cells). Error bars represent the standard deviation between the mean of the three pools.

In accordance with the observation made during serial stock cultivation, the bicistronic expression of XIAP and XBP-1(s) again led to highest final titers and specific productivities when compared with the XBP-1(s) transfected control pools.

All observations made on the pool level so far supported the idea of combinatorial engineering by combining secretion and anti-apoptosis engineering. Highest XBP-1(s) expression levels were found in one of the three two transgene expressing pools when compared with control XBP-1(s) transfections. When the specific productivities and harvest titers were compared for seed-stock cultivation and fed-batch conditions, the generated polyclonal cell populations expressing both transgenes showed the highest values. Therefore, the next step was the generation and evaluation of monoclonal cell lines.

6.3.6 Generation and selection of monoclonal cell lines expressing XIAP and XBP-1(s)

Two possibilities exist for generating monoclonal cell lines: limited dilution and single-cell deposition by flow cytometry (FC). Here, the single-cell deposition using FC was used. Exponentially growing polyclonal cells were prepared for single-cell cloning as described in chapter 8.5 and subjected to the cloning procedure. Three 96-well plates containing one living cell per well were prepared per cell pool and incubated under growth conditions. The irradiated, proliferation-inhibited feeder cells died as a result of the activity of the selection antibiotic contained in the media, whereas the deposited stably transfected cell grew and formed monoclonal colonies.

In Figure 16, the total number of positive wells from three 96-well plates per pool was compared. For mock transfected cells, 33 cell lines grew on average per pool, reflecting an overall cloning efficiency of 12% derived from 9x96 wells for this genotype. For XBP-1(s)-expressing cells, 16 clones were detected on average per pool, equating to 6% cloning efficiency. On average, 38 clones were found for the XIAP expressing pools. The cloning efficiency of 13% was the highest found in the experiment. Two of the cell pools expressing

both transgenes gave rise to 24 clones on average (8% cloning efficiency) but from pool no. 3 only two clonal cell lines grew. The result of pool no. 3 was probably an outlier and was not used for the calculation.

When compared with the CFA data obtained in CHO-K1 cells (Figure 11), mock transfected and XBP-1(s)-expressing cells show the same pattern with about 50% colony count for the transcription factor expressing cells. XIAP expression did not lead to elevated clone numbers to the same extent as in CFA experiments. Also, the clone numbers did not correlate with XIAP expression level as analyzed in chapter 6.3.3. For two of the double engineered pools an increase in clone numbers was shown when compared with solely XBP-1(s)-expressing pools, as expected from CFA data. But pool no. 3 showed a lower clone number than expected from assay variation. Overall, during the cloning procedure the same pattern of clonal cell growth was found as observed during CFA experiments in CHO-K1 cells.

To select the highest mAb producing monoclonal cell lines, supernatant samples of 12 randomly selected clones per pool (= 36 clones per genotype) were collected on d11 and d13 of growth in 96-well plates after the cloning procedure. The samples were analyzed for antibody concentration by HTRF® assay as described in chapter 8.10. Additionally the plates were analyzed for colony size by the CloneSelect™ imager. Colony size as calculated by the imager software and antibody concentration data were used to calculate the specific antibody production rate. The top 6 clones were selected for each genotype according to specific productivity, expanded and further analyzed.

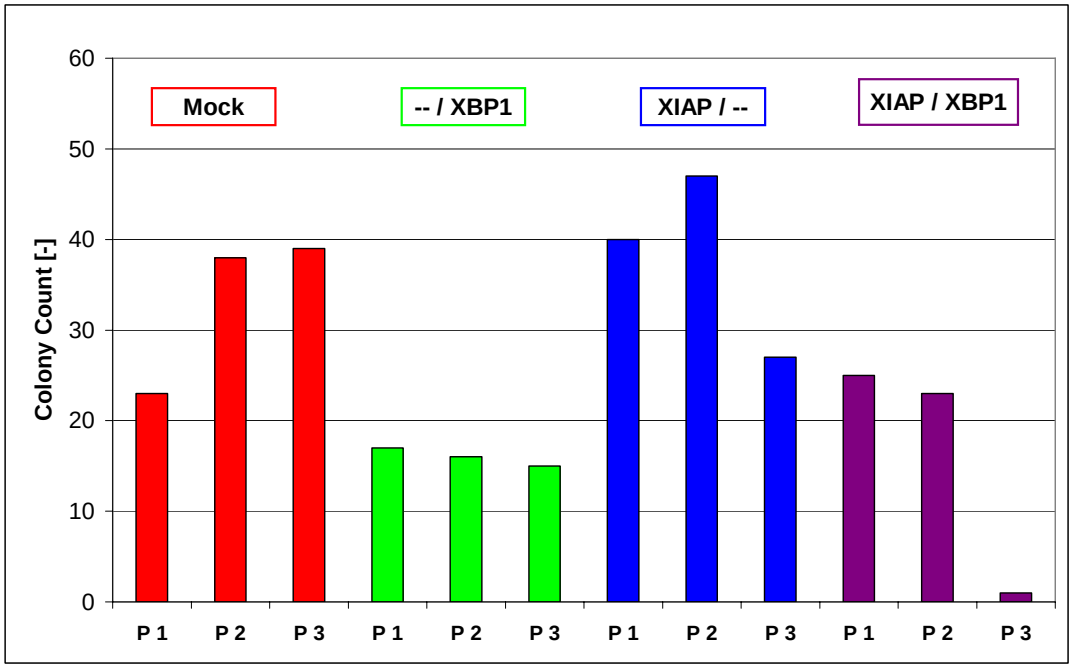

Figure 16: Cloning efficiency of stably transfected suspension DG44 cells in FACS-based single-cell cloning is comparable to the results of apoptosis induction in adherent CHO-K1 cells.

The values represent the total number of clonally growing cell lines per pool after single-cell cloning.

For mock transfected pools, the selection procedure led to clones equally distributed among the three cell pools analyzed (Table 2). Each pool gave rise to two clones. The same was found for XIAP transfected cell pools. Of pools expressing two transgenes, pool no. 1 showing the highest XBP-1(s) expression level, giving rise to 5 of the top 6 clones. The remaining clone was selected from pool no. 2. Unlike double engineered pools, XBP-1-Pool no. 3, exhibiting highest XBP-1(s) expression, did not lead to a clone in the top 6. Pool no. 1 gave rise to 4 and pool no. 2 gave rise to 2 selected clones.

Table 2: Number of clones selected per cell pool

Number of top 6 clones selected for highest Qp in 96-well plates originating from the stated cell pools and XBP-1(s) expression level of the parental pool relative to beta tubulin as measured by qPCR. Nd = not determined

	Mock **# clones/level**	**-- / XBP1** **# clones/level**	**XIAP / --** **# clones/level**	**XIAP / XBP1** **# clones/level**
Pool 1	2/nd	4/0.7	2/0.3	5/3.9
Pool 2	2/nd	2/1.1	2/0.1	1/1.0
Pool 3	2/nd	0/2.5	2/0.04	0/1.0

In line with the hypothesis and results that high XBP-1(s) expression led to a survival disadvantage, no clones originated from the pool with the highest solely XBP-1(s) expression level. On the other hand, co-expression of XIAP seemed to support the outgrowth of clonal cell lines during single cell deposition. The selection of 5 of the 6 top-producing clones from the double engineered pool with highest XBP-1(s) expression emphasized the combinatorial approach.

6.3.7 Expression analysis of monoclonal cell lines stably transfected with XIAP and XBP-1(s)

For the top 6 clones selected based on their productivity, the mRNA expression level for both transgenes was analyzed by qPCR.

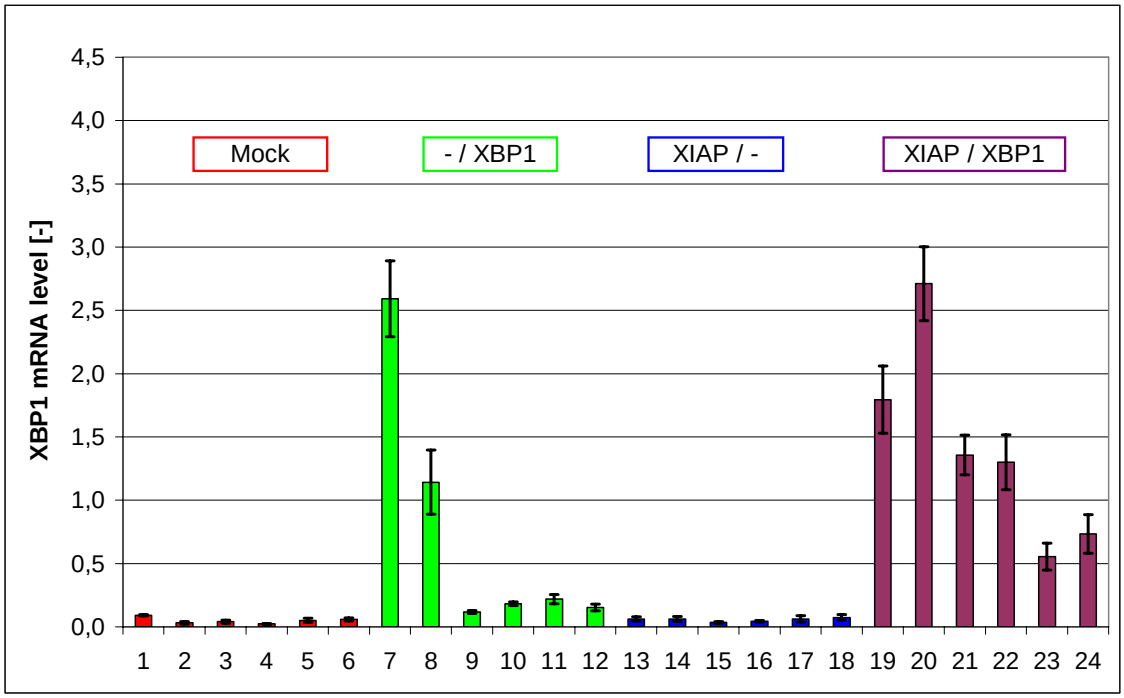

Figure 17: The XBP-1 mRNA expression level in stable clones is not increased compared with the pool level.

The XBP-1 mRNA abundance was measured by real-time PCR. The analysis was run in triplicate samples and error bars represent the standard deviation.

As described in chapter 6.3.3, the level of XBP-1(s) mRNA was determined for all of the 24 clones generated (Figure 17). As expected, mock transfected and XIAP expressing clones showed the lowest levels of XBP-1(s) expression, representing the method's background level. Primers for XBP-1(s) qPCR were designed to amplify the spliced and the unspliced mRNA differing by the 26 nucleotides which are physiologically cut out. To test whether endogenous, unspliced hamster mRNA was co-amplified, PCR products of clone 19 and 20 were digested with PstI and NcoI enzymes. The results confirmed that the PCR product originated from the spliced variant template (data not shown). For XBP-1(s) and clones expressing both transgenes, the mRNA level of XBP-1(s) varied from 0.25-fold to 2.5-fold over beta tubulin levels. Maximum XBP-1(s) mRNA levels were the same for single and double engineered cell lines. Nevertheless, clones expressing two transgenes showed, on

average, higher transgene levels compared with single engineered clones. For solely XBP-1(s) expressing cell lines, clone 7 showed the highest expression level, 2.5-fold over beta tubulin. The expression level of clones 9 to 12 was close to the background levels detected in mock transfected clones. Clone 20, expressing both transgenes, also showed a 2.5-fold XBP-1(s) expression over beta tubulin. The remaining clones of the genotype ranged from 0.5-fold to 1.7-fold expression levels compared with beta tubulin. In clones 19 to 23 no increase in XBP-1(s) expression level was observed when compared with their parental pool no. 1 (Figure 13, XBP-1(s) level of 4). Therefore, the selection of clones expressing higher levels of XBP-1(s) than the average reflected by the pool value was not possible.

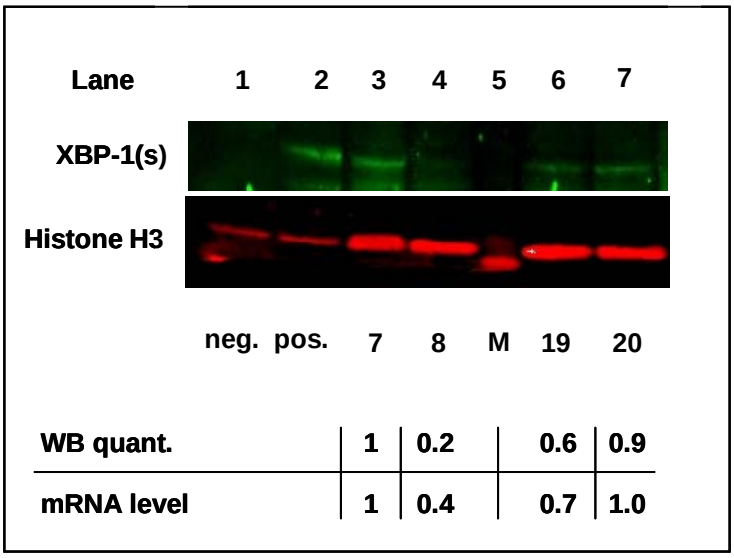

Figure 18: XBP-1 Western blot analysis of two clonal cell lines per genotype correlated with mRNA level

XBP-1(s) protein level in nuclear extracts was determined by Western blot for two clones per genotype (upper lane) and compared with histone H3 level as loading control (lower lane). Lane 1: CHO-K1 mock transfected as negative control, Lane 2: CHO-K1 XBP-1(s) transfected as positive control, M = marker lane. Lane 3, 4 and 6,7: Nuclear extracts of the stated clones. Relative to clone 7, the quantified protein level as well as the relative XBP-1(s) mRNA level are stated.

For two clones of XBP-1(s) expressing genotypes showing the highest XBP-1(s) mRNA level nuclear protein extracts were prepared to detect intracellular levels of the heterologous protein. Nuclear extracts were separated on SDS-PAGE and proteins transferred to nitrocellulose membranes. Antibodies directed against XBP-1(s) and histone H3 were used for detection. NIRdye-coupled secondary antibodies and scanning at 680 nm (red) and 800 nm (green) were used for visualization as described in chapter 8.7. For stably XBP-1(s) expressing cells, clone 7 and clone 8 were selected. For the cell lines expressing both transgenes, clones 19 and 20 were analyzed. Nuclear extracts of mock and XBP-1(s) transiently transfected CHO-K1 cells served as negative and positive controls, respectively. The Western blot detection of XBP-1 (Figure 18) showed a band of about 50-55 kD size for the positive control in lane 2, which corresponds to the theoretical size of the spliced form of XBP-1. Detection of histone H3 protein was used to confirm loading of equal protein amounts. The transgene expression level was quantified by the scanner software based on cumulated signal intensity and calculated relative to the loading control. This quantification revealed that clone 7 showed a 5-fold higher XBP-1 protein level compared with clone 8 and the same protein level when compared with clone 20. Clone 19 exhibited about half the expression level when compared with clone 7. For clone 8 the signal was found close to the detection limit of the near infrared scanning method. The results of the Western blot quantification were in good agreement with the mRNA expression levels quantified by qPCR. The detection limit of XBP-1(s) in Western blot analysis, however, could not be improved by detection of the tagged C-terminus of the protein. The signal intensity remained unchanged when different antibodies against either XBP-1(s) or Flag-Tag were compared. Also, an enrichment of XBP-1(s) by immunoprecipitation failed as well as intracellular detection by FACS analysis of stable cell lines (data not shown).

For all 24 clones, the heterologous XIAP mRNA expression level was also analyzed (Figure 19). Clones 1 to 12 were below the detection limit and clones 13 to 24 showed XIAP mRNA levels between 0.5-fold and 6-fold over beta tubulin mRNA levels. As expected for the IRES coupled expression, XIAP levels of clones 19 to 24 showed the same profile as for XBP-1(s) mRNA expression levels. Compared with expression levels of cell pools (Figure 12), again, no increase in XIAP mRNA expression level was observed. In accordance with XBP-1(s) protein analysis, two clones with high mRNA levels were selected for Western blot analysis of cytosolic cell extracts. The cytosolic extracts of mock or transiently XIAP transfected CHO-K1 cells served as controls (Figure 20). Actin as loading control was detected as a single band of about 40 kD size (red signal) and XIAP as a band of about 50 kD size (green signal).

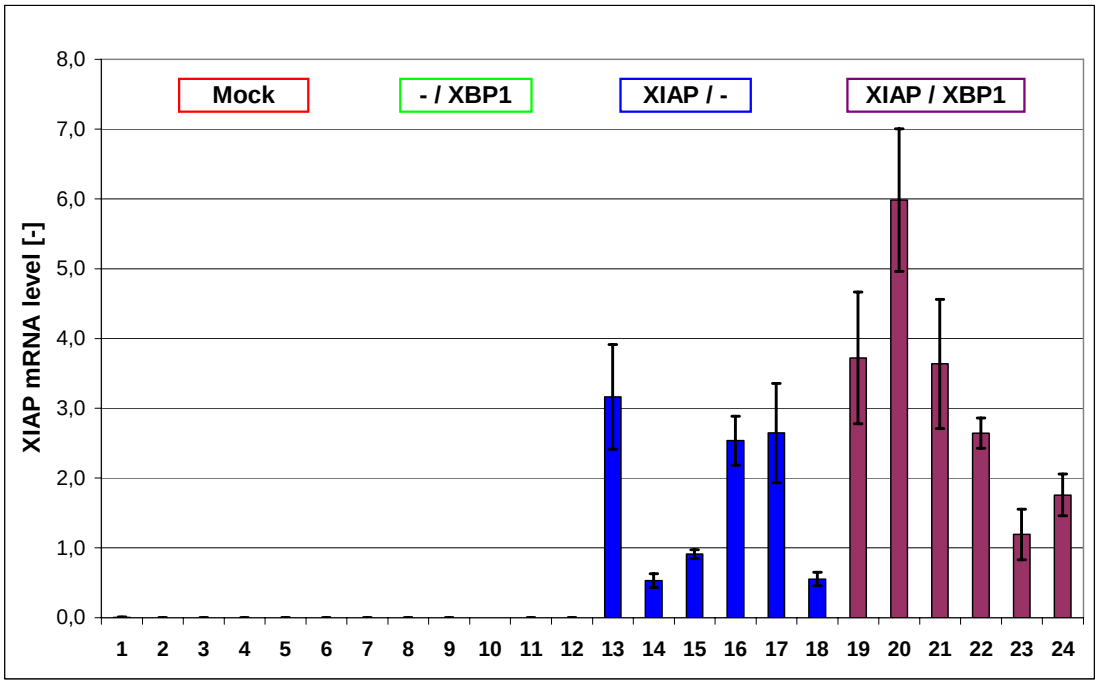

Figure 19: XIAP mRNA expression level in top 6 stable cell clones per genotype

The heterologous XIAP mRNA abundance was measured by real-time PCR relative to beta tubulin. The analysis was run in triplicate samples and error bars represent the standard deviation.

XIAP and actin protein amounts were quantified by the scanner software as integrated signal intensity and XIAP level was calculated relative to actin. Clone 19 expressing both transgenes showed about 2-fold higher XIAP protein levels when compared with solely XIAP-expressing clones 13 and 16. From the mRNA levels measured, the protein level of clone 19 was expected to be in the range of single engineered clones. From qPCR data, only the protein level of clone 20 was expected to be twice as high when compared with the three cell clones further analyzed.

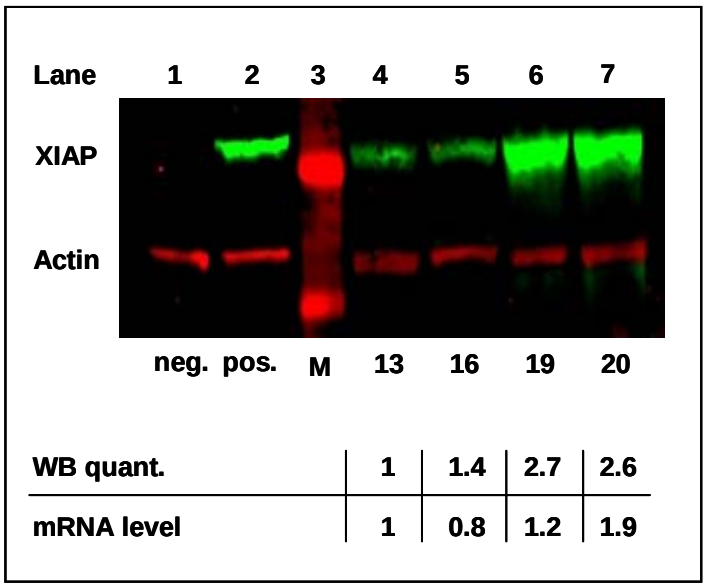

WB quant.	1	1.4	2.7	2.6
mRNA level	1	0.8	1.2	1.9

Figure 20: Western blot analysis of XIAP of two selected clones per genotype revealed low correlation to mRNA levels

Protein level of XIAP was detected in cytosolic cell extracts by Western blot. Actin served as loading control. Lane 1: Cytosolic extract of mock transfected CHO-K1 as negative control, Lane 2: Cytosolic extract of XIAP transfected CHO-K1 as positive control, Lane 3: Marker, Lane 4-7 Cytosolic extracts of stated clones. The quantified protein level relative to clone 13 as well as the relative XIAP mRNA level are stated.

In summary, the expression of both transgenes was verified on mRNA and in selected clones on the protein level. In accordance with the working hypothesis, XBP-1(s) mRNA level in double engineered clones was enhanced on average when compared with mono-transgenic

clones. However, no correlation of XIAP expression and XBP-1(s) level was found, as protein levels of the transcription factor were the same regardless of XIAP co-expression. This result could suggest that the presence of heterologous XIAP was not sufficient to support the survival of cells with high XBP-1(s) expression levels.

6.3.8 Analysis of IgG productivity of monoclonal cell lines expressing XIAP and XBP-1(s)

To analyze the specific antibody productivity in engineered clonal cell lines, titers of seed-stock cultures were measured over three passages and Qp was calculated.

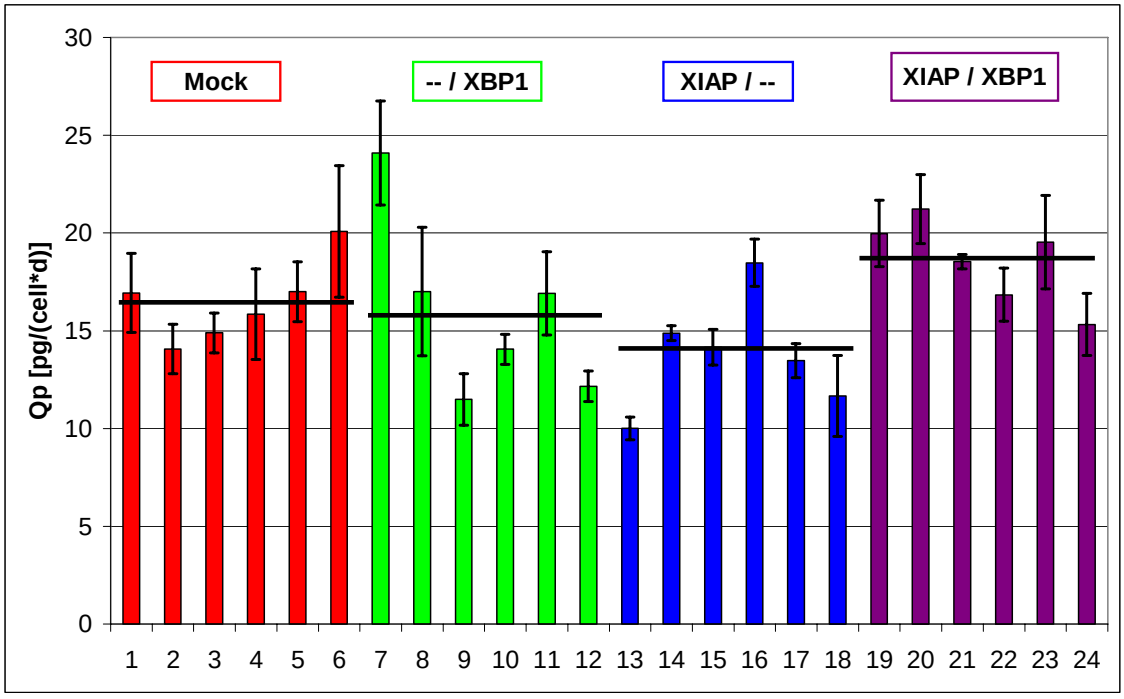

Figure 21: The specific antibody productivity of stable cell clones is not enhanced in two transgene expressing CHO cells in seed-stock cultures.

The data represent the mean specific productivity (Qp) of the 6 top clones per genotype across 3 passages in seed-stock cultures. The horizontal bars represent the mean of the 6 corresponding clones and the error bars represent the standard deviation of triplicate measurements.

Figure 21 plots the specific productivity of all 24 clones. Mock transfected clones varied between 14 pg/(cell*d) and 20 pg/(cell*d). The variation for solely XBP-1(s) expressing cell lines was found to be higher, ranging from 11 pg/(cell*d) to 24 pg/(cell*d). The solely XIAP-expressing clones varied from 10 pg/(cell*d) to 18 pg/(cell*d). Clones expressing two transgenes showed a range in productivity between 15 pg/(cell*d) to 22 pg/(cell*d).

Overall, double engineered clones showed the highest specific productivity on average when compared with single engineered and mock transfected clones. The difference, however, was not statistically significant.

6.3.9 Fed-batch production of an IgG antibody from CHO cells expressing XIAP and XBP-1(s)

The final yield in a fed-batch process is the integrative result of growth performance and productivity. As the final harvest titer of a production process does not solely rely on Qp but also on overall IVC, the performance in a fed-batch process was investigated. For each clone, triplicate shake flasks were seeded in the screening model. Overall, 72 flasks were inoculated and run for 10 days as described earlier in chapter 6.1.3. Viable cell numbers and viability were assessed every other day from day 4 on, using the CEDEX system (Figure 22 A, B). Titer was analyzed by HTRF® assay. The mean of triplicate samples from 6 clones per genotype is shown.

Compared with the clones expressing both transgenes showing the highest integral of viable cells, the clones expressing solely the transcription factor exhibited the lowest IVC in the experiment (lower peak cell density, earlier decline phase and lower viability profile). The growth characteristics were found to support the working hypothesis that XBP-1(s) expressing clones showed the lowest overall cell mass due to the negative impact of the active

form of the transcription factor. This effect was counteracted by the co-expression of the anti-apoptosis protein XIAP. The viability profile was found to be the same when compared with the fed-batch evaluation of polyclonal cell lines (Figure 22 B). Clones expressing XIAP and XBP-1(s) showed on average the highest viability on day 8 indicating a positive effect of XIAP on culture longevity.

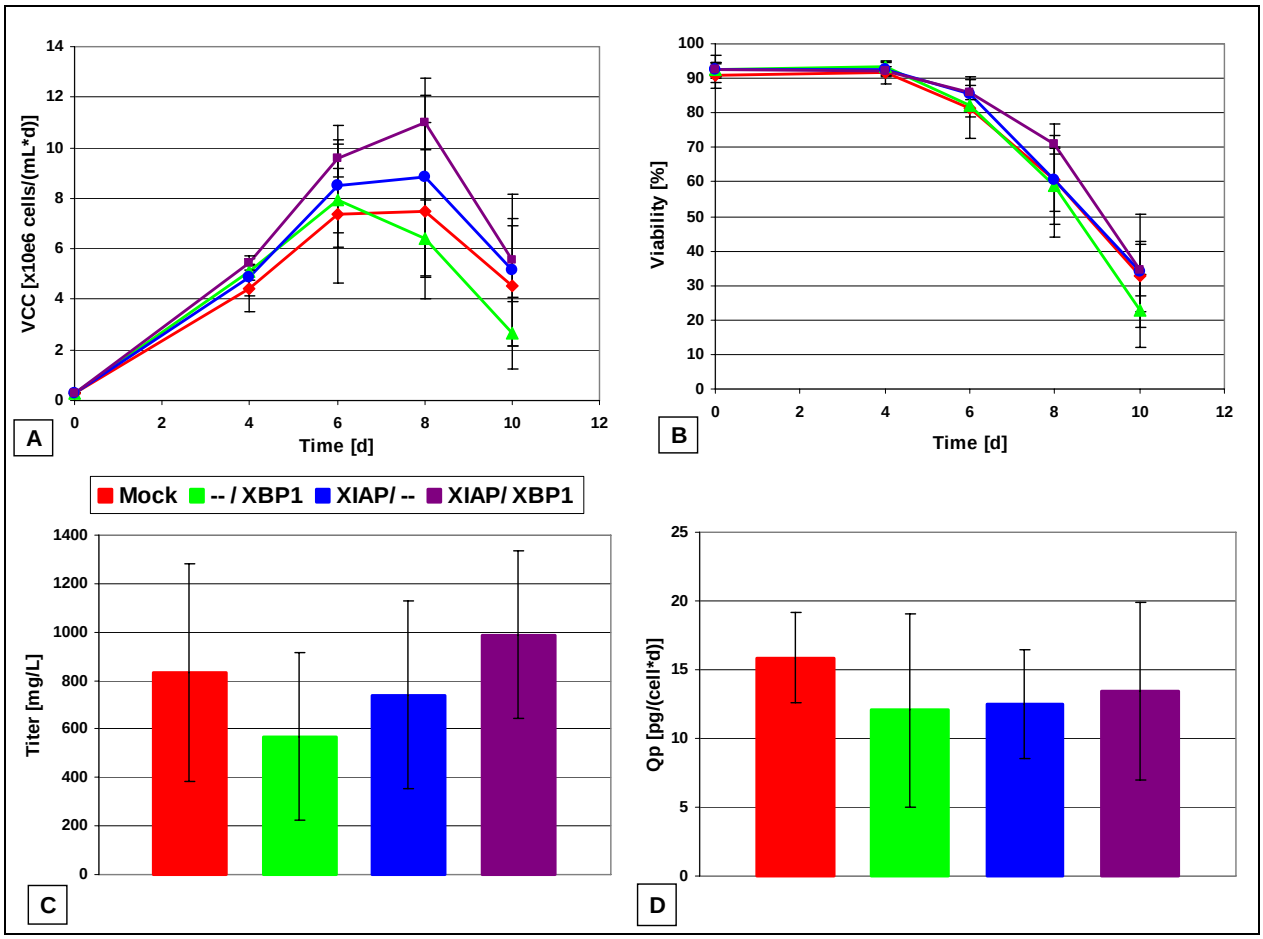

Figure 22: Bicistronic expression of h-XBP-1(s) in combination with h-XIAP in CHO cells did not lead to higher antibody (IgG) yield in a chemically defined serum-free fed-batch process in clonal cell lines.

A fed-batch was performed in shake flasks for all top 6 clones (n=3). Viable cell count (A) and viability (B) were assessed by the CEDEX system. The product concentration of the harvest day (d10) was determined by HTRF® assay (C) and the specific productivity (D) was calculated as final product concentration divided by final IVC (integral of viable cells). Error bars represent the deviation between the mean of the six clones.

Due to the lowest overall cell numbers in solely XBP-1(s) expressing clones, the final titer was found to be lowest on average with a range of 200 mg/L to 900 mg/L (Figure 22 C). Mock transfected and solely XIAP-expressing clones showed the same range in final product concentration, ranging from 400 mg/L to around 1,200 mg/L. Clones expressing both transgenes showed the highest titer on average (1,000 mg/L), ranging between 600 mg/L and 1,300 mg/L. When final titers were compared between the different genotypes, no statistically significant difference could be detected. For specific productivity (Figure 22 D), mock transfected clones ranged from 13 pg/(cell*d) to 19 pg/(cell*d), reflecting the specific productivity of the parental cell line (15 pg/(cell*d)). On average, none of the engineered genotypes showed enhanced specific productivity.

Despite the higher productivity and harvest titer in polyclonal cell lines (chapter 6.3.5), the performance neither of single nor of double engineered clonal cell lines was significantly altered in fed-batch processes.

It was found that, for the successful ER engineering of suspension CHO cells to increase their specific production rate, high levels of the active form of the transcription factor X-box-binding protein 1 were necessary. On the other hand, high levels of XBP-1 were found to induce apoptosis in transient expression experiments and to lower the colony count in CFA assays. The combination of the secretion-enhancing transcription factor together with the caspase inhibitor XIAP was thought to enable cell survival with high XBP-1(s) levels, thus allowing the selection of higher producing cell lines when compared with the single engineering approach. It was found that co-expression of XIAP provided apoptosis protection in transient expression studies. Also, the number of colonies formed after stable integration of the bicistronic plasmid increased when compared with control transfections. This proved that XIAP was able to diminish XBP-1(s)-induced apoptosis. During the generation of polyclonal cell populations it was found that pools expressing both transgenes, linking XBP-1(s) and XIAP translation to the same transcript, secreted more therapeutic antibody molecules when

compared with the single engineering approach, thus proving the worth of the combinatorial engineering approach in an industrially relevant setting. Cellular transcript levels of XBP-1(s), however, were not enhanced on average by the co-expression of XIAP when compared with the single engineering approach. When the cloning procedure, flow cytometry based single cell deposition, was applied to generate monoclonal cell lines, no significant differences in Qp and harvest titer were found for single or double engineered clones. The transcript level of the transcription factor was indeed elevated when XIAP was co-expressed, but no significantly elevated productivity was found when compared with solely XBP-1(s)-expressing clones. After promising results in transient studies as well as on the pool level for enhanced antibody secretion rates, the data generated for cell clones prove the challenge in transferring the two transgene approach to the final stages of industrial cell line development.

6.4 2D-DIGE analysis of supernatants from CHO cells grown in chemically defined serum-free media

In recent years, several studies have described the intracellular proteome of mammalian cells used for therapeutic protein production such as CHO and NS0 cells. The focus of these studies was a better understanding of how the protein composition inside the cell reflects the cell culture environment (Kaufmann et al., 1999; Lee et al., 2003b; Yee et al., 2008; Seow et al., 2001; Meleady et al., 2008) or finding key differences between so called high-producer or low-producer cells that can be visualized by two-dimensional electrophoresis (Dinnis et al., 2006; Nissom et al., 2006; Smales et al., 2004). While technologically the field has evolved and given rise to more reproducible data sets, and while high-throughput mass spectrometry can now generate spectra for proteins of very low abundance, the time required for sample preparation and the lack of reproducibility have prevented the use of such data for process monitoring and control.

In this thesis, the aim was to establish the methodology for monitoring the proteins that are present in the cell culture fluid (CCF) during bioreactor cultivation. This CCF proteome is characterized by reduced complexity compared with the intracellular proteome and one hypothesis is that it would provide a distinct picture for different culture conditions. Furthermore, some of the proteins secreted by the host cell have an impact on the overall process performance such as growth factors or proteases that could potentially degrade the product.

However, several hurdles need to be overcome to establish a methodology for describing and quantifying the CCF proteome such as low protein concentration and the presence of the protein product at high concentrations.

A proposed workflow for the analysis of cell culture fluid (CCF) by 2D analysis is shown in Figure 23. Cells from a process sample need to be removed followed by a clearing step to

remove debris from the supernatant. To achieve suitable protein concentrations, the supernatant sample needs to be concentrated prior to protein labelling. The 2D separation is then analyzed and proteins spots with different abundance among samples are identified by the DeCyder™ software. On the basis of the software analysis, identified protein spots are collected and analyzed by peptide mass fingerprinting using mass spectrometry. The schematic workflow also illustrates questions which had to be addressed first. One question is whether the antibody secreted by a production cell line will hamper later process steps. One way to address this problem would be protein A purification of the CCF prior 2D separation. Additionally, the concentration method had to be defined to reproducibly yield a protein concentration high enough for the subsequent 2D separation.

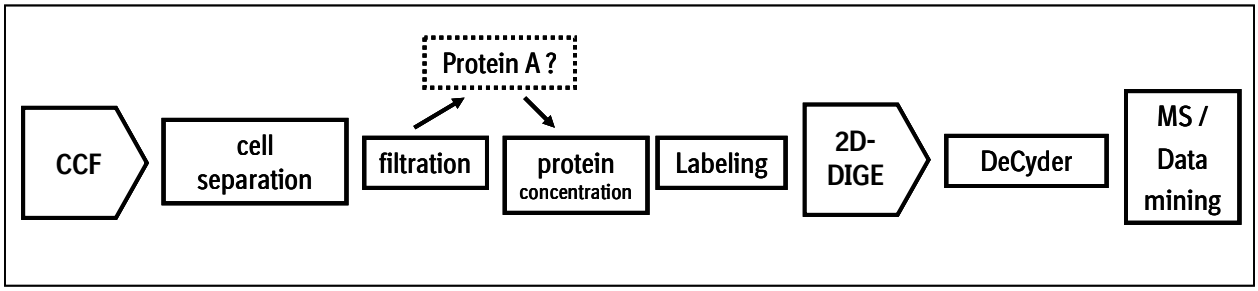

Figure 23: Schematic workflow from cell culture fluid (CCF) to the identification of protein spots separated by 2D-DIGE.

Another hurdle is the lack of hamster genome sequences. Even though CHO cells are the main host for biopharmaceutical production, the full genome sequence has not yet been published (Jayapal et al., 2007). At the beginning of the project it was unclear to which extent hamster proteins would be able to be identified based on data base entries of single genomic hamster sequences or homology to rat or mouse sequences.

6.4.1 Description of the total protein content in batch culture supernatant

In order to establish a protocol for the two-dimensional proteomic analysis of cell culture supernatants, the protein composition of supernatant of day 4 suspension batch cultures of the host CHO-DG44 cell line was compared with the protein content of IgG-producing cells of the same origin. To separate the proteins according to their size an SDS-PAGE was run and proteins were silver-stained for visualization (Figure 24).

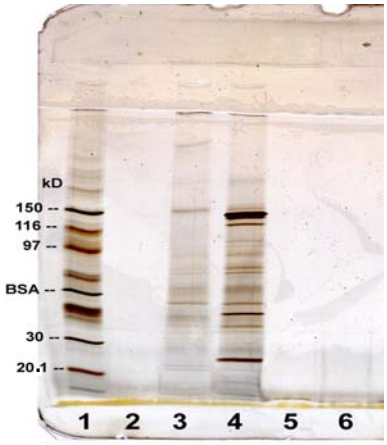

Figure 24: SDS-PAGE showing mAb as most prominent protein in supernatant of producer cell lines

Silver-stained SDS-PAGE of protein content in the supernatant of host (lane 3) and parental cell line (lane 4) as well as two different unconditioned media which were 40x concentrated (lane 5 + 6). Fresh growth medium was separated for control in lane 2 and marker protein in lane 1.

As expected for an IgG product, the SDS-PAGE showed a major band at 150 kD representing the mAb product. Additionally, bands at 25 kD and 50 kD appeared when compared with the proteins secreted by the host cell line (most probably representing light and heavy chain of the antibody, respectively). Lanes 2, 5 and 6 showed that no bands originated solely from the medium used. Neither the medium itself nor the 40x concentration led to detectable band patterns. Therefore it can be concluded that all bands visualized by silver staining in cell

culture supernatants originate from the cells but not from media additives such as soy hydrolysates.

Also, the results proved that the antibody product was the predominant protein in the supernatant of current cell culture processes. This would greatly hamper proteome analysis using 2D gels as it would lead to masking of low abundance proteins. To be able to detect low abundance proteins in 2D-DIGE analysis, thus providing the best possible picture of the CCF, a methodology resulting in product-free CCF had to be developed.

6.4.2 Generation and selection of a monoclonal CHO-DG44 derived mock cell line

Two possibilities for removing the protein product from the CCF were investigated. One was protein-A purification of the supernatant and the other was the generation of a mock cell line. Purification of cell supernatants by protein-A affinity binding is generally the first step in the purification of monoclonal antibodies used as biopharmaceuticals. As this purification step would add variation to the sample preparation process and bear the risk of proteins binding unspecifically to the resin or the antibody itself the generation of a mock cell line was favored.

A mock cell line is defined as containing all genetic elements present in a production cell line except for the product. Additionally, the mock cell line to be used as a prediction tool for the identification of process marker proteins should exhibit growth characteristics similar to those of a CHO-derived, DHFR-amplified producer cell line. To be able to start all experiments from a defined cell population, a pre-existing polyclonal mock transfected cell pool was re-cloned using FC-based single-cell deposition. Five monoclonal cell lines were expanded and analyzed for their growth characteristics in the shake flask fed-batch screening model (Figure

25). Peak cell density of the five cell lines varied from 8 x10^6cells/mL to 15 x10^6cells/mL on day 6 to day 7 of a shortened fed-batch run.

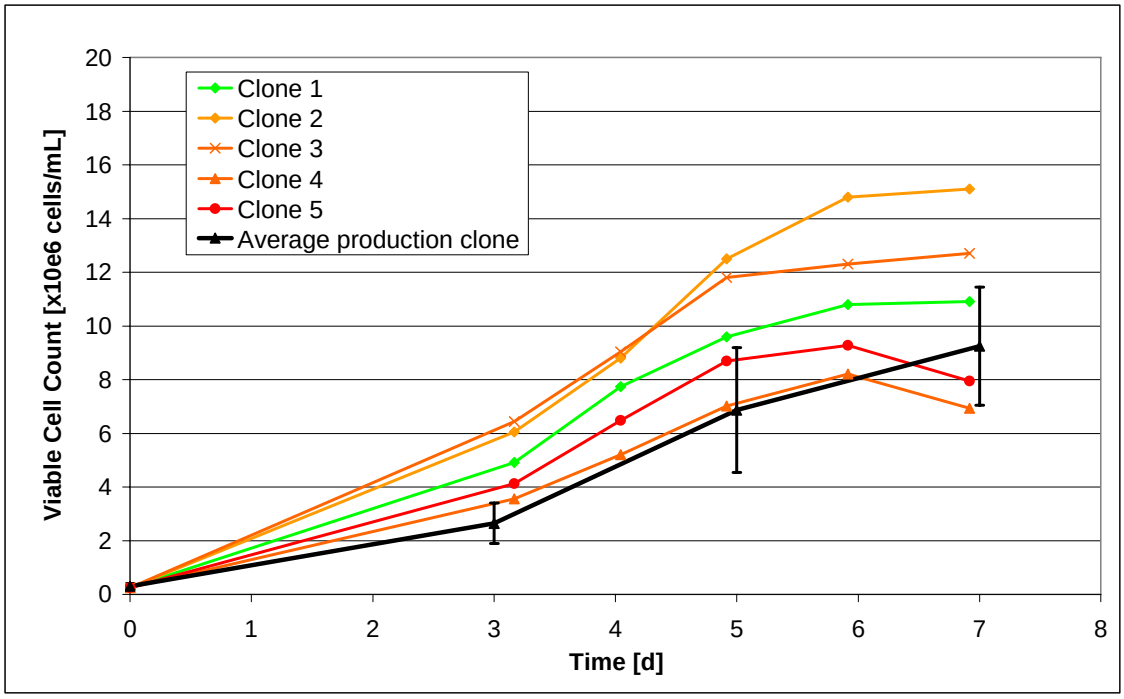

Figure 25: Mock transfected Clone 1 showed similar growth characteristics in fed-batch cultures as production clones

Viable cell number during a 7 day fed-batch process for different monoclonal cell lines was determined with the CEDEX system and compared with the mean growth profile of four different production clones.

The growth profile of four monoclonal cell lines expressing different antibody products grown under the same conditions was averaged from independent experiments and compared. The monoclonal cell lines represent the typical growth performance observed during the production of biopharmaceuticals.

Clone 1, growing at a rate on the upper limit of the average production clone with comparable growth characteristics was selected as model cell line for further experiments (green line in Figure 25), thus closely reflecting the growth characteristics present in a production process.

6.4.3 Comparison of methods for concentrating the protein content in CHO batch culture supernatants

After selection of the mock clone, the question of an adequate protein concentration method was addressed. For the preparative 2D-DIGE analysis procedure, 50 µg of protein from the supernatant had to be dissolved in a final volume of about 140 µL resulting in a minimum protein concentration of 0.36 µg/µL. To achieve this total protein concentration the supernatant had to be concentrated 60 to 100-fold. Two methods were evaluated: precipitation of proteins by trichloroacetic acid (TCA) and ultrafiltration (UF) using a polyether sulfone (PES) filter membrane.

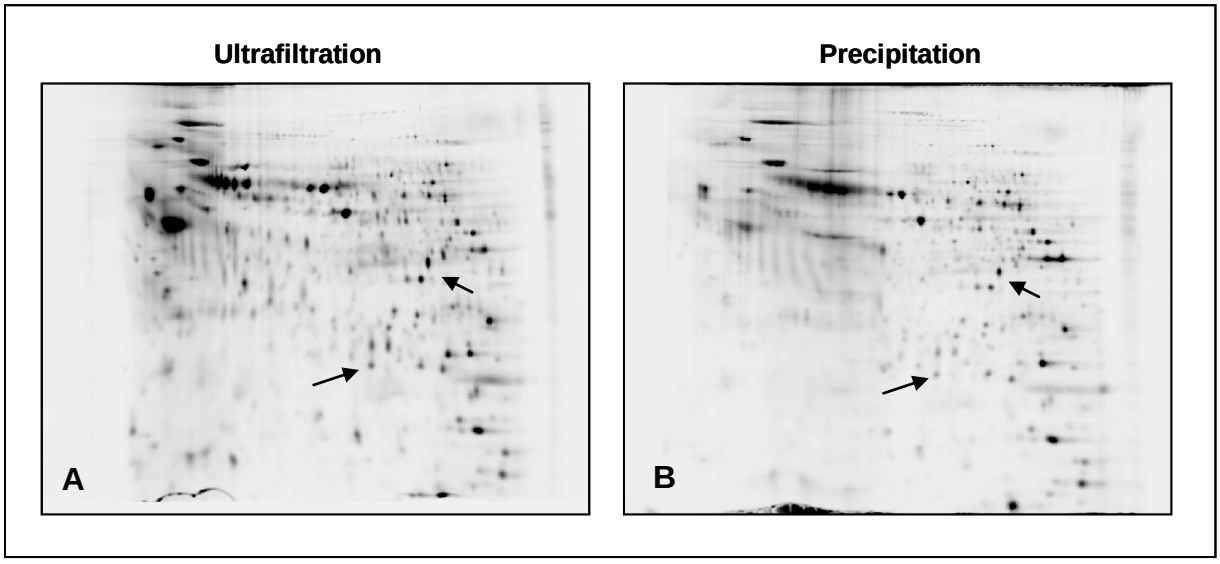

Figure 26: Comparison of ultrafiltration (UF) and precipitation revealed UF to be the superior concentration method

2-D comparison of protein separation from supernatant (A) concentrated 100-fold by ultrafiltration and TCA-precipitated proteins (B). Arrows indicate examples for spots with different intensity and focussing.

Day 3 cell culture supernatants of the mock cell line grown in chemically defined BI proprietary medium were concentrated or precipitated as described in chapter 8.19. To evaluate the two concentration methods, 10 µg of total protein per method were separated on

minigels (Figure 26). The gel with the sample concentrated by ultrafiltration showed more visually detectable protein spots when compared with the gel with the precipitated sample. Additionally, the spot intensity was higher than on the precipitated sample, a fact which suggests that more protein is present. Both gels showed smearing in the upper left part of the gel resulting from unresolved proteins of higher molecular weight and lower pH. The individual spots of the precipitated sample were more focused than the spots in the ultrafiltered sample (see arrows in Figure 26).

The method provided the highest protein recovery as evaluated by spot number and spot intensity and was therefore selected for all subsequent experiments. The unfocused appearance of individual spots was addressed and found to be caused by Pluronic® F68. It was shown that this 8.4 kD large surfactant used in the original medium caused this smear effect on individual spots (data not shown). To further improve the resolution of individual spots in 2D-GE, the chemically defined, Pluronic®-free CD-DG44 medium was used for all following experiments.

The finally selected concentration protocol started with cell and debris removal in two centrifugation steps at 200 g and 3,000 g for 5 min and 10 min, respectively. Protease inhibitor was added to protect proteins from cleavage. For concentration, 20 mL of supernatant were centrifuged in vivaspin columns with a 10 kD cut-off ultrafiltration membrane at 4°C and at 4,000 g for 1 h. The concentrate of less than 1 mL was washed by addition of 20 mL of PBS to remove free amino acids. After a further concentration step, the protein concentrate was quantitatively transferred to a 5 kD cut-off vivaspin column using PBS, followed by an additional centrifugation step for concentration. To transfer the concentrated proteins to the buffer needed for subsequent protein labelling, DIGE buffer was added three times in consecutive concentration steps. The final volume was adjusted to result in a 100-fold concentration of the initial volume. After determination of the protein

concentration by Bradford assay, equal protein amounts per sample were labelled, separated by 2D-DIGE and further analyzed.

In summary, the concentration method was shown to yield sufficiently high protein concentrations in samples from cell culture supernatant to be separated by 2D-GE. The generation of a mock cell line to remove the antibody product from the sample together with the selection of a suitable concentration method were the basis for further investigations into proteomic changes in cell culture supernatants.

6.4.4 Differential proteome analysis of cell culture supernatant and cell lysate of suspension CHO cultures

To establish the 2D-DIGE separation method and to confirm that the concentration method did not enrich for specific proteins, a cell lysate sample was differentially compared with concentrated proteins from d2 supernatant.

To this end, cell culture fluid of cells grown in chemically defined media was sampled on d2 for concentration. The cell pellet was lysed directly in DIGE buffer. Proteins of the supernatant were labelled with Cy3 dye (green) and proteins of the lysates for comparison in red with Cy5 dye. Protein spots visible on the 2D gel (Figure 27) appeared either solely in green, representing proteins prominently present in the supernatant, or in red, showing proteins dominating in the cell lysates and representing intracellular proteins. Yellow appeared for proteins present in similar concentration in the lysates and the concentrated supernatant.

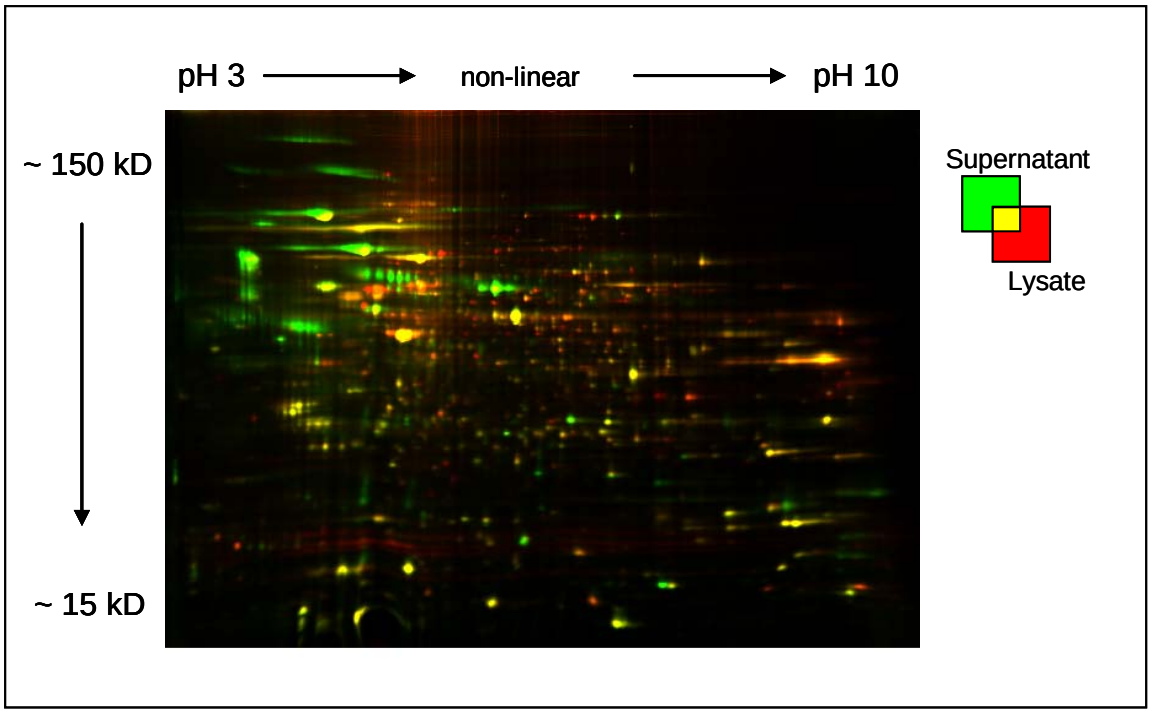

Figure 27: Differential comparison of proteins of cell culture supernatant and cell lysates

Proteins concentrated from d2 supernatant of CHO cells grown in suspension were green-labelled and compared with red-labelled proteins derived from a cell lysate of the same cell line. Proteins present in both samples appear as yellow in the overlay picture.

Combined, the data show that concentration of the supernatant sample by ultrafiltration was able to enrich specifically for proteins solely present in the cell culture fluid. Furthermore, the supernatant proteins were distributed over the full separation range, indicating that the method did not specifically enrich for proteins with certain properties. The results thereby allow to focus on secreted proteins in subsequent analysis.

6.4.5 Analysis of supernatants derived from mock transfected CHO-DG44 cells grown in suspension batch culture

To further develop and test the method up to the point of protein identification, supernatants of d2, d3 and d6 of a batch culture were prepared. Mock transfected clone 1 was seeded at

0.3x10^{6}cells/mL in CD-DG44 medium in n=9 shake flasks. Cell growth was monitored using the CEDEX system. The cells grew to 2x10^{6}cells/mL with a viability of about 90% on all days (Figure 28). Macroscopically, cell aggregates were detected from day 2 on which were not accounted for in the automated CEDEX system. Insufficient growth factor concentration was the reason for the observed cell clumping. This could be prevented by the addition of appropriate amounts of growth factor to the media for subsequent analysis to result in a growth profile that is comparable to the standard medium used. On each sampling day, n=3 flasks were sacrificed for 100-fold concentration of the supernatant as described in chapter 8.19. A total of five preparative 2D-DIGE gels were run by the laboratory staff of PD Dr. Lenter.

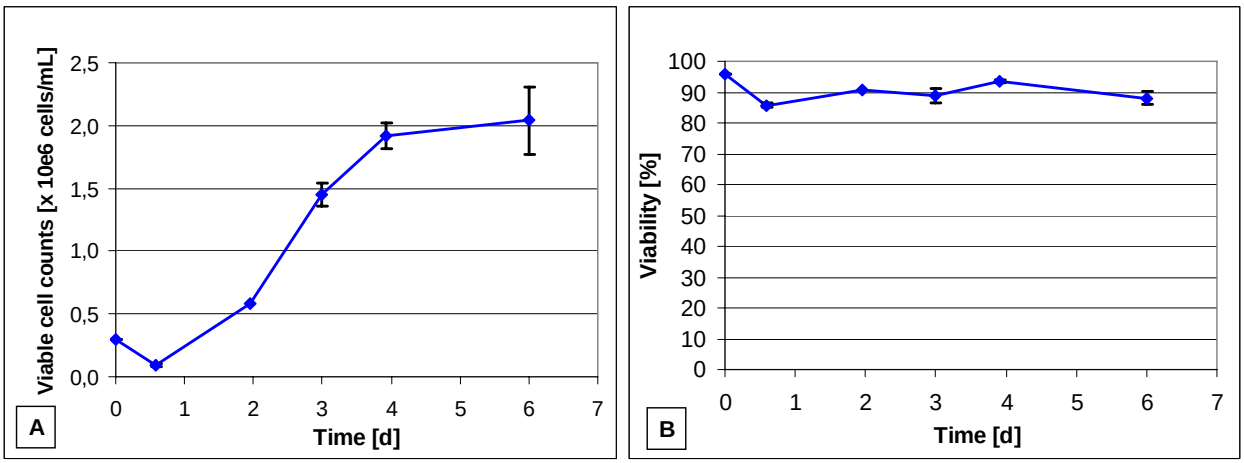

Figure 28: Viable cell count and viability of batch cultures of a mock transfected CHO cell line grown in suspension in chemically defined medium

Viable cell count (A) and viability (B) were determined using the CEDEX system. Error bars represent the standard deviation of triplicate samples.

The three samples per timepoint were distributed among the five gels and a dye switch was performed to prevent a dye bias. A mixture of all samples was prepared as internal standard and run on each gel. From all five gels, the DeCyder™ software selected gel 1 as master gel

(Figure 29) and matched the remaining gels to this master gel. All detectable protein spots were uniquely numbered by the software for subsequent analysis. The abundance of each protein spot in any given timepoint sample was calculated from its fluorescence intensity. In a next step, culture days 2 and 3 were compared as well as culture days 2 and 6 to reveal proteins with different abundance which could serve as process marker proteins with distinct profiles during the process and which correlate with, for example process phase shifts.

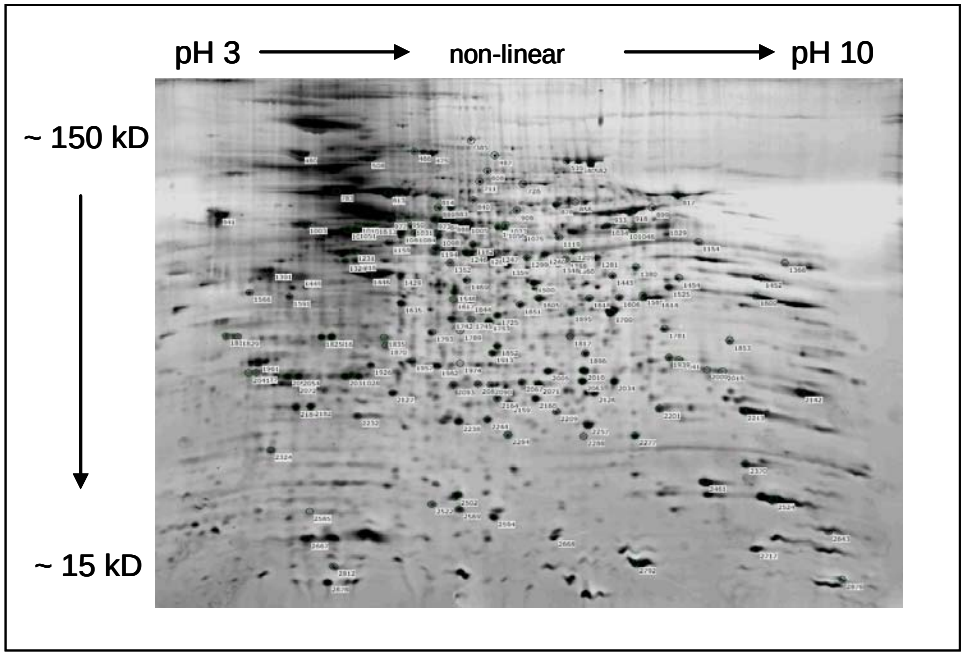

Figure 29: Master Gel from 2D-DIGE analysis of suspension batch cultures

The selected master gel shows a black and white overlay picture of Cy2, Cy3 and Cy5 signals from the scan representing supernatant samples from batch d2, d3 and d6. Numbers mark spots identified by MS analysis.

The abundance of individual spots was compared by a Student's t-test to reveal spots differentially abundant at the different timepoints. Between d2 and d3 a total of 13 spots with different abundance were identified, 12 spots showing higher and one spot lower abundance at d3. When day 2 was compared with day 6, a total of 40 protein spots were present with higher intensities and 23 were identified with lower abundance at d6. All spots identified as

differentially abundant in either the first or the second comparison were selected for protein identification.

To further characterize proteins existing in the cell culture supernatant, unregulated spots distributed over the gel were manually selected in addition to give to a total of 192 spots to be identified. The selected 192 spots were picked and, after subsequent trypsin digestion, analyzed by mass spectrometry. The resulting peptides were blasted against SwissProt Database for protein identification.

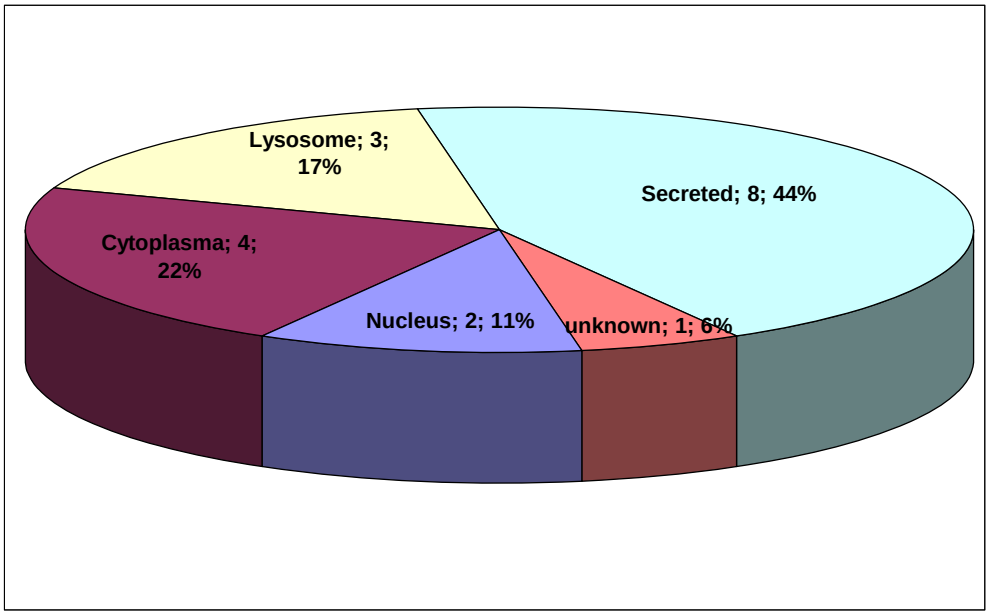

Figure 30: Location of differentially abundant proteins between d2 and d3 of CHO batch cultures

Proteins with different abundance between d2 and d3 were clustered according their cellular origin. Numbers indicate the total protein number and relative distribution in percent.

In up to 40% of the differentially abundant protein spots more than one protein was identified. In the comparison between d2 and d3 a total of 18 proteins were identified as present in the 13 “deregulated” spots. The identified proteins were first classified according to their cellular location. About half of the different abundant proteins (44% or 8 proteins) were found to have been secreted, as determined by the presence of a signal peptide according to the protein

database (Figure 30). The remaining proteins originated from cytoplasm, nucleus or the cellular lysosome.

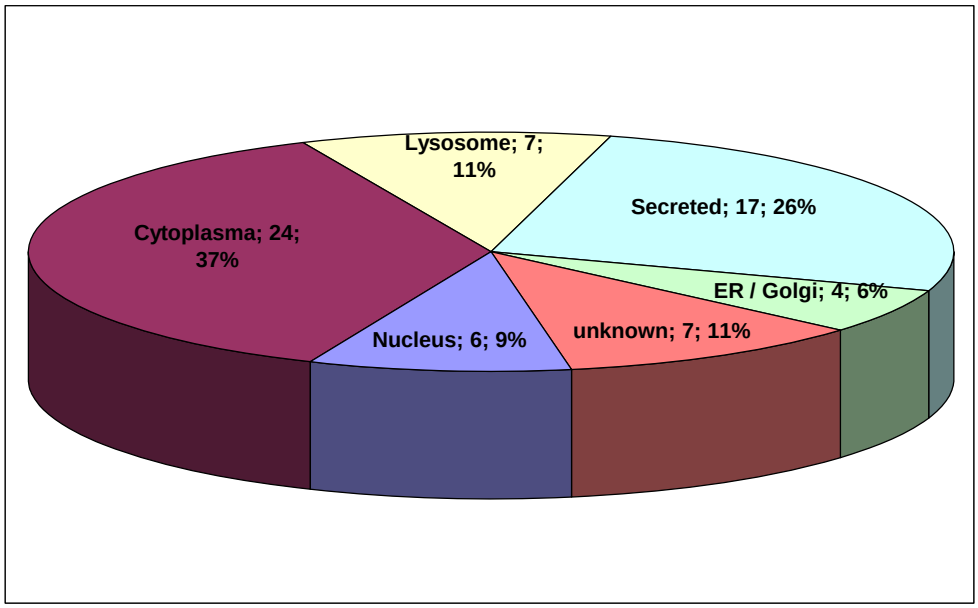

Figure 31: Location of differentially abundant proteins between d2 and d6 of CHO batch cultures

Proteins with different abundance between d2 and d6 were clustered according their cellular origin. Numbers indicate the total protein number and relative distribution in percent.

A different distribution of the cellular location was found when d2 and d6 were compared. A total of 77 proteins were found in the 63 deregulated protein spots. The majority of identified proteins originated from the cytoplasm (37%) followed by secreted proteins (26%). Lysosomal proteins were found in 11% of the identified proteins and proteins associated with the nucleus were found in 9%, the remaining 6% of proteins originated from the ER or Golgi network (Figure 31). In 12 cases, the same protein was found in more than one spot, mainly when adjacent protein spots were picked. A different position on the gel could result from post-translational modifications such as altered glycosylation or phosphorylation. The increase in cytoplasmic proteins on day 6 resulted most probably from cell death due to the cell aggregation observed. Microscopic inspection showed the cell aggregates to consist

mainly of dead cells. Intracellular proteins might have been released into the culture supernatant As a result of disruption of the plasma membrane.

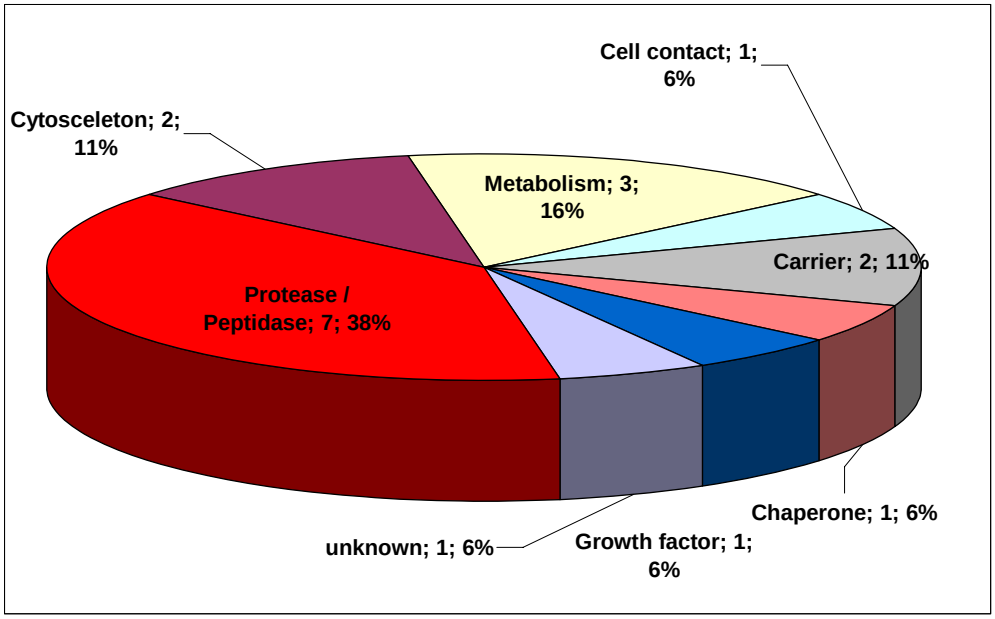

Figure 32: Function of differentially abundant proteins between d2 and d3 of CHO batch cultures

Proteins with different abundance between d2 and d3 were clustered according to their function. Numbers indicate the total protein number and relative distribution in percent.

Next, the identified proteins were classified according their function. The first comparison between d2 and d3 revealed seven proteins with protease or peptidase activity corresponding to 45% of the differentially abundant proteins (Figure 32).

19% of the proteins were found to be associated with metabolic functions and the remaining proteins were equally distributed among functions such as cell contact, carrier or chaperone function, growth factors and structural function in the cytoskeleton. The function of the remaining protein was unknown. The functional distribution changed when the abundance of proteins in the supernatant of d2 and d6 was compared. Proteins with protease or peptidase activity as well as regulator proteins accounted for 20%. Proteins of the cellular metabolism were found in 18% of all cases.

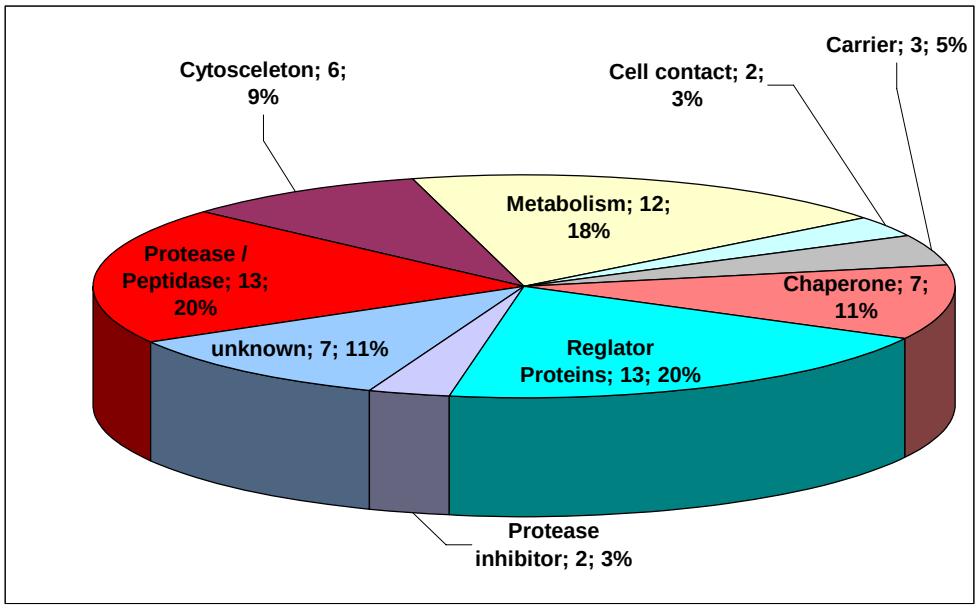

Figure 33: Function of differentially abundant proteins between d2 and d6 of CHO batch cultures

Proteins with different abundance between d2 and d6 were clustered according to their function. Numbers indicate the total protein number and relative distribution in percent.

Chaperone function was found for 11% of the proteins and proteins of unknown function were found with the same percentage. Proteins of the cytoskeleton were identified as 9% of the differentially abundant proteins, followed by 5% proteins with carrier function. Between d2 and d6, 3% of the proteins exhibited protease inhibitory functions. As shown in Figure 34, 10 of the 12 differentially abundant proteins identified between d2 and d3 were also identified when d2 and d6 where compared. For proteins of lower abundance, the only protein identified for the comparison of the early process phase was also identified in the later.

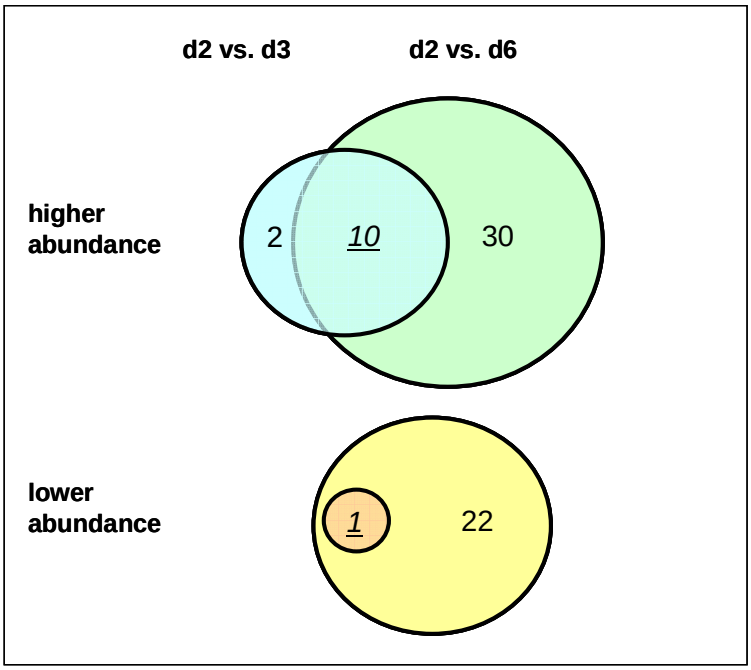

Figure 34: Overlap of differentially abundant spots

This graph shows the total numbers of spots differentially abundant in the comparison of d2/d3 and d2/d6. Underlined numbers indicate the overlap of both comparisons.

Of the total of 192 protein spots analyzed, 94 proteins (58%) originated from the cytoplasm (data not shown). A further 20% was found to be associated with the nucleus, followed by 10% of secreted proteins. The remaining 12% of identified proteins originated from, for example, cell membrane, lysosomes, mitochondria or the peroxisome.

The results proved that differentially abundant proteins were able to be identified using 2D-DIGE analysis of concentrated supernatant from batch process samples. Even when there was only a 24 h period between two samples, the method was able to detect differences in protein abundance and identified 12 proteins with higher abundance on d3 and one with lower abundance. Since the cell number increased between d2 and d3, it would have been expected that proteins with different abundance due to active secretion processes would be identified. This result also indicated that the sensitivity of the method would be sufficient for

characterizing mammalian cell cultures, where typically processes are sampled once a day. The same was expected when d2 was compared with culture d6. Since the comparison of d2 and d6 incorporated a time span of four days rather than one day for the comparison between d2 and d3, it was not surprising either that more proteins of different abundance were identified on d6 compared with d3. In the case of the “upregulation” this could have been a result of active protein secretion or of passive release due to cell death. For the proteins of lower abundance the differences observed may have resulted from proteolytic activity in the supernatant or from cellular endocytotic activity. The observed overlap of proteins identified as “deregulated” during the two comparisons indicated an expected progression of protein release. Protein abundance steadily increased from d2 to d6 for 34 (85%) of the proteins identified as being of higher abundance. The profile for the remaining six proteins (15%) showed no differential abundance between d2 and d3 followed by a significant increase up to d6.

To verify the results of the large-scale exploration of differentially abundant proteins in CHO supernatants, initially one 2D-DIGE result was tested with Western blot. The stress-induced phosphoprotein 1 (STIP1), which mediates the association of the molecular chaperones HSC70 and HSC90 by complex formation, was found by the 2D method to be 2.3 times less abundant on d6 when compared with d2. This characteristic was verified by Western blot analysis of supernatant samples prepared in an independent experiment under exactly the same conditions as used for the previous study (Figure 35). Equal amounts of protein, as determined by BCA assay, were separated on SDS-PAGE and analyzed for STIP1 presence in Western blot. Quantification of the single STIP1 band revealed a 2-fold decrease in abundance on d6 when compared with d2. The result confirmed the identical finding of the 2D-DIGE analysis and MS identification.

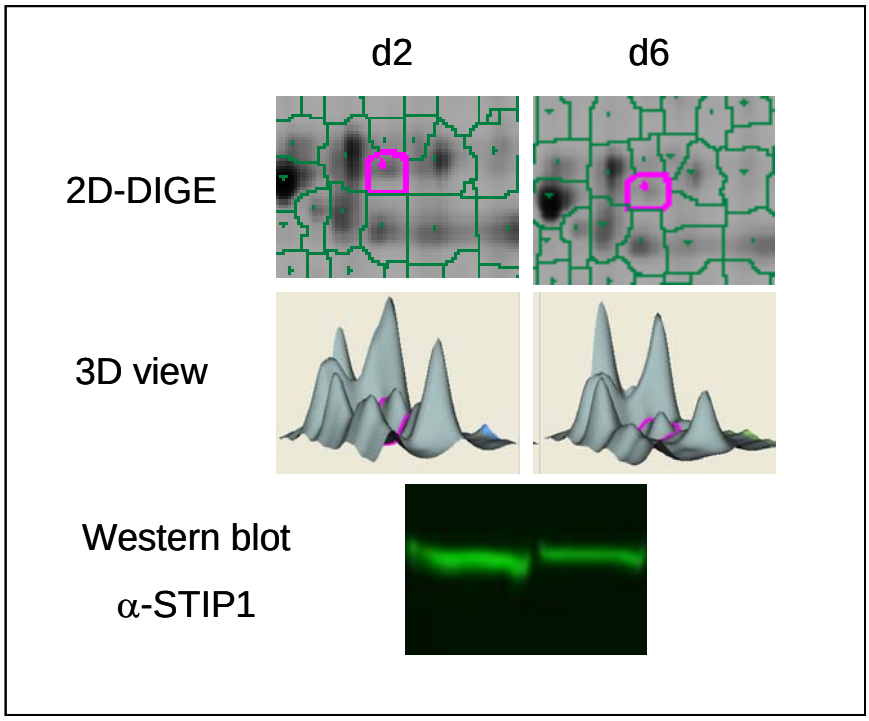

Figure 35: Verification of 2D-DIGE result by Western blot for STIP1

The upper panels show the differentially abundant spot in the 2D-DIGE analysis corresponding to STIP1. In the middle panel, the area is shown as a 3D diagram in the DeCyder software. In the lower panel STIP1 was detected in a Western blot experiment of equal protein amounts of cell culture supernatant from d2 and d6.

In summary, a cell line suitable for the proteomic characterization of industrially relevant suspension cell culture supernatants was generated. Furthermore a protocol for the investigation of cell culture supernatants was developed and optimized. With the optimized concentration method for cell culture supernatant, the analysis of cell lysate and supernatant samples was able to prove the suitability of the procedure. Additionally, a first batch experiment to establish the total workflow from sample preparation to protein identification by mass spectrometry revealed differentially abundant proteins secreted in an early process phase between d2 and d3, a fact indicating the good sensitivity of the method. Also, a comparison of early d2 and late phase d6 showed as expected more differentially abundant proteins when compared with the d2 and d3 analysis. Finally, the findings were verified for

one protein by Western blot analysis and were in good agreement between the different methods, thus successfully completing the establishment of the method.

7 DISCUSSION

7.1 Overexpression of XBP-1(s) in mAb producing CHO cells

Although many mammalian cell engineering approaches based on gene overexpression have been described in the literature (Kuystermans et al., 2007), only a few, such as overexpression of Bcl-2 and BclxL (Meents et al., 2002), have been evaluated in a setting that is relevant to the industrial-scale manufacture of therapeutic proteins for use in humans by using cells growing in serum-free suspension cultures.

Recently, post-translational transport and processing steps have been the focus of cell engineering science. Targeting single ER-resident chaperones in the secretory pathway such as binding protein (BiP or GRP78) and protein disulfide isomerase (PDI) to increase heterologous protein production was successful in yeast (Smith et al., 2004; Shusta et al., 1998; Gasser et al., 2006) and insect cells (Hsu and Betenbaugh, 1997; Ailor and Betenbaugh, 1998) but was found to yield inconsistent results in mammalian cells (Borth et al., 2005; Davis et al., 2000; Kitchin and Flickinger, 1995). Moreover, reduction of the level of endogenous BiP, rather than overexpression, was found to improve tissue plasminogen activator (tPA) production in CHO cells (Dorner et al., 1988).

Given the complex regulation of mammalian protein secretion, targeting single components of the secretory pathway may not always produce the desired effect. Therefore, engineering the level of key regulators that influence the activity of multiple proteins involved in protein transport and secretion seems a particularly promising approach. The spliced form of the transcription factor X-box-binding protein 1 (XBP-1(s)) fulfils such a target profile as it regulates the transcription of >500 genes relevant to the transport of secreted proteins (costa-Alvear et al., 2007). XBP-1(s) is a key regulator of plasma cell differentiation and secretory organ development (Lee et al., 2005). Furthermore XBP-1(s) is a critical effector of the

mammalian UPR, whose activity is regulated by inositol-requiring enzyme 1 (IRE1), an ER-resident kinase/ribonuclease that acts as an ER-stress sensor/transducer. XBP-1(s) drives ER expansion and chaperone induction, which are aspects desirable for the generation of highly productive cell lines. Thus, the aim of this study was to evaluate secretion engineering of suspension CHO cells by XBP-1(s) overexpression under industrially relevant process conditions.

The study results show that the constructed XBP-1(s)-expressing plasmid was functional, as its expression leads to extension of ER in transiently transfected CHO-K1 cells. As a model, a monoclonal CHO-DG44 cell line producing a therapeutic IgG in suspension culture in chemically defined serum-free media was chosen to evaluate the potential of XBP-1 engineering for improving production processes for biopharmaceuticals. It was demonstrated that introducing XBP-1(s) leads to novel monoclonal production cell lines that secreted more IgG molecules per cell and day in seed-stock cultures as well as in a small-scale fed-batch format. Furthermore the data presented here suggest a correlation between XBP-1(s) expression level and increase in IgG productivity. Interestingly, another study in NS0 cells is inline with this finding when NS0 cells were transiently transfected with erythropoietin (EPO) and murine XBP-1(s) in parallel, showing highest product concentrations in cells transfected with the highest amount of XBP-1(s) plasmid (Ku et al., 2007). However, in the same study, adherently growing CHO-K1 cells in comparable experimental settings did not evince an obvious XBP-1(s)-dependent dose response on product secretion. The authors speculated that XBP-1(s) can only increase the productivity of cells operating at their secretory limit. Again, in the same study the productivity of stably monoclonal antibody (mAb) and interferon γ (IFNγ) producing cells was not altered when XBP-1(s) was transiently overexpressed. Furthermore, stable overexpression of hamster XBP-1(s) failed to enhance the secretion of antithrombin III (ATIII) in adherent CHO-K1 cells (Ohya et al., 2007). The authors found an

already activated UPR in the parental cell line and speculated that an additional overexpression of the transcription factor could therefore would not further enhance the secretion capacity of the cell. More recently, a study has evaluated the production of recombinant human factor VIII (FVIII) in HepG2 and CHO cells (Campos-da-Paz et al., 2008). Again, transient expression of XBP-1(s) provided inconsistent results with regard to productivity enhancement: XBP-1(s) failed to enhance the productivity in CHO cells but increased the productivity of HepG2 cells measured 24 h after co-transfection of the product coding gene. Finally, a cell line-dependent effect of XBP-1(s) overexpression has been described by Tigges and Fussenegger, where the productivity of human cell lines HEK-293, HeLa and HT-1080 was not impacted by this engineering approach (Tigges and Fussenegger, 2006).

Taken together, these results suggest that the increase in specific productivity by overexpression of XBP-1(s) can depend on the species, cell type, production level, the product molecule, the UPR status of the cell and finally on the expression level of XBP-1(s) itself. All of this leads to the conclusion that evaluating the actual benefit of this cell engineering strategy requires a study truly reflecting conditions relevant to industrial manufacturing.

When post-translational processing machinery is targeted, it is critical to assess the impact of the transgene on the quality of the protein product secreted. Therefore, the IgG product from the supernatants of the fed-batch cultures described was purified by protein-A and a physico-chemical characterization study of this material was performed. It was found that cell lines producing more antibody due to heterologous expression of XBP-1(s) did not display discernable product differences with regard to microheterogeneity, as revealed by SDS-PAGE, isoelectric focusing, size exclusion chromatography and carbohydrate mapping. It was clearly demonstrated that the secretory capacity of a monoclonal antibody-producing cell line was enhanced by the heterologous expression of the spliced form of XBP-1 without affecting

the quality of the product. These results demonstrate the potential of XBP-1(s) as a potential candidate for successful host cell engineering in biopharmaceutical process development and production. XBP-1(s) may, as a result of its physiological role, bypass a secretory bottleneck in highly productive cell lines, further pushing the limits of secretion of protein products. Despite the positive effect on specific productivity (Qp) shown for XBP-1(s)-overexpressing cells, it appeared difficult throughout the entire study to generate stable XBP-1(s)-expressing monoclonal CHO cell lines. Only very few cell lines grew after selection and sub-cloning and only a small fraction of these cell lines expressed detectable amounts of XBP-1(s). This was in contrast to data obtained when other transgenes were evaluated (unpublished data). Additionally, under fed-batch conditions both XBP-1(s)-expressing cell clones exhibited lower peak cell densities and higher doubling times during the exponential growth phase. These are indications that expressing high levels of XBP-1(s) might impose a negative selection pressure on the relevant clonal cell populations resulting in an increased likelihood of instable genotypes in long-term serial cultivations.

Ultimately, a novel host cell line improved by engineeringshould exhibit the following characteristics: (i) The described correlation of XBP-1(s) expression and enhancement in specific productivity should aims at a high transgene expression. (ii) The cell line should exhibit the same growth rate and peak cell density when compared with its predecessor. (iii) The viability profile in fed-batch cultures should not be affected by transgene expression. (iv) Stable expression of the transgene over a prolonged period of time is a further requirement for a production cell line.

Common to most studies is, when hamster cells were used, the employment of serum-dependent, adherently growing CHO-K1 cells as model system. None of the aforementioned studies provided data on or even mentioned long-term stability or negative impacts of XBP-1(s) overexpression.

7.2 Stability of XBP-1(s) overexpression in mAb-producing CHO cells and its negative impacts

The aim of this study was to test the applicability of XBP-1(s) engineering in an industrially relevant environment. This includes the feasibility of transgene expression for prolonged periods in culture in monoclonal cell lines. Currently, the most prominent regime for the large-scale manufacture of proteins from mammalian cells starts with the thawing of a working cell bank (WCB) vial and includes establishing serial cultures in spinner or shake flasks as a typical industrial inoculum setting. Several scale-ups can then be performed to expand cultures to the final bioreactor volume of usually more than 5000L. This means that several batches are generated from a single primary seed culture after WCB thaw. Therefore, for long industial-scale manufacturing runs a typical requirement for the “limit of in vitro cell age (LCA)” of a production cell line after WCB thaw would be 100 days or more.

Notably, this study shows that after about 60 days (25 passages) of culture both XBP-1(s)-expressing cell lines E23 and E27 expressed only 35% of their initial transgenic XBP-1 mRNA level. When the antibody productivity of cells of different age in culture was compared, both clones showed lower average Qp values in the fed-batch cultures initiated at later points in time. However, only for clone E27 was the decrease found to be significant, so that in summary the decrease in expression level could not be conclusively correlated with loss in antibody productivity. It is interesting to note, however, that in yeast a constitutively active UPR by overexpression of the yeast XBP-1 homolog Hac1p reduced cell growth (Cox and Walter, 1996), correlating with the observation in this study during the generation of XBP-1(s)-expressing clones E23 and E27. Such a growth impairment results in a negative selection pressure in long-term cultures. Cells circumventing high expression levels, e.g. by deletion of transgene copies, would overgrow cell lines expressing higher amounts of the

transgene. To test for such a possible negative impact of heterologous XBP-1(s) expression on growth and/or survival in CHO cells, colony formation experiments were carried out. It was shown that transfection of cells with the active spliced form of X-box-binding protein gave rise to 7 times fewer colonies when compared with mock transfected controls. In a similar set of experiments, the XBP-1 homolog Hac1p was overexpressed, resulting in smaller colonies (Cox and Walter, 1996), whereas in the present CHO-K1 cell study the size of colonies was the same when compared with the controls. As these colonies are the progeny of single cells, the colony count is a measure of the result of transfection efficiency, cell survival after transfection and attachment characteristics, in total a survival assay. To further dissect possible reasons for the lower colony counts, apoptosis induction was determined after 48 h in transiently transfected cells. A 25% higher apoptosis rate was found in XBP-1(s)-expressing cells when compared with controls. This increase can not solely account for the reduced colony counts but is one significant aspect contributing to the observed outcome. So far, a direct apoptosis induction by XBP-1(s) overexpression has not been reported in the literature. However, to date, four different activation routes for UPR-mediated apoptosis induction have been proposed: (i) Activation of the ER stress response element (ERSE) by ATF6 in the promotor region of CHOP (also known as growth arrest and DNA-damage-inducible protein GADD153) activates its expression and induction of apoptosis (Zinszner et al., 1998; Yoshida et al., 1998). (ii) The association of the cytosolic domain of activated IRE1α with TNF receptor-associated factor 2 (TRAF2) and apoptosis signal-regulating kinase 1 (ASK1) activates the c-Jun amino-terminal kinase (JNK) pathway to induce apoptosis (Urano et al., 2000). (iii) The activated IRE1α-TRAF2 complex can activate ER-associated procaspase-12 to induce death signalling via caspase 9 activation (Yoneda et al., 2001; Groenendyk and Michalak, 2005). (iv) The cytosolic Bcl-2 family members Bak and Bax, upon ER stress, modulate Ca^{2+} release from the ER, resulting in m-Calpain-mediated activation of caspase 12

as well as Ca^{2+}-mediated opening of the mitochondrial permeability transition pore (PTP) and subsequent cytochrome C release (Nakagawa and Yuan, 2000; Walter and Hajnoczky, 2005). Interestingly, the branching point with a link to the apoptotic signalling cascade was shown to be IRE1α in two signalling pathways. As this ER-membrane protein mediates the splicing of XBP-1(u) mRNA, it is located upstream of the XBP-1 signalling cascade. Therefore, it seems unlikely that apoptosis induction due to XBP-1(s) overexpression is transmitted by IRE1α. However, the spliced form of XBP-1 was shown to activate the ERSE element, controlling its own activity and also that of the pro-apoptotic protein CHOP (Yamamoto et al., 2004). The activation of the response element was lower when compared with activation via ATF6 binding, but it could be speculated that this activation might still be sufficient to induce cell death.

The complex protein regulation in mammalian cells employs redundant mechanisms for many of the important regulatory networks. Overexpression of a single protein may therefore not be enough to result in the desired phenotype, because negative feed-back mechanisms may counteract. The data in this study showed that the intracellular protein level of XBP-1(s) was low in stably transfected CHO cell lines and close to the detection limit even in nuclear extracts despite the fact that in this setup heterologous XBP-1(s) expression was driven by the strong CMV promotor. The low XBP-1(s) protein abundance in the nucleus could be explained by the finding that the protein encoded by the unspliced XBP-1 mRNA (XBP-1(u)) forms a complex with XBP-1(s) protein, overwriting its nuclear localization signal (Yoshida et al., 2006). Furthermore, the complex was found to degrade rapidly in the cytoplasm as a negative feedback loop for the transcriptional activity of XBP-1. This regulatory circuit under ER stress allows fine tuning of the stress response and might account for the low protein abundance since XBP-1(s) binds and transactivates its own promotor to increase the production of unspliced mRNA (costa-Alvear et al., 2007). The difficulty in detecting the

protein in Western blot is also supported by the fact that none of the studies evaluating effects of XBP-1(s) overexpression on cellular productivity showed Western blot results confirming XBP-1(s) protein expression (Tigges and Fussenegger, 2006; Ku et al., 2007; Ohya et al., 2007; Campos-da-Paz et al., 2008).

Taken together, the observed distinct survival disadvantage mediated by XBP-1(s) and the described regulatory loop to downregulate the XBP-1(s) levels potentially explain the observed low protein abundance in stably transfected CHO cell lines. Apoptosis induction in cells expressing high levels of XBP-1(s) would ultimately lead to outgrowth of low expressing cells. The feedback loop could then further decrease XBP-1(s) protein levels in stable cell lines and also account for the instability observed.

The use of the active splice form of XBP-1 was chosen because of its known physiological functions of ER expansion and chaperone induction which could contribute to enhanced heterologous protein secretion from an improved mammalian host cell line. The shown link to negative impacts by decreasing the number of surviving cells and apoptosis induction suggested the combination of anti-apoptosis engineering and secretion engineering by XBP-1(s) overexpression. Simultaneous engineering of mammalian cells with two transgenes has already been proposed (Fussenegger et al., 1997) and proven for simultaneous proliferation control by p27 and anti-apoptosis engineering by BclxL in CHO-K1 cells (Fussenegger et al., 1998). However, all previously tested multiple gene engineering approaches were conducted with different aims, such as growth enhancement combined with anti-apoptosis engineering (Ifandi and Al-Rubeai, 2003) or the combination of two anti-apoptosis proteins (Sauerwald et al., 2006). The present study provides the first data on the combination of a secretion-enhancing protein in combination with an anti-apoptotic protein.

7.3 Evaluation of a combinatorial cell engineering approach

The ultimate goal of the combined engineering approach by co-expressing secretion-enhancing XBP-1(s) and caspase inhibitor XIAP as anti-apoptosis regulator was the generation of highly productive cell lines. The basic hypothesis is that increasing the number of surviving cells with high XBP-1(s) expression leads to higher productive cell lines. According to the data presented in this study, reduction of the negative impacts of XBP-1(s) expression is crucial for implementing such a strategy.

It was shown that in CHO-K1 cells transiently transfected with both transgenes, XBP-1 dependent apoptosis induction was reduced by the action of XIAP. In addition, more colonies were found in a survival assay when CHO-K1 cells were stably transfected with both transgenes in the colony formation assay. Together, both results proved that: (i) human XIAP was functionally expressed in CHO cells, (ii) XIAP was able to decrease XBP-1(s) dependent apoptosis induction and (iii) XIAP was thus able to increase the number of cells surviving heterologous XBP-1(s) expression. In a next step, the approach was transferred to industrially more relevant CHO-DG44 derived suspension cultures. A well characterized IgG-producing and monoclonal cell line was transfected with novel bicistronic expression vectors encoding either XIAP or XBP-1(s) or both genes linked by an IRES element. The mAb productivity of polyclonal cell pools was assessed in seed-stock cultures as well as in fed-batch cultures. In both conditions, cell lines expressing both transgenes showed improved specific productivities when compared with mock transfected controls. In contrast, overexpression of either one of the examined proteins did not lead to altered productivities. It is important to note that these data originate from polyclonal cell populations. For XBP-1(s) it was shown and described in chapter 6.1 of this study that two clonal cell lines expressing the active transcription factor alone show elevated IgG1 levels compared with control cell lines. These data are therefore another indication that a significant amount of heterologous XBP-1(s)

protein is needed to affect productivity. A few studies have analyzed the effect of expressing XIAP alone in CHO cells. Although XIAP overexpression was shown to lower cell death after apoptosis induction by different stimuli in CHO-K1 and HEK293 cultures, no data for an improved fed-batch culture viability have been provided to date (Sauerwald et al., 2002; Sauerwald et al., 2003; Sauerwald et al., 2006). In none of the stably XIAP-expressing cell lines examined here, a significant impact on cell viability was observed under fed-batch conditions. Again, the expression level in stable cell lines could be a challenge to achieve positive effects in long-term fed-batch cultures. Similar observations were made for BclxL expression in CHO suspension cells, where the desired effect of a prolonged viability profile of batch cultures by BclxL overexpression was only observed after dhfr-based amplification of the BclxL gene (Meents et al., 2002). Despite any obvious effect of heterologous XIAP expression on cell viability, harvest titers of polyclonal stable cell lines were significantly improved for cell lines expressing both transgenes compared with the controls. The expression of both transgenes in cell pools was confirmed on the mRNA level by RT-PCR. In the case of XBP-1, the variance of expression level was high. Although the highest XBP-1 mRNA level of all cell lines generated was found in a cell pool expressing both transgenes, on average, the mRNA level of the transcription factor was on average not increased by XIAP co-expression. The work done in polyclonal cell populations did thus did not support the hypothesis that XIAP co-expression would lead to higher XBP-1(s) expression. Nevertheless, up to the point of polyclonal cell populations, the combination of secretion-enhancing protein XBP-1(s) and anti-apoptosis protein XIAP was shown to be effective in elevating the productivity of monoclonal antibodies under fed-batch conditions.

In a next step, heterogeneous cell lines were subjected to single cell cloning to test the engineering approach as comprehensively as possible compared with standard industrial cell line development programs. Unlike in the first study where limited dilution was applied, here a cloning procedure using flow cytometry was applied. Under the stringent conditions of

single cell cloning, XBP-1(s) transfected pool gave rise to lower numbers of surviving cells compared with mock transfected cells. The number of surviving cells expressing heterologous XIAP was insignificantly enhanced by 1% when compared with the mock control. Co-expression of XIAP improved the cloning efficiency when compared with solely XBP-1(s)-expressing clones for 2 out of 3 pools of the two transgene genotype. From pool no. 3 only two clonal cell lines grew. The reason for this deviation could be a technical problem within the flow cytometry device and may not be representative. Overall, the results of the cloning procedure of CHO suspension cells were in agreement with the data obtained in CFA experiments and support the theory that XIAP co-expression might allow high XBP-1(s) expressing cells to survive the cloning procedure.

The clones generated were then subjected to an immediate early clone screening procedure by determining product concentration before the cells were passaged for the first time as described recently (Kaufmann and Fieder, 2008). The 6 best producing clones out of 36 per genotype were selected. As anticipated for mock and XIAP transfected cells, equal numbers of clonal cell lines were selected from each pool for top 6 cell lines representing an even statistical distribution. However, for solely XBP-1(s) expressing clones, no clone was selected for the top 6 from pool no. 3 which showed highest XBP-1(s) expression. This observation would reflect the hypothesis that cells with high XBP-1(s) levels do not survive and consequently, no high producer cell lines could be selected. The number of cells surviving the cloning procedure was found to be lowest for pool no. 3 supporting this observation; the difference to the two other pools of this genotype, however, was not significant. By contrast, pool no. 1 of the polyclonal cell populations expressing both transgenes gave rise to 5 of the top 6 clones of this genotype. This cell pool showed highest XIAP and highest XBP-1(s) levels when compared with two further pools of this genotype. Here, in contrast to the single engineering approach, most of the selected clonal cell lines originated from the pool with the

highest levels of XBP-1(s) mRNA encoding the secretion-enhancing protein indicating that co-expression of XIAP possibly allowed high expressing XBP-1(s) cells to survive.

All clones were analyzed for transgene expression by real-time PCR and for selected clones by Western blot analysis. The mean XBP-1(s) expression was higher in cell lines co-expressing XIAP. However, maximum XBP-1(s) levels found were to be the same for cells expressing only XBP-1(s). In addition, the cloning procedure did not lead to cell lines expressing higher amounts of both transgenes. This unusual observation may be a result of the regulatory feed-back loop described above for XBP-1 (Yoshida et al., 2006). Furthermore, it needs to be taken into account that the protein level was close to Western blot detection limits regardless of the expression construct used and mRNA level measured, suggesting that not all mRNA was translated to protein. The data proved that XIAP co-expression can inhibit XBP-1(s) dependent apoptosis induction in transient studies; however, for stably transfected cell lines however, the XIAP level may not be sufficient to promote the survival of XBP-1(s) high-producing cell lines. Another possibility is that the described feed-back regulation for XBP-1(s) activity is the dominating effect.

When the productivity of the clonal cell lines was compared in seed-stock cultures and fed-batch cultivation, no significant differences between the genotypes compared were found in productivity and final titer. Despite the proven transgene expression no enhancement of specific or total antibody productivity was found for XBP-1(s) or double engineered clones. The expectations that engineered monoclonal cell lines will exhibit elevated XBP-1(s) levels and consequently higher specific productivities were not met: Although the average XBP-1(s) level was enhanced by XIAP co-expression, this initial set of experiments did not lead to the generation of cell lines with productivity levels that were not reached previously mentioned. During fed-batch cultivation, XBP-1(s) expressing cells again showed low cell concentrations resulting in lower harvest titers. By comparison, cell lines expressing XBP-1(s) and XIAP

showed high peak cell densities and higher mean titers. However, these differences were not statistically significant as the variance between the six selected clones was high for all genotypes. Again, as seen on the pool level, with regard to viability profiles XIAP expression did not correlate with prolonged or higher harvest viabilities. Despite the promising results with polyclonal cell lines, the engineering approach described did not lead to monoclonal cell lines with significantly higher specific productivities. One reason could be that no or only few cells expressing high amounts of XBP-1(s) survived the stringent cloning procedure. In favor of this hypothesis is the fact that during the cloning procedure lower cloning efficiencies were found for stably XBP-1(s)-expressing cells. To overcome this limitation limited dilution could be used to lower the stringency, thus increasing the probability of selecting for cells expressing higher amounts of XBP-1(s).

To ensure that a colony originates from a single-cell by limited dilution investigators commonly use two rounds of subcloning. The same result can be achieved using flow cytometry (FC) in a single cloning round in less time, the reason why many companies prefer this method. However, depositing a single cell in a 96-well plate exerts stress on the cells resulting in low numbers of outgrowing clonal cell lines. Thus, single cell deposition is a stringent selection step for cell survival and despite XIAP co-expression no XBP-1(s) high expressers could be enriched. The cloning procedure was one of the main differences between the studies evaluating the mono- and bicistronic engineering approach. This difference may also be the reason why no clones with elevated Qp were found for solely XBP-1(s) expressing cells.

Since a transgenic approach for generating superior host cells for biopharmaceutical production has to prove its applicability in all stages of a cell line development program, the performance of the tested transgene combination was not satisfactory. The described first attempt to increase the specific productivity by overexpressing two transgenes beyond the limits of expressing XBP-1 alone was not successful on the level of monoclonal cell lines - a

prerequisite for manufacturing – when the described cloning procedures were applied. While further studies are necessary to assess the potential of XBP-1(s) engineering the described detailed study emphasizes the need for stringent application of relevant experimental procedures to be able to truly evaluate cell engineering strategies.

7.4 Proteomic analysis of supernatant from suspension CHO cultures grown in chemically defined serum-free media

Describing the proteome of the cell culture supernatant of mammalian cells in production processes is a novel approach with the final aim of establishing new methods for sophisticated process monitoring and control. The proteomic analysis of cell culture supernatants up to now was mainly focused on the investigation of cell-cell communication (Wegrzyn et al., 2007) and the discovery of marker proteins secreted from cancer cells (Maurya et al., 2007). Initially, supernatant from IgG secreting CHO cells was tested for its total protein content to estimate the amount of protein present and to visualize the complexity and distribution of proteins present in the cell culture fluid. As expected, the protein constituent predominant by far in the cell culture media of a producer cell line was the antibody product as shown by SDS-PAGE for day four supernatant samples. To avoid detection limits for low abundance proteins, mock cell lines were created and a model cell line was selected with growth characteristics comparable to mAb producing cell lines. As the total protein content in the supernatant was too low for direct 2D analysis, an appropriate concentration method was established. Another challenge in this project was the lack of complete genomic sequences for any hamster organisms in public databases.

In an initial set of experiments the novel sample preparation procedure was evaluated and at the same time proteins identified using sequences from related organisms and novel CHO sequences accessible to Boehringer Ingelheim as part of a CHO sequencing consortium.

Three timepoints of a scale-down batch process were analyzed by 2D-DIGE analysis of the cell culture supernatant. Overall, 192 spots were analyzed from the master gel and from 91% of the spots a total of 189 proteins were identified when peptides were matched against SwissProt database.

During establishment of the method several questions had to be addressed. Several parameters could be used to normalize the analyzed samples, such as culture volume, cell number or protein concentration. Since the protein amount is crucial for comparable protein labelling among different samples as well as for the resolution on the 2D gel, this parameter was kept constant in all analyses. On the contrary, because of cell growth, applying equal sample volumes would result in highly variable protein amount among samples of different timepoints in batch and fed-batch experiments. However, since equal protein amounts were used per sample the high antibody concentration in the samples would lower the absolute amount of low abundance proteins to be present in the sample. Therefore, mock cell lines were generated to obtain representative supernatants without the therapeutic protein. The chosen mock cell line was characterized as growing with a comparable fed-batch growth profile as cells used typically for production. Since production cells and mock cell lines descended from a joint CHO-DG44 host cell line it is expected that their fed-batch cell culture supernatant proteome is highly similar.

In a next step, two concentration methods were compared to identify an appropriate method for enriching the proteins within the supernatant sample to concentrations high enough to allow subsequent 2D analysis. The two methods are based on different physicochemical principles, ultrafiltration selects proteins by size whereas precipitation depends on solubility. Even for early process phases, a single ultrafiltration step was found to result in sufficiently high protein concentrations concentrating the sample 60 to 100-fold. The integral of viable cell numbers (IVC) can be used for estimating the accumulated secreted protein in the cell culture fluid. In this study, when $0.3x10^6$cells/mL were seeded to initiate batch cultures, on

day 2 the IVC reached a value of about 1 x 10^6 cells/(mL*d) then increasing to 7 x 10^6 cells/(mL*d) on d6. This illustrates the dramatic increase in host cell protein content in the supernatant of batch and fed-batch cultures during fermentation. Furthermore, ultrafiltration was regarded as highly reproducible (Dr. Lenter personal communication). On the other hand, precipitation of proteins using TCA is less time consuming and easy to handle. However, it was found to result in less protein spots and to some extend in lower spot intensities. Additionally, the precipitation method did not improve individual spot focusing when compared with the filtration method. Proteins smaller than 10 kD which are lost by the filtration method using 10 kD cut-off membrane are precipitated and are part of the sample. However, the minimum protein size detectable on 2D gels is about 15 kD to 20 kD; precipitation is therefore not advantageous for the aim of this project. For these reasons, ultrafiltration was selected as best concentration method for further experiments.

Another hurdle was the vertical and horizontal streaking seen on 2D gels of the initial experiments. It was found that the media additive Pluronic® was partially responsible for these effects. Furthermore, a screen with different cell culture media was conducted and finally, a commercially available medium was selected which showed sufficient resolution for this 2D gel study.

The aim of this study was to be able to detect as many proteins as possible and to globally describe the cell culture fluid proteome. Therefore, the broadest pH range available, ranging from pH 3 to pH 10, was chosen for the first dimension. Decreasing this range would ultimately enhance protein separation but at the same time be a preselection and exclude proteins from the analysis. The broad pH range used could also be the reason for the fact that up to 40% of the spots analyzed contained more than one protein.

Differential gel electrophoresis was selected as the method of choice for its ability to enable quantification of differences between two samples. The modified 2D gel electrophoresis (2D-GE) was shown to be highly reproducible, sensitive and enabling comparison of two

samples on a single gel and named 2D-DIGE (2D differential gel electrophoresis) (Unlu et al., 1997). Furthermore, the comparison of more than one gel is enabled by the use of a so-called internal standard representing a mixture of all analyzed samples present on all gels. Thus, the method is a valuable tool for the large-scale analysis of process samples collected at different timepoints during cell cultures. Additionally, multiple samples can be combined to one study when the information of different gels is analyzed thus the abundance of individual proteins over time can be analyzed.

To finally establish and test the whole sample preparation and separation procedure, a differential display of proteins from cell lysates and proteins from concentrated supernatant was performed. Proteins originating from cell culture supernatant were found over the full ranges of pH and size, thus confirming that the ultrafiltration method did not preselect for proteins with certain characteristics. The 2D separation was controlled by using the cell lysates sample.

To test the entire established workflow for the analysis of cell culture supernatant from sample preparation to protein identification, an experiment using batch cultures was performed and samples were collected at three different timepoints namely d2, d3 and d6. The comparison of protein abundance in d2 and d6 samples revealed a total of 65 differentially abundant protein spots. These spots and an additional 127 spots that were not altered between the samples were chosen for MS analysis. Despite the incomplete sequence information on the CHO genome 91% of the spots could be assigned to at least one protein using SwissProt database and additional BI data on CHO sequences. This result confirmed that by applying the workflow it was possible to generate samples from culture supernatants that had sufficient quality and protein amount to visualize the cell culture fluid proteome on 2D-GE and finally gave rise to annotated protein identities. Certainly, these data need to be verified by a second independent method such as Western blot for accurate interpretation of the results. To start this verification process, one protein identified as stress-induced phosphoprotein 1 (STIP1)

was selected for further analysis. The protein was analyzed by the 2D-DIGE method to be 2.3 times less abundant on d6 compared with d2 based on a protein content normalization. A comparable value of a 2.0-fold decrease was found when concentrated supernatant from an independent experiment was analyzed by Western blot confirming identity as well as the change of protein abundance over time. It is unclear whether the 2-fold change in protein abundance was actively regulated by the cells or if STIP1 is being degraded by proteolytic cleavage during cell culture in the supernatant. The relevance of the protein to be used for process monitoring or process control needs further investigation correlating the concentration of this protein with a distinct cellular status relevant to the process. In addition, a higher sampling frequency would enable protein kinetics to be followed in more detail.

Identified marker proteins such as the concentration of critical proteases can be evaluated for their use to determine for example the harvest timepoint of sensitive therapeutic proteins such as coagulation factors or hormones. These types of protein products are prone to proteolytic cleavage and the harvest timepoint can be a critical process parameter (Sandberg et al., 2006). Additionally, if marker proteins were found to be indicative of changes in cellular status, for example cell viability, this would open up the opportunity to adopt and develop more sophisticated feeding strategies. Another field of interest is the search for autocrine growth factors secreted by the autonomously growing cell. Only a few studies have investigated cell culture supernatants. Secreted autocrine growth factors were analyzed with the aim of enhancing growth of recombinant cell lines by modifying of media formulations (Spens and Haggstrom, 2005). Using size exclusion chromatography, the authors were able to select a fraction of supernatant which positively affected cell growth of the NS0 cell line under investigation. The identification of the exact autocrine growth factor postulated is still pending. However, in another study, authors applied a modified mass spectrometry method to

analyze secreted proteins from adherently growing CHO cells but did not report any annotation (Kumar et al., 2007).

To our knowledge, the established method is the first report investigating proteomic changes in the supernatant of production processes of suspension CHO cells. The method can now be used as a basis for the thorough investigation of changes in process supernatants to identify possible marker proteins for the development of next-generation process control and feeding strategies.

8 MATERIALS AND METHODS

All materials, unless mentioned otherwise, were obtained from Sigma-Aldrich, Schnelldorf, Germany.

8.1 Cell culture

CHO-K1 (ATCC CRL-9618) cells were maintained as monolayer in F12 medium (Invitrogen, Karlsruhe, Germany) supplemented with 5% fetal calf serum (FCS) (Biological Industries, Kibbutz Beit Haemek, Israel). The cells were incubated in surface-aerated T-flasks (Thermo Fisher Scientific, Waltham, USA) in humidified incubators (Thermo Fisher Scientific, Waltham, USA) with 5% CO_2 at 37°C. The cultures were split by trypsination and re-seeding twice a week. The seeding density was typically 3-6×10^4 cells/cm^2, allowing the cells to reach confluency in 3-4 days.

Suspension cultures of monoclonal antibody (mAb) producing CHO DG44 cells (Urlaub et al., 1986) and stable transfectants thereof were incubated in Boehringer-Ingelheim (BI) proprietary chemically defined, serum-free medium. Seed-stock cultures were sub-cultivated every 2–3 days with seeding densities of 3 ×10^5–2 × 10^5 cells/mL, respectively. The cells were grown in T-flasks or shake flasks (Thermo Fisher Scientific, Waltham, USA). The T-flasks were incubated in humidified incubators (Thermo Fisher Scientific, Waltham, USA) and the shake flasks in Multitron HT incubators (Infors HT, Bottmingen, Switzerland) at 5% CO_2, 37°C and 120 rpm.

Cell concentration and viability were determined either by trypan blue exclusion using a Fuchs-Rosenthal hemocytometer (Brand, Wertheim, Germany) or the automated CEDEX system (Innovatis, Bielefeld, Germany).

8.2 Expression vectors

The pCDNA3-XBP-1(s) was kindly provided by Prof. Fussenegger (ETH Zurich, Switzerland) and contained the spliced variant of human X-box-binding protein-1.

pCDNA3-XBP-1(s) was *Xba*I digested and blunted using Klenow enzyme. A second digestion was carried out using *Hind*III. The fragment was then cloned into pBIP (BI proprietary), which was *BsrG*I (blunt) and *Hind*III digested (all enzymes were obtained from New England Biolabs, Ipswich, USA), resulting in pBIP-XBP-1. For selection of stably transfected cells, the pBIP vector contained a puromycin resistance cassette. Expression of the heterologous gene was driven by a CMV promoter/enhancer combination.

For the generation of a bicistronic expression construct, both multiple cloning sites and the IRES of pIRES (Clontech, Mountain View, USA) were cloned into the MCS of the pBIP vector. For this purpose, pIRES was digested with *Not*I and blunted by Klenow enzyme. Next, the vector was digested with *EcoR*I. The pBIP vector was digested with BsrGI (blunt) and *EcoR*I. Ligation resulted in the pBIP-IRES vector.

For expression of the anti-apoptotic protein X-linked inhibitor of apoptosis (XIAP) from the first cistron, the ImaGenes (formerly RZPB) full-length cDNA clone IRATp970H0655D (human XIAP, IMAGE ID 5532247) was employed (ImaGenes, Berlin, Germany). The pCMV-SPORT6 vector obtained was digested with *EcoR*I and the 1678 bp insert encoding XIAP ligated to pBI15P (BI proprietary) as shuttle vector. The resulting pBI15P-XIAP vector was digested with *Sal*I and *EcoR*I and the fragment cloned into *Xho*I and *EcoR*I cut pBIP-IRES to give pBIP-IRES-XIAP.

To clone the XBP-1(s) sequence into the second cistron, an *Xba*I restriction site was added 5’ and 3’ by PCR reaction using the pCDNA3-XBP-1(s) as template and the following primers:

XBP1-*Xba*I-for: 5’CCAATT*TCTAGA*ATGGTGGTGGTGGCAGCCGC3’ and

XBP1-Flag-*Xba*I-rev:

5'CCAATT*TCTAGA*TTA***CTTATCGTCGTCATCCTTGTAATC***GACACTAATCAGCTGG GGAAAG3' adding a ***Flag-Tag*** to the C-terminus of the protein as well. The resulting fragment was *Xba*I digested and cloned either into pBIP-IRES or pBIP-IRES-XIAP to give pBIP-IRES-XBP1 and pBIP-IRES-XIAP-XBP1, respectively.

Table 3: Plasmid overview showing name, insert, backbone, resistance (Neomycin (G418 = neo, puromycin = puro, ampicillin = amp) and the origin of the different plasmids

Name	Insert	Backbone/Resistance	Origin
pCDNA3-XBP1(s)	Human spliced XBP-1	pCDNA3 / neo	Prof. Fussenegger (ETH Zurich)
pBIP	none	pBIP / puro	Dr. Florin (BI)
pBIP-XBP1	Human spliced XBP-1	pBIP / puro	constructed
pBI15P	IRES GFP	pBIP / puro	Dr. Enenkel (BI)
pIRES	MCS-IRES-MCS	pIRES / neo	Commercial (Clonetech)
pBIP-IRES	MCS-IRES-MCS	pBIP / puro	constructed
pBIP-IRES-XBP1	Human spliced XBP-1-Flag (2nd Cistron)	pBIP-IRES / puro	constructed
pBIP-IRES-XIAP	Human XIAP (1st Cistron)	pBIP-IRES / puro	constructed
pBIP-IRES-XIAP-XBP1	Human spliced XBP-1-Flag	pBIP-IRES / puro	constructed
pBI15P-XIAP	Human XIAP -IRES-GFP	pBI15P / puro	constructed
pCMV-SPORT6-XIAP	Human XIAP	pCMV-SPORT6 / amp	Commercial (ImaGenes)

8.3 Generation of stable CHO cell lines

All cells were transfected in 6-well plates using Lipofectamine™ and Plus™ reagent (Invitrogen, Karlsruhe, Germany) according to the manufacturer's protocol. CHO-K1 cells were seeded 24 h prior to transfection with 1.5×10^5 cells/well to reach 50-60% confluency. Prior to the addition of the transfection mixture, the cells were washed with PBS and 1 mL of serum-free growth medium was added. Best results were obtained using 1 µg DNA, 6 µL of Plus™ reagent and 4 µL of Lipofectamine™. After 3 h, the serum concentration was restored by adding 1 mL of medium supplemented with 10% FCS. CHO-DG44-derived suspension cells were transfected at a concentration of 7.5×10^5 cells/mL in CHO-S-SFMII medium (Invitrogen, Karlsruhe, Germany) according to the same, but serum-free protocol.

For the generation of stably transfected cell populations from DG44 derivatives, the antibiotic puromycin was added 48 h after transfection at a concentration of 5 to 10 mg/L. Suspension cells were cultivated in static cultures until growth was observed by microscopic inspection and then subjected to seedstock cultivation in shake flasks in chemically defined BI proprietary medium.

Clones were generated either by limited dilution or flow cytometry, or fluorescence-activated cell scanning or sorting (FACS).

8.4 Limited dilution

Limited dilution was one way to obtain clones of single-cell origin. For limited dilution cells were seeded in twelve 96-well plates corresponding to cell densities in the range between 0.3 cells/well to 640 cells/well. After one week under growth condition plates were microscopically inspected for cell growth and wells with monoclonal growing cell lines were

marked. After an additional week under growth conditions, monoclonal cell lines were further expanded and analyzed.

8.5 Single cell cloning by cell sorting

Flow cytometric single cell sorting is designed to selectively deposit cells from particular populations into tubes or other collection vessels (e.g. well). These sorted cells, essentially unharmed by the process, can then be used for further culturing or experimental analysis. In order to sort the cells, the sorter electronics interprets the signals collected for each cell as it is interrogated by the laser beam, and compares the signals with the sorting criterion settings. If the cell meets the criteria, an electrical charge is applied to the liquid cell stream which is being accurately broken into droplets containing the cell. This charge is applied to the stream at the precise moment the cell of interest is about to break off the stream, and removed once the charged droplet has broken from the stream. As the droplets fall, they pass between two metal plates strongly positively or negatively charged. These charged droplets are drawn towards the metal plate of the opposite polarity, and deposited in the collection well.

Autologous feeder cells were used to increase cloning efficiency from single-cell cloning using the cell sorter. After irradiation with 100 Gy from a Cs137 gamma ray source 10,000 feeder cells were plated per well in growth medium containing the appropriate selection antibiotics one day prior SCC. For SCC exponentially growing cell pools were centrifuged for 5 min at 200 g and washed in HBSS (Invitrogen, Karlsruhe, Germany). After an additional centrifugation step the cells were resuspended in HBSS and filtered through a 70 µm cell strainer sieve (BD Biosciences, Erembodegem, Belgium) to remove cell aggregates. The cell suspension was then sorted using the auto clone program of an Epics Altra Hss cell sorter (Beckman Coulter, Fullerton, USA) and small cells of the living gate (forward/side scatter

diagram) were plated into the previously prepared 96-well plates as single-cells. The plates were the cultivated under growth conditions to allow single-cells to grow and form colonies. After 12 to 16 days the colonies were large enough for further expansion and analysis. To asses the colony size in 96-well plates, colonies were classified in three categories (small, medium, large) by microscopic inspection or colony size was measured by the CloneSelect™ Imager (Genetix Ltd., New Milton, UK).

8.6 ER-quantification

For the quantification of the endoplasmic reticulum, ER-Tracker™Green (Invitrogen, Karlsruhe, Germany), a fluorescently labeled antidiabetes drug glibenclamide was used. The drug binds to sulfonylurea receptors of ATP-sensitive K+ channels prominent in the ER membrane (Hambrock et al., 2002). CHO-K1 cells were transfected with mock plasmids containing either neomycin or puromycin resistance genes or with an XBP-1 expression construct carrying a puromycin resistance cassette. After 48 h, cells were harvested by trypsination and centrifuged for 5 min at 200 g. For ER staining, 1×10^6 cells were resuspended in 400 µL of glucose-containing phosphate-buffered saline (HBSS, Invitrogen, Karlsruhe, Germany) containing 2 mM ER-Tracker™Green and incubated for 15 min at 37°C. The cells were washed with HBSS. For detection, the cells were resuspended in 400 µL of HBSS and living cells were analyzed for green fluorescence by flow cytometry using a Beckmann Coulter Epics XL MCL at ex/em wavelength 488/524 nm (Beckman Coulter, Fullerton, USA).

8.7 Preparation of cell lysates and Western Blot

For specific detection of proteins, they were separated according to size and transferred to a membrane where immunological detection was based on specific antibody binding. For visualization and detection, either an enzyme-linked secondary antibody or a near infrared dye (NIR)-labeled antibody was used.

For whole cell lysates, 5 x 10^6 cells were pelleted by centrifugation for 5 min at 200 g, washed in ice-cold PBS and resuspended in lysis buffer (see below) and incubated for 15 min on ice. The cell debris was pelleted for 10 min at 16,000 g, and the supernatant was further analyzed.

For nuclear extracts, 5 x 10^6 cells were pelleted by centrifugation for 5 min at 200 g and washed in ice-cold PBS. The pellet was resuspended in 250 µL of NP40 buffer (see below) and incubated for 5 min on ice to lyse cells. Nuclei were spun down for 5 min at 800 g. The pellet was washed in 500 µL of CE buffer (see below) and nuclei were then resuspended in 250 µL of NE buffer (see below) and broken up with three freeze-thaw cycles (liquid nitrogen and 37°C water bath). Debris was pelleted for 10 min at 16,000 g, and the supernatant was further analyzed.

To determine the protein concentration of the lysates, the bicinchoninic acid assay (BCA) was used (Smith et al., 1985). The lysates were diluted 1:10 in PBS and 25 µL was mixed with 175 µL of freshly prepared reagent according to the manufacturer's protocol. The samples were incubated at 37°C for 30 min and color formation was measured at 562 nm with an absorbance reader (Tecan, Maennedorf, Switzerland). To calculate the protein concentration, the absorbance of the samples was compared with the absorbance of a bovine serum albumin (BSA) standard curve.

For Western blot analysis, equal volumes of nuclear extracts or equal amounts of protein from whole cell lysates were separated on a NuPAGE 10% Bis-Tris-gel (Invitrogen, Karlsruhe, Germany) with MOPS buffer according to the manufacturer's protocol. The proteins were transferred onto a nitrocellulose or PVDF membrane (Millipore, Billerica, USA) using transfer buffer in an XCell II blot module (all Invitrogen, Karlsruhe, Germany). Blocking was run for 1 h at room temperature with blocking reagent (Invitrogen, Karlsruhe, Germany).

	Lysis buffer	**NP40 buffer**	**CE buffer**	**NE buffer**
NP40	1%	0.5%	none	none
HEPES	50 mM	10 mM	10 mM	none
KCl	none	10 mM	10 mM	60 mM
Tris	none	none	none	250 mM
EDTA	1 mM	1 mM	1 mM	1 mM
EGTA	5 mM	none	none	none
NaCl	150 mM	none	none	none
NaF	25 mM	none	none	none
Complete	40 µL/mL	40 µL/mL	40 µL/mL	40 µL/mL

Rabbit anti-XBP-1 (Biolegend, San Diego, USA) was used as primary antibody in 1:1,000 dilution. The secondary antibody was goat anti-rabbit IgG (H+L) HRP Conjugate (BioRad, Hercules, USA) in 1:10000 dilution or goat anti-rabbit NIR800-coupled antibody (1:15000, Licor Biosciences, Lincoln, USA). As loading controls mouse anti-actin (1:1000) and rabbit anti-Histone H3 (1:5000, kindly provided by Dr. Olayioye, University Stuttgart, Germany) were used. For detection the ECL Plus system (GE Healthcare, Munich, Germany) was used. For the detection of XIAP the rabbit anti-XIAP antibody (3b6, Cell Signaling, Danvers, USA) was used in a 1:1,000 dilution. For visualization the NIRdye-coupled secondary antibody goat anti-rabbit NIR800 coupled (1:15000, Licor Biosciences, Lincoln, USA) was used and scanned with the Odyssey scanning system (Licor Biosciences, Lincoln, USA). Detection of stress-induced phosphoprotein 1 (STIP1) was done by use of a polyclonal rabbit anti-STIP1

antibody (Abcam, Cambridge, UK) in 1:500 dilution. For visualization, the aforementioned secondary goat anti-rabbit NIR800 antibody was used in 1:15000 dilution.

8.8 Fed-batch cultivation

To simulate a production process, the cells were cultivated in shake flasks over a period of 10 days with daily feeding and daily addition of pH correction media.

The cells were seeded at 2.5 to $3x10^5$ cells/mL into shake flasks in BI-proprietary production medium without antibiotics or MTX. The cultures were agitated at 120 rpm at 37°C and 5% CO_2 which was later reduced to 2% as cell numbers increased. Culture parameters (including pH, glucose and lactate concentrations) were determined daily and the pH was adjusted to 7.0 using $NaCO_3$ as required. BI-proprietary feed solution was added every 24 h. Cell densities and viability were determined by trypan-blue exclusion using an automated CEDEX cell quantification system (Innovatis, Bielefeld, Germany). Samples from the cell culture fluid were collected and subjected to titer measurement by enzyme-linked immunosorbent assay (ELISA).

Cumulative specific productivity was calculated as product concentration on the given day divided by the integral of viable cells (IVC) at this point in time.

8.9 Product quantification by ELISA

Monoclonal antibody concentration was determined by ELISA or homogeneous time-resolved fluorescence assay (HTRF®assay). For ELISA, the protein of interest was captured by an immobilized first antibody followed by the binding of an enzyme-labeled second

antibody. For quantification, an enzymatic-driven change in color was measured and the absorbance of the samples was compared with the absorbance of a standard curve.

For ELISA detection of the mAb product, anti-human Fc-fragment (Jackson Immuno Research Laboratories, Newmarket, UK) and anti-human kappa light chain HRP conjugated were used as capture and detection antibodies, respectively.

8.10 Product quantification by HTRF assay

The HTRF® assay generates a signal by fluorescence resonance energy transfer (FRET) between donor and acceptor molecule. Laser excitation of the donor at 337 nm results in the transfer of energy to the acceptor when in close proximity (~690 A°), leading to the emission of light at 665 nm which can be detected using an Ultra Evolution Reader (Tecan, Maennedorf, Switzerland). The donor, europium cryptate, was coupled to the capture antibody and the acceptor D2 was coupled to the anti-human kappa light chain antibody. The coupling was carried out by Cisbio (Bagnols-sur-Cèze Cedex, France). For analysis, the sample was diluted in cell culture medium to an estimated antibody concentration of 10 ng/mL. Four serial 1:2 dilution steps were carried out and 10µL of each dilution transferred in a well of 384-well plate. To start the detection reaction, 5 µL of donor and 5 µL of acceptor antibody (both at a concentration of 400 ng/mL) were added and incubated for 2 h at room temperature. After incubation, signal intensity was determined using the aforementioned reader with ex./em. wavelength 337 nm/665 nm, respectively. For quantification, the signal intensity was compared with the signal intensity of a standard curve ranging from 25 ng/mL to 1.5 ng/mL of purified reference antibody.

8.11 Product quality analysis

Electrophoretic methods where used to investigate the size distribution and possible fragmentation as well as the isoelectric point of the mAb produced. The speed of protein movement in an electric field depends on protein size and was used for separation in sodium dodecylsulfate polyacrylamide gel electrophoresis (SDS-PAGE). Isoelectric focusing (IEF) was used to separate the proteins, based on their charge. In an electric field, proteins move to the pH where they are uncharged.

The mAb product was purified by chromatography using an rProtein-A column and the purified product was analyzed by SDS-PAGE (4-15% Bis-Tris) according to Heukeshoven and Dernick (1988).

For isoelectric focusing, 0.1 µg of antibody was applied to Phast Dry IEF gels (GE Healthcare, Munich, Germany) and proteins were separated according to the manufacturer's protocol using 80% Pharmalyte (8-10.5) and 20% Servalyte (3-10). Staining was performed as described by Heukeshoven and Dernick including a prior washing step with 20% trichloro-acetic acid for 5 min at 20°C to remove the ampholyte (Heukeshoven and Dernick, 1988). Both quality analysis were conducted in the laboratory of Dr. Jacobi in the purification development department.

8.12 Carbohydrate mapping

To differentiate carbohydrates linked to the monoclonal antibody, they were enzymatically released from the antibody and separated by high pressure liquid chromatography (HPLC).

The samples and the reference standard were diluted with enzyme buffer (50 mM phospate pH 7.5), purified water and reduction reagent. The samples were incubated for 10 min at 56°C. 25 µL of Triton X-100 solution was added to each sample, the solutions were mixed

and 5 µL of PNGase F (Roche Diagnostics, Mannheim, Germany) was added. The samples were then incubated overnight at 37°C. They were then desalted by polygraphitized carbon (solid-phase extraction) and dried (TurboVap LV Evaporator, Zymark). Dried samples were labeled with 2-AB for 2 h at 65°C and purified by amino-cartridges. Purified and dried samples were analyzed using an amide 80- column with a gradient of acetonitrile/ammonia/formic acid pH 4.0. The flow rate was set to 0.4 mL/min (HPLC Spectra System, Thermo Fisher Scientific, Waltham, USA). The analysis was performed in the quality control laboratory of Dr. Kopp.

8.13 Colony formation assay

For investigating the survival ability of cells after transfection of different transgenes the cells were plated in low densities. Growing cells form individual colonies which can then be quantified. The CHO-K1 cell line was transfected with plasmids as described in Chapter 8.3. One day after transfection the cells were trypsinated and counted using the CASY® cell counter (Innovatis, Bielefeld, Germany). Either one well of a 6-well plate or $1x10^5$ cells were plated in fresh cell culture medium on a 10 cm cell culture dish (Thermo Fisher Scientific, Waltham, USA). The culture dishes were incubated overnight under standard conditions (37°C, 5% CO_2) to allow the cells to adhere. On the day following the re-plating, the selection antibiotic puromycin was added (15 mg/L). The dishes were then incubated in a humidified atmosphere containing 5% CO_2 at 37°C for 12 to 14 days. Because of the selection antibiotic, only stably transfected cells survived and formed individual colonies large enough for counting. The plates were washed in PBS and fixed in ice-cold acteon/methanol (1:1) for 5 min. After a wash with water, a freshly made Giemsa solution was added for 15 min to stain the cells. The stain was washed away with water and the dishes were air-dried. Finally, the blue colonies were counted manually.

8.14 Apoptosis assay

To analyze cell death by apoptosis the high-affinity binding of Annexin V to phosphatidylserine was used. Fluorescently labeled Annexin V binding could then be quantified by FACS. For counterstaining, the DNA-binding fluorescent dye propidium iodide (PI) was used. PI can only penetrate a damaged plasma membrane such as is found in necrosis and the endphase of apoptosis. Consequently, the method can differentiate between healthy (Annexin V and PI negative), early apoptotic (Annexin V positive, PI negative), late apoptotic (Annexin V positive, PI positive) and necrotic cells (only PI positive).

To detect apoptotic cells, the Annexin V-FITC Kit I (No.: 556547) from BD Biosciences (Erembodegem, Belgium) was used according to the manufacturer's protocol. Equal cell numbers were washed with PBS and resuspended in binding buffer. For staining, 100 µL of the cell suspension was transferred to a new reaction tube and 5 µL of an Annexin V conjugate followed by 2 µL of propidium iodide (PI) for counterstaining were added. After an incubation period of 20 min in the dark, the cells were resuspended in 400 µL of PBS and analyzed by a flow cytometer (Beckmann Coulter Epics XL MCL ex./em. wavelength for FITC 488/524 nm and for PI 488/620 nm).

8.15 RNA isolation and cDNA synthesis

To compare and quantify the abundance of specific transcripts in the different cell lines, total RNA was isolated and mRNA was reverse transcribed into cDNA.

$5x10^6$ cells were washed in PBS and lysed in 1 mL of TRIzol® (Invitrogen, Karlsruhe, Germany). For RNA preparation, 100 µL of chloroform was added to 500 µL of TRIzol solution and the mixture was incubated for 5 min at room temperature. To separate the two phases, the solution was centrifuged for 5 min at 13,000 g. The chloroform phase containing

the RNA was then transferred in a fresh tube where 250 µL isopropanol was added and the mixture was incubated for 10 min. The RNA was pelleted at 13,000 g for 10 min and washed in 500 µL of ethanol (75%). The pellet was dried and dissolved in 50 µL of diethylpyrocarbonate (DEPC)- treated water. For cDNA synthesis, 4 µg RNA were reverse transcribed using the Cloned AMV First-Strand cDNA Synthesis Kit (Invitrogen, Karlsruhe, Germany) according to the manufacturer's protocol. The kit contains oligo d(T) and random hexamer primers.

8.16 RT-PCR (quantitative)

Real-time PCR or qPCR was used for quantification of specific mRNA transcript levels. Here, the cDNA is quantified after each amplification cycle by measuring the fluorescence intensity of an intercalating dye. Relative concentrations of DNA present were determined by plotting fluorescence against cycle number on a logarithmic scale. The cycle at which the fluorescence from a sample crossed the threshold (cycle threshold = cT) was taken for sample comparison.

For quantitative mRNA analysis, 1 µL of cDNA was mixed with 1x diluted Sybr®-Green 2x Mastermix (Applied Biosystems, Foster City, USA), 10 nmol of forward Primer, 10 nmol of reverse Primer and 17 µL of water. Triplicate samples were measured in an iCycler iQ5 (BioRad, Hercules, USA) according to the manufacturer's protocol. The annealing temperature was 58°C and data were collected at the end of every 72°C extension cycle.

For normalization the housekeeping gene beta tubulin was measured for each sample in triplicate and its mean cycle threshold (cT value) subtracted from the mean cT from the gene of interest. The primers used were as follows:

Tub_for: 5'CTCAACGCCGACCTGCGCAAG3',

Tub_rev: 5’ACTCGCTGGTGTACCAGTGC3’,

XBP1_for: 5’TGGTTGAGAACCAGGAGTTA3’,

XBP1_rev: 5’GCTTCCAGCTTGGCTGATG3’,

XIAP_for: 5’GACTCAGCAGTTGGAAGAC3’,

XIAP_rev: 5’GTCCAGCACTTGCTAACTC3’

8.17 RT- PCR (semi quantitative)

For reverse transcription PCR 1 µL of cDNA was mixed with 10 nmol of forward primer, 10 nmol of reverse primer, 7.5 µL of 2x Green master mix (Invitrogen, Karlsruhe, Germany) and 4.5 µL of water. The primers and conditions used were the same as for qPCR (see 8.16). A MyCycler thermocycler (BioRad, Hercules, USA) was used for temperature control..

8.18 Modified medium and batch procedure for 2D-DIGE analysis

For the 2D-DIGE analysis of proteins in the supernatant of suspension CHO cells grown in chemically defined serum-free batch cultures, a medium free of detergent Pluronic® F68 was used (CD-DG44 Medium, Invitrogen, Karlsruhe, Germany). Pluronic® F68 was developed as a serum replacement to protect cells from shear stress arising from sparging and agitation in bioreactors (Papoutsakis, 1991). Pluronic® F68 is a water-soluble triblock copolymer of polyethylene oxide (PEO) and polypropylene oxide (PPO) of 8.4 kDa acting as non-ionic surfactant (BASF Corporation, 2004). With the characteristics of size and hydroxyl groups F68 was expected to disturb the protein separation in 2D analysis.

For the analysis of batch cultures, the CD-DG44 medium was supplemented with 800 mg/L of glutamine and cells were grown with a starting cell density of 3 x10^5cells/mL in shake flasks. A clonal cell line derived from DG44 stably transfected with mock plasmid was used as model cell not secreting an antibody product. The cell line was selected for the same growth profile in fed-batch cultures when compared with cells secreting different therapeutic antibodies. The transfection and selection of polyclonal cells was carried out by Dr. Florin. Cloning, selection and characterization of the monoclonal cell lines was accomplished during the course of this work.

8.19 Concentration of cell culture supernatant

The protein concentration in batch cultures of suspension CHO cells was too low for the direct analysis by two-dimensional gel electrophoresis (2D-GE). Therefore, the supernatant was concentrated 100-fold by ultrafiltration.

The cells were separated by centrifugation for 5 min at 200 g followed by a further 10 min 3,000 g centrifugation step to clear cellular debris. To prevent protease activity, Pefabloc SC (Roche Diagnostics, Mannheim, Germany) was added in 100 µg/mL concentration. 20 mL of supernatant was transferred to a 10 kD Vivaspin tube (polyethersulfone membrane (PES), Sartorius, Goettingen, Germany) and concentrated by centrifugation for 1 h at 4,000 g and 4°C. The specification “10 kDa” refers to the nominal membrane cut-off retaining molecules bigger than 10 kDa in the retentate and molecules smaller in the flow-through filtrate. The concentrate (typically < 1 mL) was washed by adding 20 mL of PBS followed by centrifugation under the conditions described above. The remaining concentrated protein solution was then transferred with PBS into a 2 mL Vivaspin followed by a further centrifugation step. The 2 mL tube comprises a 5 kD PES cut-off membrane. After

concentration, DIGE buffer (see below) was added three times after subsequent centrifugation steps. The final sample volume was adjusted to 200 µL and the samples were stored at -70°C for further analysis.

DIGE buffer:	Urea	7 M
	Thiourea	2 M
	CHAPS	4%
	TrisHCl	30 mM

The DIGE buffer was purified with a slurry of 1% ion-exchange resin Amberlite™ IRN-150L (GE Healthcare, Munich, Germany) for 1 h at room temperature followed by filtration to remove the resin.

For comparison the precipitation of proteins was also tested. Precipitation was carried out using trichloroacetic acid (TCA). TCA removes the hydrate shell around the proteins by displacing water which results in precipitate formation.

The supernatant was prepared as described above by sequential centrifugation at 180 g and 3,000 g. Then, 1.8 mL supernatant were mixed with 200 µL TCA to result in a 10% TCA solution. The mixture was incubated for 30 min on ice and then centrifuged for 5 min at 15,000 g at 4°C. The pellet was washed in 500µL ice-cold acetone and air dried. Finally, the protein pellet was dissolved in 200µL DIGE buffer and stored at -70°C for further analysis.

8.20 Determination of protein concentration

Bradford 5x concentrate (BioRad, Hercules, USA) was used to determine the protein concentration. The samples were diluted in distilled H_2O to appropriate concentrations <10 µg/mL and 50 µL dilutions were analyzed in duplicate by addition of 150 µL 1:3.8 diluted Bradford reagent in 96-well plates. After incubation for 20 min at room temperature in

the dark, the samples were analyzed at 595 nm in an absorption reader (Tecan, Maennedorf, Switzerland). The sample absorption was compared with the absorption of a BSA standard curve ranging from 0 to10 µg/mL of BSA protein.

8.21 CyDye labeling of samples

All analyzes described in the following were carried out by the proteome research laboratory staff of PD Dr. Lenter.

Differential two-dimensional gel electrophoresis (2D-DIGE) is based on labeling two samples with different fluorescent dyes. When the proteins of both samples are separated by 2D electrophoresis on a single gel, the individual protein abundance of each spot can be assigned to the corresponding sample.

For analytical gels, 50 µg of protein from each sample was labeled with 400 pmol of CyDye. The internal standard (mixture of all samples) was labeled with Cy2. The samples from different days of the batch culture were labeled either with Cy3 or Cy5. At least one of the triplicate samples was labeled different from the others to prevent a dye bias, as the dye may influence the protein spot position on the gel. After 30 min incubation on ice (in the dark) the labeling reaction was stopped by the addition of 1 µL of 10 mM lysine. After additional 10 min on ice (in the dark) the labeling reaction was completed. Subsequently, two samples (Cy3 and Cy5 labeled) and 50 µg of the internal standard (Cy2 labeled) were mixed. This mix was filled up to 140 µL with buffer 1, and the resulting mixture was incubated for 15 min on ice and vortexed several times. Next, 270 µL of buffer 2 was added and the mix was incubated 20 min on ice and vortexed again several times. Finally the sample mix was centrifuged for 5 min at 13,000 rpm and 4°C.

	Buffer 1	**Buffer 2**
Urea	9 M	7 M
DTE	65 mM	10 mM
CHAPS	4%	4%
TrisHCl	35 mM	none
Bromophenol blue	0.0025%	none
Thiourea	none	2 M
Ampholytes 3-10	none	0.8%

For 7 cm test gels (minigels) the same protocol was adjusted for the use of 10 µg of protein by using 80 pmol CyDye, adjustment to 46 µL with buffer 1 and addition of 84 µL of buffer 2.

8.22 First dimension: isoelectric focusing

For analytical gels the sample loading onto a 24cm Immobiline DryStrip® pH 3-10 NL (GE Healthcare, Munich, Germany) was performed by in-gel rehydration. The sample was added to the focusing tray of the PROTEAN IEF Cell (BioRad, Hercules, USA) and the precast IPG strip was placed on top of the sample. To avoid crystallization of urea, all strips were overlaid with 2 mL of mineral oil (700µL for the minigels). After rehydration for 6 h at room temperature in the dark, electrode papers moistened with purified water were placed between the strips and the electrodes to remove excess salts. The strips were focused in the PROTEAN IEF Cell (BioRad, Hercules, USA) at a constant temperature of 20°C. The strips were further rehydrated for about 12 h. Subsequently an isoelectric focusing protocol comprising five steps of increasing voltages was applied: 1 h at 50 V and 1 h at 100 V for a good sample entry, 1 h at 500 V, 1 h at 1,000 V and 8 h at 8,000 V for the focusing. At the end of the run about 55,000 volt hours had been reached. The program was adjusted for the minigels to reach about 5,000 volt hours: 30 min at 50 V, 30 min at 500 V, 30 min at 1000 V and 2 h at 5,000 V for the focusing.

8.23 Equilibration of IPG strips

For an efficient protein transfer from the first to the second dimension, an equilibration step was needed. The strips were therefore incubated with 2.5 mL of 1.4-dithioerythritol equilibration solution (DTE buffer) under low agitation for 7 min (750 µL for minigels). The solution was then replaced by fresh 2.5 mL DTE-buffer and the strips were incubated again 7 min under low agitation (750 µL for minigels). Then, 2.5 mL of iodacetamide buffer was added to each strip. After 5 min incubation under low agitation, the solution was replaced by 2.5 mL of the same buffer and incubated for another 5 min (750 µL for minigels). The equilibrated IPG gel strips were placed on SDS polyacrylamide gradient gels as indicated below.

	DTE buffer	**Iodacetamide buffer**
Urea	6 M	6 M
DTE	2%	none
SDS	2%	2%
TrisHCl	50 mM	50 mM
Glycerol	30%	30%
pH	6,8	6,8
Iodacetamide	none	2.5%
Bromophenol blue	none	0.004%

8.24 Second dimension: SDS-PAGE

The analytical samples were separated in the second dimension on 9-18% polyacrylamide gradient gels (Tris-HCl Optigel-LF, 9-18% linear from Nextgenescience).

For the 7 cm minigels, self-made 12% polyacrylamide gels were used with a thickness of 1.5 mm according to the following recipe (amount per gel):

3 mL purified-H_2O
2.3 mL of 1,5 M TrisHCl pH 8.8
3.6 mL of 30% acrylamide/0.8% PDA (piperazine diacrylamide)
45.2 µL of 5% sodiumthiosulfate
34.7 µL of 10% APS (ammonium persulfate)
3.47 µL of TEMED (tetramethylethylenediamine)

The IPG strips were placed on top of the polyacrylamide gels and embedded in 0.5% agarose, dissolved in 1-fold running buffer (TGS buffer: 25 mM Tris/HCl, 192 mM glycine, 0.1% SDS, pH 8.3, BioRad, Hercules, USA), for a better contact between strip and gel. The run was performed using the Ettan DALT system (GE Healthcare, Munich, Germany). In the upper chamber 2-fold TGS and in the lower chamber 1-fold TGS running buffer was applied. During the run the temperature was kept constant at 15°C. For optimal sample entry, the low current was limited to 10 mA/gel for about 1 h and subsequently increased to 15 mA/gel for the run, which was performed overnight. Bromophenol blue was used as a front marker and the run was stopped after 13 to 14 h (for minigel 1.5 h at 120 V). After the glass plate surface had been cleaned with ethanol, the gels were scanned using the Typhoon 9400 laser scanner (GE Healthcare, Munich, Germany) at an excitation/emission setting of 488/520 nm for Cy2, 532/580 nm for Cy3 and 633/670 nm for Cy5.

8.25 Image analysis

The 2-D-DIGE analysis was performed using the DeCyder 2D™ Software 6.5 (GE Healthcare, Munich, Germany). Samples concentrated from a triplicate batch process were analyzed on five 2-D gels as follows: each gel contained a Cy2-labeled standard and a sample from two

different culture days. Statistical analysis and quantification of protein abundance were carried out using the biological variation analysis module (BVA) of the DeCyder software. One gel was selected as master gel and all other gels in the study were matched to this master gel by the software. Proteins were defined as differentially abundant when the observed fold difference between the spots of two different conditions was greater than 1.5 with p-values of less than 0.05 (Student's t-test).

8.26 Picking protein spots of interest

As CyDyes only stain about 3% of the total protein and slightly influence the spot position, picking according to the spot position of the fluorescent gel picture results in low protein recovery per spot. Therefore gels were stained differently for total protein.

After the second dimension each gel was fixed for 30 min in 400 mL of 50% methanol, 7% acetic acid under low agitation. Then the fixative was exchanged and the gels were incubated again in the same buffer for 30 min. Each gel was stained with 400 mL of Sypro® Ruby protein gel stain (Invitrogen, Karlsruhe, Germany) overnight in the dark under low agitation. After staining, the solution was removed and the gels were washed in 400 mL of 10% methanol, 7% acetic acid for 30 min under low agitation in the dark. The staining procedure was completed with two washing steps for 5 min using ultrapure water, again in the dark and under low agitation.

For spot picking, the gels were immobilized on porous cellophane foil (GE Healthcare, Munich, Germany). The foil was pretreated for 5 min in ultrapure water and clamped into a frame. The gels were mounted on the surface of the foil and dried for a few minutes. For orientation, two reference markers (GE Healthcare, Munich, Germany) were placed on each side of the gel. The gels were scanned with the Typhoon 9400 laser scanner (GE Healthcare,

Munich, Germany) at the ex/em settings of 532/610 nm. After creating the picking list in the DeCyder software, the deregulated protein spots could be picked with the Ettan DALT Spot Picker (GE Healthcare, Munich, Germany) and transferred into a 96-well plate with porous bottoms (Proxeon Biosystems, San Mateo, USA). In order to control the picking process the gels were scanned again after picking.

8.27 In-gel digest of picked protein spots

To identify the individual proteins of a spot, the picked gel had to be dissolved and contained proteins digested with trypsin. The plate containing the picked protein spots was centrifuged for 10 min at 1500 rpm and the ultrapure water used for spot uptake was removed. Then 100 µL of 100% acetonitrile was added to each spot and the resulting solution incubated for 5 min at room temperature. After removal of the liquid for 10 min at 1,500 rpm, the spots were completely dried for 10 min in a Concentrator 5301 (Eppendorf, Hamburg, Germany). One vial with 20 µg of trypsin proteomics grade was dissolved in 1 mL of 40 mM NH_4HCO_3/10% acetonitrile. 5 µL of the trypsin solution was added to each spot. After incubation for 30 min at room temperature, 10 µL of 40 mM NH_4HCO_3/10% acetonitrile was added. The digestion was run overnight in a humid chamber at 37°C. Subsequently, 10 µL ultrapure water was added to each spot and the solution incubated for 10 min. Following centrifugation, the filtrate was collected in a 96-well plate (Nerbe plus, Winsen, Germany). To the remaining spots 25 µL of 50% acetonitrile/5% trifluoroacetic acid was added to the remaining spots for further peptide extraction, followed by incubation for 1 h at room temperature under low agitation. The plate was centrifuged again for 10 min at 1,500 rpm and the flow-through was collected in the same 96-well plate as before. Next, 25 µL of 50% acetonitrile/0.1% trifluoroacetic acid was added to each protein spot, followed by incubation for 1 h at room temperature with low agitation. The plate was centrifuged again for 15 min at

1,500 rpm and the flow-through obtained was pooled with those previously obtained. Then, the samples were dried completely in the Concentrator 5301 (Eppendorf, Hamburg, Germany).

8.28 Protein identification by tandem mass spectrometry

NanoLC-MS/MS analysis was performed with an UltiMate nanoHPLC system (Dionex, Sunnyvale, USA) connected to a QSTAR XL quadrupole time-of-flight hybrid mass spectrometer (Applied Biosystems, Foster City, USA). The dried peptide sample was dissolved in 10 µL of 2% acetonitrile, 0.1% trifluoroacetic acid, and the solution applied to a precolumn (PepMap C18, 0.3 mm i.d.×5 mm length; Dionex, Sunnyvale, USA) and separated using an analytical column (PepMap C18, 0.075 mm i.d×15 mm length; Dionex, Sunnyvale, USA) at a flow rate of 250 nL/min. The mobile phases were: A = 2% acetonitrile, 0.1% formic acid and B = 80% acetonitrile, 0.1% formic acid. The gradient for separation was 5-15% B in 3 min, 15–45% B in 25 min and 45–100% B in 2 min. A survey scan from m/z 350 to 1300 was run for 1 sec with subsequent 2 MS/MS scans of 2.5 sec each. Precursor ions were dynamically excluded for 120 sec. Under script control (Analyst software, Applied Biosystems, Foster City, USA), the product ion spectra acquired were submitted to the Mascot search engine (Matrix Science, Boston, USA) searching against the SwissProt database with the following parameters: maximum of one missed trypsin cleavage, cysteine carbamidomethylation, methionine oxidation, and a maximum 0.15 Da error tolerance in both the MS and MS/MS data.

9 REFERENCE LIST

Ailor,E. and Betenbaugh,M.J. 1998. Overexpression of a cytosolic chaperone to improve solubility and secretion of a recombinant IgG protein in insect cells. Biotechnol. Bioeng. *58*, 196-203.

al-Rubeai,M. and Singh,R.P. 1998. Apoptosis in cell culture. Curr. Opin. Biotechnol. *9*, 152-156.

Arden,N. and Betenbaugh,M.J. 2004. Life and death in mammalian cell culture: strategies for apoptosis inhibition. Trends Biotechnol. *22*, 174-180.

Barnes,L.M., Bentley,C.M., Moy,N., and Dickson,A.J. 2007. Molecular analysis of successful cell line selection in transfected GS-NS0 myeloma cells. Biotechnol. Bioeng. *96*, 337-348.

BASF Corporation 2004. Pluronic F68 Block Copolymer Surfactant. Technical Bulletin www.basf.com/performancechemical/pdfs/Pluronic_F68.pdf.

Benton,T., Chen,T., McEntee,M., Fox,B., King,D., Crombie,R., Thomas,T.C., and Bebbington,C. 2002. The use of UCOE vectors in combination with a preadapted serum free, suspension cell line allows for rapid production of large quantities of protein. Cytotechnology *38*, 43-46.

Borth,N., Mattanovich,D., Kunert,R., and Katinger,H. 2005. Effect of increased expression of protein disulfide isomerase and heavy chain binding protein on antibody secretion in a recombinant CHO cell line. Biotechnol. Prog. *21*, 106-111.

Brewer,J.W. and Hendershot,L.M. 2005. Building an antibody factory: a job for the unfolded protein response. Nat. Immunol. *6*, 23-29.

Calfon,M., Zeng,H., Urano,F., Till,J.H., Hubbard,S.R., Harding,H.P., Clark,S.G., and Ron,D. 2002. IRE1 couples endoplasmic reticulum load to secretory capacity by processing the XBP-1 mRNA. Nature *415*, 92-96.

Campos-da-Paz,M., Costa,C.S., Quilici,L.S., de,C.S., I, Kyaw,C.M., Maranhao,A.Q., and Brigido,M.M. 2008. Production of recombinant human factor VIII in different cell lines and the effect of human XBP1 co-expression. Mol. Biotechnol. *39*, 155-158.

Chiang,G.G. and Sisk,W.P. 2005. Bcl-x(L) mediates increased production of humanized monoclonal antibodies in Chinese hamster ovary cells. Biotechnol. Bioeng. *91*, 779-792.

Chu,L. and Robinson,D.K. 2001. Industrial choices for protein production by large-scale cell culture. Curr. Opin. Biotechnol. *12*, 180-187.

costa-Alvear,D., Zhou,Y., Blais,A., Tsikitis,M., Lents,N.H., Arias,C., Lennon,C.J., Kluger,Y., and Dynlacht,B.D. 2007. XBP1 Controls Diverse Cell Type- and Condition-Specific Transcriptional Regulatory Networks. Molecular Cell *27*, 53-66.

Cox,J.S. and Walter,P. 1996. A novel mechanism for regulating activity of a transcription factor that controls the unfolded protein response. Cell *87*, 391-404.

Davis,R., Schooley,K., Rasmussen,B., Thomas,J., and Reddy,P. 2000. Effect of PDI overexpression on recombinant protein secretion in CHO cells. Biotechnol. Prog. *16*, 736-743.

Decision Resources/Pharmaview 2008. ProductView 2008. http://www. decisionresourcesgateway. com/Pharmaview/index. aspx?StoryID=0&ReportID=0&Lang=en&MainPage=extra. aspx.

Deveraux,Q.L., Roy,N., Stennicke,H.R., Van,A.T., Zhou,Q., Srinivasula,S.M., Alnemri,E.S., Salvesen,G.S., and Reed,J.C. 1998. IAPs block apoptotic events induced by caspase-8 and cytochrome c by direct inhibition of distinct caspases. EMBO J. *17*, 2215-2223.

Deveraux,Q.L., Takahashi,R., Salvesen,G.S., and Reed,J.C. 1997. X-linked IAP is a direct inhibitor of cell-death proteases. Nature *388*, 300-304.

Dinnis,D.M., Stansfield,S.H., Schlatter,S., Smales,C.M., Alete,D., Birch,J.R., Racher,A.J., Marshall,C.T., Nielsen,L.K., and James,D.C. 2006. Functional proteomic analysis of GS-NS0 murine myeloma cell lines with varying recombinant monoclonal antibody production rate. Biotechnol. Bioeng.

Dorner,A.J. and Kaufman,R.J. 1994. The levels of endoplasmic reticulum proteins and ATP affect folding and secretion of selective proteins. Biologicals *22*, 103-112.

Dorner,A.J., Krane,M.G., and Kaufman,R.J. 1988. Reduction of endogenous GRP78 levels improves secretion of a heterologous protein in CHO cells. Mol. Cell Biol. *8*, 4063-4070.

Florin,L., Pegel,A., Becker,E., Hausser,A., Olayioye,M.A., and Kaufmann,H. 2008. Heterologous expression of the lipid transfer protein CERT increases therapeutic protein productivity of mammalian cells. J. Biotechnol. *submitted*.

Fussenegger,M., Moser,S., Mazur,X., and Bailey,J.E. 1997. Autoregulated multicistronic expression vectors provide one-step cloning of regulated product gene expression in mammalian cells. Biotechnol. Prog. *13*, 733-740.

Fussenegger,M., Schlatter,S., Datwyler,D., Mazur,X., and Bailey,J.E. 1998. Controlled proliferation by multigene metabolic engineering enhances the productivity of Chinese hamster ovary cells. Nat. Biotechnol. *16*, 468-472.

Gasser,B., Maurer,M., Gach,J., Kunert,R., and Mattanovich,D. 2006. Engineering of Pichia pastoris for improved production of antibody fragments. Biotechnol. Bioeng. *94*, 353-361.

Groenendyk,J. and Michalak,M. 2005. Endoplasmic reticulum quality control and apoptosis. Acta Biochim. Pol. *52*, 381-395.

Hambrock,A., Löffler-Walz,C., and Quast,U. 2002. Glibenclamide binding to sulfonylurea receptor subtypes: dependence on adenine nucleotides. Br. J. Pharmacol. *136*, 995-1004.

Hanada,K., Kumagai,K., Yasuda,S., Miura,Y., Kawano,M., Fukasawa,M., and Nishijima,M. 2003. Molecular machinery for non-vesicular trafficking of ceramide. Nature *426*, 803-809.

Heukeshoven,J. and Dernick,R. 1988. Improved silver staining procedure for fast staining in PhastSystem Development Unit. I. Staining of sodium dodecyl sulfate gels. Electrophoresis *9*, 28-32.

Hooker,A.D., Green,N.H., Baines,A.J., Bull,A.T., Jenkins,N., Strange,P.G., and James,D.C. 1999. Constraints on the transport and glycosylation of recombinant IFN-gamma in Chinese hamster ovary and insect cells. Biotechnol. Bioeng. *63*, 559-572.

Hsu,T.A. and Betenbaugh,M.J. 1997. Coexpression of molecular chaperone BiP improves immunoglobulin solubility and IgG secretion from Trichoplusia ni insect cells. Biotechnol. Prog. *13*, 96-104.

Ifandi,V. and Al-Rubeai,M. 2003. Stable transfection of CHO cells with the c-myc gene results in increased proliferation rates, reduces serum dependency, and induces anchorage independence. Cytotechnology *41*, 1-10.

Iwakoshi,N.N., Lee,A.H., and Glimcher,L.H. 2003. The X-box binding protein-1 transcription factor is required for plasma cell differentiation and the unfolded protein response. Immunol Rev *194*, 29-38.

Jain,E. and Kumar,A. 2008. Upstream processes in antibody production: evaluation of critical parameters. Biotechnol. Adv. *26*, 46-72.

Jayapal,K.P., Wlaschin,K.F., Hu,W.S., and Yap,M.G.S. 2007. Recombinant protein therapeutics from CHO Cells - 20 years and counting. Chemical Engineering Progress *103*, 40-47.

Jiang,Z., Huang,Y., and Sharfstein,S.T. 2006. Regulation of recombinant monoclonal antibody production in chinese hamster ovary cells: a comparative study of gene copy number, mRNA level, and protein expression. Biotechnol. Prog. *22*, 313-318.

Kaufmann,H. and Fieder,J. 2008. Methods of selecting cell clones. Patent Application *WO2008031873*.

Kaufmann,H. and Fussenegger,M. 2003. Metabloic engineering of mammalian cells for higher protein yield. In: S.C.Markrides, ed. Gene Transfer and Expression in Mammallian Cells, Elsevier Science B.V., pp. 457-469.

Kaufmann,H. and Fussenegger,M. 2004. Caspase Regulation at the molecular level. In: M.Al-Rubeai and M.Fussenegger, eds. Cell Engineering, Kluwer Acadamic Publishers, pp. 1-23.

Kaufmann,H., Mazur,X., Fussenegger,M., and Bailey,J.E. 1999. Influence of low temperature on productivity, proteome and protein phosphorylation of CHO cells. Biotechnol. Bioeng. *63*, 573-582.

Kim,J.M., Kim,J.S., Park,D.H., Kang,H.S., Yoon,J., Baek,K., and Yoon,Y. 2004. Improved recombinant gene expression in CHO cells using matrix attachment regions. J. Biotechnol. *107*, 95-105.

Kim,R., Emi,M., Tanabe,K., and Murakami,S. 2006. Role of the unfolded protein response in cell death. Apoptosis. *11*, 5-13.

Kitchin,K. and Flickinger,M.C. 1995. Alteration of hybridoma viability and antibody secretion in transfectomas with inducible overexpression of protein disulfide isomerase. Biotechnol. Prog. *11*, 565-574.

Knappskog,S., Ravneberg,H., Gjerdrum,C., Tro[beta]e,C., Stern,B., and Pryme,I.F. 2007. The level of synthesis and secretion of Gaussia princeps luciferase in transfected CHO cells is heavily dependent on the choice of signal peptide. Journal of Biotechnology *128*, 705-715.

Ku,S.C., Ng,D.T., Yap,M.G., and Chao,S.H. 2007. Effects of overexpression of X-box binding protein 1 on recombinant protein production in Chinese hamster ovary and NS0 myeloma cells. Biotechnol. Bioeng. *99*, 155-164.

Kumar,N., Maurya,P., Gammell,P., Dowling,P., Clynes,M., and Meleady,P. 2007. Proteomic Profiling of Secreted Proteins from CHO Cells Using Surface-Enhanced Laser Desorption Ionization Time-of-Flight Mass Spectrometry. Biotechnol. Prog.

Kuystermans,D., Krampe,B., Swiderek,H., and Al-Rubeai,M. 2007. Using cell engineering and omic tools for the improvement of cell culture processes. Cytotechnology *53*, 3-22.

Lahm,H.W. and Langen,H. 2000. Mass spectrometry: a tool for the identification of proteins separated by gels. Electrophoresis *21*, 2105-2114.

Lee,A.H., Chu,G.C., Iwakoshi,N.N., and Glimcher,L.H. 2005. XBP-1 is required for biogenesis of cellular secretory machinery of exocrine glands. EMBO J. *24*, 4368-4380.

Lee,A.H., Iwakoshi,N.N., Anderson,K.C., and Glimcher,L.H. 2003a. Proteasome inhibitors disrupt the unfolded protein response in myeloma cells. Proc. Natl. Acad. Sci. U. S. A *100*, 9946-9951.

Lee,K., Tirasophon,W., Shen,X., Michalak,M., Prywes,R., Okada,T., Yoshida,H., Mori,K., and Kaufman,R.J. 2002. IRE1-mediated unconventional mRNA splicing and S2P-mediated ATF6 cleavage merge to regulate XBP1 in signaling the unfolded protein response. Genes Dev. *16*, 452-466.

Lee,M.S., Kim,K.W., Kim,Y.H., and Lee,G.M. 2003b. Proteome analysis of antibody-expressing CHO cells in response to hyperosmotic pressure. Biotechnol. Prog. *19*, 1734-1741.

Liu,C. and Hong,L. 2001. Development of a shaking bioreactor system for animal cell cultures. Biochem. Eng J. *7*, 121-125.

Manz,R.A. and Radbruch,A. 2002. Plasma cells for a lifetime? Eur. J. Immunol. *32*, 923-927.

Maurya,P., Meleady,P., Dowling,P., and Clynes,M. 2007. Proteomic approaches for serum biomarker discovery in cancer. Anticancer Research *27*, 1247-1255.

Meents,H., Enenkel,B., Eppenberger,H.M., Werner,R.G., and Fussenegger,M. 2002. Impact of coexpression and coamplification of sICAM and antiapoptosis determinants bcl-2/bcl-x(L) on productivity, cell survival, and mitochondria number in CHO-DG44 grown in suspension and serum-free media. Biotechnol. Bioeng. *80*, 706-716.

Meleady,P., Henry,M., Gammell,P., Doolan,P., Sinacore,M., Melville,M., Francullo,L., Leonard,M., Charlebois,T., and Clynes,M. 2008. Proteomic profiling of CHO cells with enhanced rhBMP-2 productivity following co-expression of PACEsol. Proteomics *8*, 2611-2624.

Mohan,C., Kim,Y.G., Koo,J., and Lee,G.M. 2008. Assessment of cell engineering strategies for improved therapeutic protein production in CHO cells. Biotechnol. J. *3*, 624-630.

Muller,D., Katinger,H., and Grillari,J. 2008. MicroRNAs as targets for engineering of CHO cell factories. Trends Biotechnol. *26*, 359-365.

Nakagawa,T. and Yuan,J. 2000. Cross-talk between two cysteine protease families. Activation of caspase-12 by calpain in apoptosis. J. Cell Biol. *150*, 887-894.

Nissom,P.M., Sanny,A., Kok,Y.J., Hiang,Y.T., Chuah,S.H., Shing,T.K., Lee,Y.Y., Wong,K.T., Hu,W.S., Sim,M.Y., and Philp,R. 2006. Transcriptome and proteome profiling to understanding the biology of high productivity CHO cells. Mol. Biotechnol. *34*, 125-140.

O'Callaghan,P.M. and James,D.C. 2008. Systems biotechnology of mammalian cell factories. Brief. Funct. Genomic. Proteomic. *7*, 95-110.

Ohya,T., Hayashi,T., Kiyama,E., Nishii,H., Miki,H., Kobayashi,K., Honda,K., Omasa,T., and Ohtake,H. 2007. Improved production of recombinant human antithrombin III in Chinese hamster ovary cells by ATF4 overexpression. Biotechnol. Bioeng. *100*, 317-324.

Pak,C.O., Hunt,M.N., Bridges,M.W., Sleigh,M.J., and Gray,P.P. 1996. Super-CHO-A cell line capable of autocrine growth under fully defined protein-free conditions. Cytotechnology *V22*, 139-146.

Papoutsakis,E.T. 1991. Media additives for protecting freely suspended animal cells against agitation and aeration damage. Trends Biotechnol. *9*, 316-324.

Reimold,A.M., Iwakoshi,N.N., Manis,J., Vallabhajosyula,P., Szomolanyi-Tsuda,E., Gravallese,E.M., Friend,D., Grusby,M.J., Alt,F., and Glimcher,L.H. 2001. Plasma cell differentiation requires the transcription factor XBP-1. Nature *412*, 300-307.

Sandberg,H., Lutkemeyer,D., Kuprin,S., Wrangel,M., Almstedt,A., Persson,P., Ek,V., and Mikaelsson,M. 2006. Mapping and partial characterization of proteases expressed by a CHO production cell line. Biotechnol. Bioeng. *95*, 961-971.

Sauerwald,T.M., Betenbaugh,M.J., and Oyler,G.A. 2002. Inhibiting apoptosis in mammalian cell culture using the caspase inhibitor XIAP and deletion mutants. Biotechnol. Bioeng. *77*, 704-716.

Sauerwald,T.M., Figueroa,B., Jr., Hardwick,J.M., Oyler,G.A., and Betenbaugh,M.J. 2006. Combining caspase and mitochondrial dysfunction inhibitors of apoptosis to limit cell death in mammalian cell cultures. Biotechnol. Bioeng. *94*, 362-372.

Sauerwald,T.M., Oyler,G.A., and Betenbaugh,M.J. 2003. Study of caspase inhibitors for limiting death in mammalian cell culture. Biotechnology and Bioengineering *81*, 329-340.

Sautter,K. and Enenkel,B. 2005. Selection of high-producing CHO cells using NPT selection marker with reduced enzyme activity. Biotechnol. Bioeng. *89*, 530-538.

Schirrmann,T., Al-Halabi,L., bel,S., and Hust,M. 2008. Production systems for recombinant antibodies. Frontiers in Bioscience *13*, 4576-4594.

Schlatter,S., Stansfield,S.H., Dinnis,D.M., Racher,A.J., Birch,J.R., and James,D.C. 2005. On the optimal ratio of heavy to light chain genes for efficient recombinant antibody production by CHO cells. Biotechnol. Prog. *21*, 122-133.

Seow,T.K., Korke,R., Liang,R.C., Ong,S.E., Ou,K., Wong,K., Hu,W.S., and Chung,M.C. 2001. Proteomic investigation of metabolic shift in mammalian cell culture. Biotechnol. Prog. *17*, 1137-1144.

Seth,G., Hossler,P., Yee,J.C., and Hu,W.S. 2006. Engineering cells for cell culture bioprocessing--physiological fundamentals. Adv. Biochem. Eng Biotechnol. *101*, 119-164.

Shaffer,A.L., Shapiro-Shelef,M., Iwakoshi,N.N., Lee,A.H., Qian,S.B., Zhao,H., Yu,X., Yang,L., Tan,B.K., Rosenwald,A., Hurt,E.M., Petroulakis,E., Sonenberg,N., Yewdell,J.W., Calame,K., Glimcher,L.H., and Staudt,L.M. 2004. XBP1, downstream of Blimp-1, expands the secretory apparatus and other organelles, and increases protein synthesis in plasma cell differentiation. Immunity. *21*, 81-93.

Shusta,E.V., Raines,R.T., Pluckthun,A., and Wittrup,K.D. 1998. Increasing the secretory capacity of Saccharomyces cerevisiae for production of single-chain antibody fragments. Nat. Biotechnol. *16*, 773-777.

Sitton,G. and Srienc,F. 2008. Mammalian cell culture scale-up and fed-batch control using automated flow cytometry. J. Biotechnol. *135*, 174-180.

Smales,C.M., Dinnis,D.M., Stansfield,S.H., Alete,D., Sage,E.A., Birch,J.R., Racher,A.J., Marshall,C.T., and James,D.C. 2004. Comparative proteomic analysis of GS-NS0 murine myeloma cell lines with varying recombinant monoclonal antibody production rate. Biotechnol. Bioeng. *88*, 474-488.

Smith,J.D., Tang,B.C., and Robinson,A.S. 2004. Protein disulfide isomerase, but not binding protein, overexpression enhances secretion of a non-disulfide-bonded protein in yeast. Biotechnol. Bioeng. *85*, 340-350.

Smith,P.K., Krohn,R.I., and Hermanson,G.T. 1985. Measurement of protein using bicinchoninic acid. Analytical Biochemistry *150*, 76-85.

Spens,E. and Haggstrom,L. 2005. Defined protein-free NS0 myeloma cell cultures: stimulation of proliferation by conditioned medium factors. Biotechnol. Prog. *21*, 87-95.

Tigges,M. and Fussenegger,M. 2006. Xbp1-based engineering of secretory capacity enhances the productivity of Chinese hamster ovary cells. Metab Eng *8*, 264-272.

Unlu,M., Morgan,M.E., and Minden,J.S. 1997. Difference gel electrophoresis: a single gel method for detecting changes in protein extracts. Electrophoresis *18*, 2071-2077.

Urano,F., Wang,X., Bertolotti,A., Zhang,Y., Chung,P., Harding,H.P., and Ron,D. 2000. Coupling of stress in the ER to activation of JNK protein kinases by transmembrane protein kinase IRE1. Science *287*, 664-666.

Urlaub,G., Mitchell,P.J., Kas,E., Chasin,L.A., Funanage,V.L., Myoda,T.T., and Hamlin,J. 1986. Effect of gamma rays at the dihydrofolate reductase locus: deletions and inversions. Somat. Cell Mol. Genet. *12*, 555-566.

(VFA.) Zulassungen für gentechnisch hergestellte Arzneimittel. www.vfa.de Verband Forschender Arzneimittelhersteller e.V. ((2008)

Walsh,G. 2006. Biopharmaceutical benchmarks 2006. Nat. Biotechnol. *24*, 769-776.

Walter,L. and Hajnoczky,G. 2005. Mitochondria and endoplasmic reticulum: the lethal interorganelle cross-talk. J. Bioenerg. Biomembr. *37*, 191-206.

Wegrzyn,J., Lee,J., Neveu,J.M., Lane,W.S., and Hook,V. 2007. Proteomics of neuroendocrine secretory vesicles reveal distinct functional systems for biosynthesis and exocytosis of peptide hormones and neurotransmitters. Journal of Proteome Research *6*, 1652-1665.

Wurm,F.M. 2004. Production of recombinant protein therapeutics in cultivated mammalian cells. Nat. Biotechnol. *22*, 1393-1398.

Yamamoto,K., Yoshida,H., Kokame,K., Kaufman,R.J., and Mori,K. 2004. Differential contributions of ATF6 and XBP1 to the activation of endoplasmic reticulum stress-responsive cis-acting elements ERSE, UPRE and ERSE-II. J. Biochem. (Tokyo) *136*, 343-350.

Yee,J.C., de Leon,G.M., Philp,R.J., Yap,M., and Hu,W.S. 2008. Genomic and proteomic exploration of CHO and hybridoma cells under sodium butyrate treatment. Biotechnol. Bioeng. *99*, 1186-1204.

Yoneda,T., Imaizumi,K., Oono,K., Yui,D., Gomi,F., Katayama,T., and Tohyama,M. 2001. Activation of caspase-12, an endoplastic reticulum (ER) resident caspase, through tumor necrosis factor receptor-associated factor 2-dependent mechanism in response to the ER stress. J. Biol. Chem. *276*, 13935-13940.

Yoshida,H., Haze,K., Yanagi,H., Yura,T., and Mori,K. 1998. Identification of the cis-acting endoplasmic reticulum stress response element responsible for transcriptional induction of mammalian glucose-regulated proteins. Involvement of basic leucine zipper transcription factors. J. Biol. Chem. *273*, 33741-33749.

Yoshida,H., Matsui,T., Hosokawa,N., Kaufman,R.J., Nagata,K., and Mori,K. 2003. A time-dependent phase shift in the mammalian unfolded protein response. Dev. Cell *4*, 265-271.

Yoshida,H., Matsui,T., Yamamoto,A., Okada,T., and Mori,K. 2001. XBP1 mRNA is induced by ATF6 and spliced by IRE1 in response to ER stress to produce a highly active transcription factor. Cell *107*, 881-891.

Yoshida,H., Oku,M., Suzuki,M., and Mori,K. 2006. pXBP1(U) encoded in XBP1 pre-mRNA negatively regulates unfolded protein response activator pXBP1(S) in mammalian ER stress response. J. Cell Biol. *172*, 565-575.

Zinszner,H., Kuroda,M., Wang,X., Batchvarova,N., Lightfoot,R.T., Remotti,H., Stevens,J.L., and Ron,D. 1998. CHOP is implicated in programmed cell death in response to impaired function of the endoplasmic reticulum. Genes Dev. *12*, 982-995.

10 ERKLÄRUNG

Ich erkläre hiermit, dass ich die vorliegende Arbeit ohne unzulässige Hilfe Dritter und ohne Benutzung anderer als der angegebenen Hilfsmittel angefertigt habe; die aus fremden Quellen direkt oder indirekt übernommenen Gedanken sind als solche kenntlich gemacht.

Hochdorf,

Unterschrift

11 DANKSAGUNG

Mein besonderer Dank gilt Prof. Dr. K. Pfizenmaier für die Betreuung meiner Arbeit und die angeregten, anspornenden Diskussionen. Insbesondere möchte ich Dr. H. Kaufmann für die Vor-Ort-Betreuung danken und dafür, dass er nie den Humor verlor und immer zu motivieren wusste. Dr. L. Florin danke ich für die unermüdliche Geduld und nie enden wollende moralische Unterstützung und verleihe ihr meinerseits die Auszeichnung „Beste Post-Doc“. Außerdem danke ich Dr. M. Olayioye und Dr. A. Hausser für die Anregungen, Diskussionen und die nette Betreuung bei den Doktorandenseminaren. Ebenfalls danke ich den Mitgliedern des Labors Zellbiologie für die außerordentlich tolle Arbeitsatmosphäre und im Besonderen Jürgen Fieder für die inspirierenden Diskussionen. Danken will ich auch Rebecca Bischoff und Eva Weber für ihre Unterstützung. Mein weiterer Dank gilt Dr. B. Enenkel und Dr. K. Sautter sowie dem gesamten Labor Molekularbiologie für die unerschöpflichen Weisheiten und Hilfestellungen rund um das Thema „Verkettung von Basenpaaren“. Mein Dank gilt auch Dr. U. Teichmann für die stets unverzügliche Bearbeitung der Fragen wie: „Dürfen wir das?“ oder „Können wir das anmelden?“. Mein herzlicher Dank gilt Dr. M. Lenter für die Unterstützung des Proteom Projektes. Jessica Bretzel danke ich für die grandiose Umsetzung und die eleganten Detaillösungen der unterschiedlichen Probenvergleiche. Danken möchte ich auch den Spezialisten Dr. W. Rist, Dr. E. Simon und Dr. T. Hildebrand für die Identifizierung und Annotationsunterstützung. Meinem Schwiegervater Darrell Charles danke ich für seine Unterstützung. Danken möchte ich meinen Eltern, Ursel und Christoph Becker sowie meiner Schwester Ina für ihren fortwährenden Beistand.

Last but not least danke ich meiner Frau Vanessa für ihr außerordentliches Verständnis und ihre mentale Unterstützung, die in der Zeit durchaus vonnöten war.